The Structural Neurobiology of Social Anxiety Disorder

A Clinical Neuroimaging Study

Coenraad J. Hattingh
Department of Psychiatry
Faculty of Health Sciences
University of Cape Town

Thesis Presented for the Degree

Doctor of Philosophy in Neuroscience - Ph.D.(Neuroscience)

By

Coenraad J. Hattingh
B.A.(Psych), Hons.B.A.(Psych), M.Sc.Med.(Neuroscience)

in the

Department of Psychiatry and Mental Health

Faculty of Health Sciences

University of Cape Town

February 2015

FACULTY OF HEALTH SCIENCES
UNIVERSITY OF CAPE TOWN

Supervisor

Professor Dan J. Stein

Co-Supervisors

Professor Christine Lochner

Dr Samantha Brooks

Word Count:

40 000

Acknowledgements:

The PhD journey is a journey that every academic has to make. It is a journey fraught with mountains to climb and horizons of new discovery to witness. And it is with the acknowledgements, written last of the entire thesis, that one is afforded the precious opportunity to thank those individuals who have made the load you carried during this journey lighter; those who have made the way clearer, and those who have stood beside you until you have reached the summit, and beyond. It is true, that success is the preserve of those who are steadfast in their desire. For those of you who have been steadfast alongside me, I am thankful - for you have seen me. There are no words to accurately express my gratitude on paper, but I list your name here, for all that it is worth to me, in my heart of hearts. Thank you.

Coenraad J. Hattingh – My father

Michelle M. Roux – My mother

In alphabetical order

Florence Adams	Graham Fieggen	Andreas Labuschagne
Jaap Brits	Jean-Paul Fouché	Christine Lochner
Samantha Brooks	Ilse Fouché	Graham Louw
Angelique Craemer	Johan Fourie	Mari Maritz
Tinus de Bruin	Chantal Fourie	Gerhard Maritz
Mariana de Bruin	Jaomie Hattingh	Nienkie Pannekoek
Jan de Bruin	Fleur Howells	Eleni Pantellis
Adri de Bruin	Pasha Javani	Bets Ruthven
Gail Edelstein	Hannelie Javani	Mark Solms
Johanna Ellis	Miriam Karjiker	Dan Stein
Chris Ellis	Lauriston Kellaway	Rachel Weiss
Betsie Ellis	Anél Kloppers	

"True, the dominance of the brain over the organism is given great emphasis, but anything possibly showing that the life of the psyche might be independent of demonstrable organic changes, or could act spontaneously, fills the psychiatrist of today with alarm, as if to acknowledge this would inevitably mean a return to the days of Natural Philosophy and the metaphysics of the soul. This mistrust on the part of the psychiatrist has placed the psyche as it were under the supervision of a guardian, and demands that it should make no movement that might reveal that it possesses a competence of its own. Yet what this attitude in fact implies is a lack of trust in the causal chain extending between the body and the psyche. Even where investigation shows the primary muse of the phenomenon to be psychical, if we go deeper, we shall one day discover that the way continues until it reaches the organic basis for the psychical. But where in the present state of our knowledge, we cannot but regard the psychical as the end of the road, that is no reason for denying it."

- *Sigmund Freud in "The Interpretation of Dreams*

"…efforts to find a neurobiological basis for psychopathology do not obviate the continuing need to address the meaning of the experience of mental illness to the patient."

- Nancy McWilliams

"Those bearing torches should pass them on to others." - Plato

Abstract:

While a number of studies have explored the functional neuroanatomy of social anxiety disorder (SAD), comparatively few studies have investigated the structural underpinnings in SAD. 18 psychopharmacologically and psychotherapeutically naïve adult patients with a primary Axis I diagnosis of generalized social anxiety disorder and 18 demographically (age, gender and education) matched healthy controls underwent 3T structural magnetic resonance imaging. A manual tracing protocol was specifically developed to compute the volume of the most prominent subcortical gray matter structures implicated in SAD by previous functional research. Cortical thickness was estimated using an automated algorithm and whole brain analyses of white matter structure were performed using FSL's tract-based spatial statistics comparing fractional anisotropy (FA), mean diffusivity (MD) in individuals with SAD. Manual tracing demonstrated that compared to controls, SAD patients showed an enlarged right globus pallidus. Cortical thickness analyses demonstrated significant cortical thinning in the left isthmus of the cingulate gyrus, the left temporal pole, and the left superior temporal gyrus. Analyses of white matter tractographic data demonstrated reduced FA in in the genu, splenium and tapetum of the corpus callosum. Additionally reduced FA was noticed in the fornix and the right cingulum. Reduced FA was also noted in bilateral corticospinal tracts and the right corona radiata. The results demonstrate structural alterations in limbic circuitry as well as involvement of the basal glanglia and their cortical projections and input pathways.

INDEX

CONTENTS

CHAPTER I

Introduction and Review of the Literature

Introduction:

Anxiety disorders are of the most prevalent psychiatric disorders, affecting 7–14% of the general population at any given time (Baxter et al., 2013) (Kessler et al., 2005). Social anxiety disorder (SAD) is the second most prevalent of the anxiety disorders (Wittchen et al., 2011). SAD is associated with significant disability, impairment and reduced quality of life (Alonso et al., 2004; Kessler, 2003; Mendlowicz & Stein, 2000; Schneier et al., 1994; Stein, Torgrud, & Walker, 2000). Understanding the associated neurobiology of SAD will undoubtedly help our understanding of the overall pathophysiology and pathogenesis of SAD, which might inform more targeted and more effective interventions.

In the following chapters, this thesis aims to examine the various structural neuroanatomical changes that are associated with SAD, and how they might contribute to our understanding of the overall neurobiological underpinnings of the symptoms of SAD. This exploration of the neurobiology of SAD hopes to further inform a novel approach to better categorizing neural alterations in those with the disorder, namely a method for manually tracing those regions most associated with SAD. However, to contextualize the findings in subsequent chapters, a review of the literature and introductory comments are presented here in the following order: 1) A brief overview of the features of the anxiety disorders in general is discussed followed by a more detailed account of SAD specifically; 2) A review of the diagnostic features of SAD according to the DSM-5; 3) A discussion of the prevalence and morbidity associated with SAD; 4) A review of SAD neurobiology, a) fear circuitry in general b) the functional anatomy of regions of interest, c) cortical thickness studies in SAD, d) studies investigating white matter in SAD, and e) manual tracing studies in SAD, and 5) An outline of the specific aims of this thesis.

1: Anxiety and Social Anxiety Disorder

As a category of psychiatric illness, anxiety disorders include conditions that share features of excessive fear and anxiety and related behavioral disturbances. Fear is the emotional response to real or perceived imminent threat, whereas anxiety is anticipation of future threat (American Psychiatric Association, 2013). These two states overlap to varying degrees, however they also differ in that fear is more closely associated with autonomic arousal whereas anxiety is characterized to a greater extent by states of hyper-vigilance and avoidant behaviour, which reduce the level of anxiety. Panic attacks feature prominently within the anxiety disorders as most of these conditions are characterized by chronic and protracted anxiety states, and severe anxiety can lead to panic.

Social anxiety disorder is often comorbid with other anxiety disorders, major depressive disorder, and substance use disorders. The onset of social anxiety disorder generally precedes that of the other disorders, except for specific phobia and separation anxiety disorder (Beesdo et al. 2007). Chronic social isolation in the course of a social anxiety disorder may result in major depressive disorder. Comorbidity with depression is high also in older adults (King-Kallimanis et al. 2009)

The anxiety disorders differ from one another in the types of objects or situations that induce fear, anxiety, or avoidance behaviour, and in the associated cognitive ideation. Thus they can be differentiated by close examination of the types of situations that are feared or avoided and the content of the associated thoughts or beliefs (American Psychiatric Association, 2013). In the case of SAD, there is marked fear and anxiety associated with social situations in which the individual feels that he may be scrutinized and potentially embarrassed. The fact that socially valenced stimuli play a key role in SAD, means that morbidity and comorbidity is often severe and chronic (Lipsitz et al., 2000; Steinert et al., 2013).

2: Diagnostic Features of SAD

The primary feature of social anxiety disorder according to the Diagnostic and Statistical Manual of Mental Disorders Fifth Edition (DSM-5) (American Psychiatric Association, 2013) is profound fear and anxiety associated with social situations in which the individual feels that others may scrutinize him or her. When an individual with SAD is exposed to social situations, such as speaking in public, riding in a bus, or meeting strangers, a profound fear dominates the situation in that he or she will be negatively evaluated or embarrassed. The individual is preoccupied with thoughts that he or she will be judged as anxious, weak, or generally unlikable. The individual fears that he or she will invariably act or appear in a certain way such as blushing, trembling, sweating, stumbling over one's words, or staring, that will be negatively evaluated by others (Burstein, M. et al., 2011)

Some individuals may fear offending others or being rejected. Fear of offending others - for example, by overly direct gaze or by showing anxiety symptoms—may be the predominant fear in individuals from cultures with strong collectivistic orientations (Heinrichs, N. et al., 2006). An individual with fear of trembling of the hands may avoid drinking, eating, writing, or pointing in public; an individual with fear of sweating may avoid shaking hands or eating spicy foods; and an individual with fear of blushing may avoid public performance, bright lights, or discussion about intimate topics. Some individuals fear and avoid urinating in public restrooms when other individuals are present (American Psychiatric Association, 2013).

Feared social situations such as social interactions (e.g., having a conversation, meeting unfamiliar people), being observed (e.g., eating or drinking), and performing in front of others (e.g., giving a speech) almost always provoke fear or anxiety in individuals with social anxiety disorder. However, the degree and type of fear and anxiety may vary (e.g., anticipatory anxiety, a panic attack) across different situations. The anticipatory anxiety may occur sometimes far in advance of upcoming events (e.g., worrying every day for weeks before attending a social event, repeating a speech for days in advance). Individuals will often avoid these feared social situations or endure them with intense dread (Gretarsdottir, E. et al., 2004).

Fear and anxiety associated with these social situations is judged to be out of proportion to the actual risk of being negatively evaluated or to the consequences of such negative evaluation. The fear, anxiety, and avoidance interfere significantly with the individual's normal routine, occupational, academic functioning, social activities or relationships, and cause significant distress and impairment in social, occupational, and other important areas of functioning (American Psychiatric Association, 2013).

3: Prevalence

The 12-month prevalence estimate of social anxiety disorder for the United States is approximately 7% (Kessler et al. 2005; Kessler et al. 2012; Ruscio et al. 2008). Lower 12-month prevalence estimates are seen in much of the world using the same diagnostic instrument, clustering around 0.5%–2.0%; median prevalence in Europe is 2.3% (Lewis-Fernández et al. 2010; Wittchen and Jacobi 2005). The 12-month prevalence estimate of social anxiety disorder in South Africa is 1.9%, whereas lifetime prevalence is 2.8% (Herman et al., 2009).

The 12-month prevalence rates in children and adolescents are comparable to those in adults (Costello et al. 2003; Kessler et al. 2012; Wittchen et al. 1999). Prevalence rates decrease with age (Wolitzky-Taylor et al. 2010). The 12-month prevalence for older adults ranges from 2% to 5% (Kessler et al. 2012; Mohlman et al. 2012; Wolitzky-Taylor et al. 2010). In general, higher rates of social anxiety disorder are found in females than in males in the general population (with odds ratios ranging from 1.5 to 2.2)(Fehm et al. 2005), and the gender difference in prevalence is more pronounced in adolescents and young adults (Wittchen et al. 1999).

Gender rates are equivalent or slightly higher for males in clinical samples, and it is thought that gender roles and social expectations play a significant role in explaining the heightened help-seeking behavior in male patients. Prevalence in the United States is higher in American Indians and lower in persons of Asian, Latino, African American, and Afro-Caribbean descent compared with non-Hispanic whites (Lewis-Fernández et al. 2010).

4: Morbidity

SAD is associated with significant disability, impairment and reduced quality of life (Alonso et al., 2004; Kessler, 2003; Mendlowicz & Stein, 2000; Schneier et al., 1994; Stein, Torgrud, & Walker, 2000). Individuals with SAD have been found to be more financially dependent (Schneier, Johnson, Hornig, Liebowitz, & Weissman, 1992), underemployed (Wittchen et al., 2000), less productive at work (Wittchen et al., 2000), and underpaid (Stein et al., 2000), compared to those without the disorder.

In addition, SAD is associated with educational impairment (Schneier et al., 1994), individuals with SAD are more likely to fail a grade or drop out of school (Stein & Kean, 2000) compared to individuals without the disorder. Finally, individuals with SAD have been found to have impairment in close relationships (Davila & Beck, 2002), including romantic relations (Sparrevohn & Rapee, 2009), friendships (Davila & Beck, 2002; Schneier et al., 1994), and family relations (Schneier et al., 1994) compared to individuals without SAD.

Even when compared to other psychiatric disorders, the impairment caused by SAD is very high, with SAD being among the 5 most impairing psychiatric disorders (Alonso et al., 2004). Whereas evidence suggests that SAD is associated with impairment across numerous areas of functioning, certain life domains may be more strongly impaired by SAD than others (Wittchen et al., 2000). Specifically, there is evidence that SAD impairs work, studies, and social life, more than family life (Wittchen et al., 2000). Similar findings have emerged in studies comparing impairment across the anxiety disorders. For instance, SAD is associated with more educational and social life impairment and less family life impairment compared to other disorders (Lochner et al., 2003; Quilty et al., 2003).

In addition, the majority of patients with SAD suffer from comorbid mental disorders, in particular depression, other anxiety disorders, substance abuse, and avoidant personality disorder (Lipsitz and Schneier, 2000; Fehm et al., 2005). Some of these comorbidities are assumed to develop as consequence of SAD (Fehm et al., 2005), and can aggravate the long-term course (Steinert et al., 2013). Moreover, it has been observed that SAD patients often seem to be unaware of interventions for their condition and do not seek treatment until they need help for any of the comorbidities (Lipsitz and Schneier, 2000; Fehm et al., 2005).

Unless an individual with SAD has become completely reclusive, they may be continuously faced with social stimuli on a daily basis, and may be in a chronic state of anxiety for protracted periods of the day, most days. To understand the changes in the neurobiology of individuals with SAD, an overview of the neurobiology of SAD is presented next.

5: A Review of the Neurobiology of SAD

To gain insight with regards to whole brain (including functional and structural aspects) contribution towards SAD neurobiology, and to work towards a functional model of SAD pathogenesis, several authors (Etkin et al., 2007; Brühl at al., 2014; Fox et al., 2014) have proposed models of SAD neurocircuitry. These models are based on findings from functional imaging research in SAD, and suggest that hyperactivation in brain regions known as the "anxiety circuit", are a consistent finding.

New neuroimaging techniques such as resting-state and functional connectivity measures (e.g. Buckner et al., 2013) as well as structural studies have further advanced our knowledge of the neurobiological underpinnings of SAD. Such data has noted increased activations in parietal and medial occipital brain regions. These regions appear decoupled from the ventral attention network, cingulo-opercular and amygdalar/limbic networks (Tomasi and Volkow, 2011; Yeo et al., 2011).

This specific form of decoupling has been noted at the level of structural and functional connectivity involving the uncinate fasciculus and superior longitudinal fasciculi. Parieto-occipital regions have been found to be hyperactive but significantly less structurally and functionally connected in SAD. Such structures include the cuneus, precuneus and the posterior cingulate cortex (PCC). The ventral cuneus and PCC have been noted previously as the most strongly connected regions in the cerebrum (Tomasi and Volkow, 2011), which makes disturbances in this region particularly significant. This functional center of the Default-Mode-Network (DMN), (Greicius et al., 2003; Raichle et al., 2001; Shulman et al., 1997) is involved in self-reference (which is negatively valenced in SAD) and emotion regulation (which is impaired in patients with SAD)(Raichle et al., 2001; Shulman et al., 1997).

Strong whole brain connectivity suggests that this posteromedial region has been associated with transfer of information, multimodal integration, internal

awareness, consciousness and processing of spontaneous thoughts (Tomasi and Volkow, 2011). The PCC/ventral cuneus is suggested to be involved in the Dorsal Attention Network (DAN) (Corbetta and Shulman, 2002). The DAN has previously been associated with working memory, alertness, attention, and externally driven cognition (Tomasi and Volkow, 2011).

The precuneus has been noted to demonstrate strong connections to prefrontal, parietal and thalamic regions (Cavanna and Trimble, 2006) which has been related to higher order cognition involved with integrative functions such as visuospatial imagery, episodic memory retrieval, voluntary shift of attention and self-referential processes (Cavanna and Trimble, 2006). The cuneus in the occipital lobe has been suggested to be involved in more circumscribed functions in visual information integration and processing (Tomasi and Volkow, 2011). Decoupling of these posteromedial regions from other brain networks could result in a preponderance particularly of limbic, ventral attention and cingulo-opercular networks, which provide bottom-up information of relevance, salience, and stimulus-driven attention (Sylvester et al., 2012).

One important functional centre linking the DMN with the fronto-parietal or executive network is located in the anterior aspect of the insula (Dennis et al., 2011; Sridharan et al., 2008). The anterior insula has previously been associated with interoceptive processes and salience (e.g. Craig, 2009; Menon and Uddin, 2010), but also with several other processes (Chang et al., 2013). The insula is often activated together with the amygdala (Kohn et al., 2014a,b; Robinson et al., 2010), particularly during the processing of emotion (Stein et al., 2007a).

In healthy individuals, increased activity in the insula is associated with anxiety (Carlson et al., 2010; Stein et al., 2007b). With an increase in anxiety, the insula becomes recruited by the DMN in healthy individuals (Dennis et al., 2011). The specific correlation between insula and amygdala connectivity with states of anxiety might explain why there is no change seen in this connection in the patients with SAD in the neuroimaging literature. Another explanation might be that only one study placed a seed in the insula (Klumpp et al., 2012). Connectivity between the amygdala, prefrontal and orbitofrontal regions were shown to be decreased in one study in highly anxious healthy subjects (Kim and Whalen, 2009). The pattern of connectivity in SAD in this regard is inconsistent; however there appears to be a tendency towards increased connectivity.

The evidence of disturbance of the usually well-balanced network system in individuals with SAD might reflect alterations in emotional arousal and in perception of potentially threatening or feared stimuli (Cisler and Koster, 2010), with difficulties in activating and applying top-down control and regulation mechanisms in anxiety disorders in general (Beck and Clark, 1997; Cisler and Olatunji, 2012; Sylvester et al., 2012). Current imaging research seems to support the role of parietal and occipital regions in anxiety disorders in addition to prefrontal and limbic circuits. Previous research has had a strong focus on the so-called "fear circuitry" (e.g. LeDoux, 2000; Marek et al., 2013), and there is evidence for the additional role of particularly medial parietal regions in anxiety and anxiety disorders, as is shown in SAD.

A) Fear circuitry:

The fear and anxiety circuit (e.g. Etkin, 2012; LeDoux, 2000; Marek et al., 2013; Paulus and Stein, 2006) is typically comprised of the amygdala, insula, anterior cingulate cortex (ACC) and prefrontal cortex. These particular brain regions appear to be hyperactive in SAD. Within the fear/anxiety circuit, activation of the amygdala is particularly associated with arousal and negative valence (Sergerie et al., 2008), and previous work on fear circuitry has noted a correlation between amygdala volume and trait anxiety (Baur et al., 2012). Hyperactivity of the fusiform gyrus (FFG), which has been implicated in an early SAD meta-analysis by Etkin and Wager (2007), may play a role in SAD. Besides its contribution to facial processing (Weiner and Grill-Spector, 2012), the FFG has also consistently been found hyperactive in response to emotional scenic stimuli in SAD (Sabatinelli et al., 2011). Therefore, hyperactivation of the FFG in patients with SAD may reflect both an increased sensitivity to facial stimuli and a heightened reactivity of the emotional system as a whole in SAD.

Prefrontal regions, which were shown to be hyperactive in SAD, have been consistently associated with emotion regulation functions (recent meta-analyses: Buhle et al., 2014; Diekhof et al., 2011; Kalisch, 2009; Kohn et al., 2014a,b; Ochsner et al., 2012). Parietal regions have received little attention: Amongst several recent meta-analyses, Kalisch found the angular gyrus bilaterally to be involved in reappraisal, but did not specifically address parietal activation (Kalisch, 2009). Diekhof et al. (2011) linked hyperactiviation in temporal and parietal cortices to the voluntary redirection of attention. Kohn et al. (2014a,b) incorporated the superior temporal and angular gyri in their model of cognitive emotional regulation, whereas

Buhle et al. (2014) associated the lateral parietal regions with monitoring and general regulatory functions. Peri-intraparietal sulcal regions are generally involved in top-down attention control or reorienting (e.g. Corbetta et al., 2008; Hutchinson et al., 2009; Langner and Eickhoff, 2012), which supports interpretations given in the field of emotion regulation.

B) Functional Anatomy of Regions of Interest

i. Caudate Nucleus

In their review, Grahn and colleagues (2008) summarize the cognitive functions of the caudate nucleus and notes that it has been implicated in several aspects of executive processes. In particular, critical processes involved in goal-directed behavior appear to consistently activate the caudate nucleus. A central element ofo goal-directed activity is the expectation of an outcome prior to the action. The expectation of particular contingencies after particular actions is integral to the shaping of goal-directed behavior, and there is mounting evidence that suggests that the caudate nucleus plays a role in this process (Grahn et al., 2008).

Tricomi et al., (2004) in a series of studies, clarified to a large extent the importance of reward and punishment in relation to the anticipation of a reward/punishment outcomes, and action-outcome contingencies. In their first experiment, neural response to reward was measured with visual stimuli. Up, down, or sideways arrow were displayed on a screen indicating an increase, decrease, or no change in subjects' monetary compensation level, and subjects in response pressed a button to the specific cue. In their second experiment, the anticipation of an outcome was measured. An anticipatory cue appeared before the arrows, indicating that a reward or punishment arrow would occur three seconds later. The respective reward or punishment arrow appeared at the expected time, and subjects responded with a button press. In the third experiment, the subjects' perception of action-outcome contingency was measured. The anticipatory cue was still present, but consisted of two types of stimuli. The first type was the same as before: it indicated proceeding reward or punishment. The second type required subjects to press their choice of buttons. Subjects were told that the subsequent reward or punishment was contingent upon their choice (though it was not).

These experiments demonstrated that the caudate was consistently active only in the conditions that subjects felt that their response determined the outcome. There

was no caudate activation to the presentation of reward or punishment on its own. Similarly, time linked anticipation of a reward or punishment (which was not contingent upon subjects' responses) did not activate the caudate nucleus. Conversely, when subjects believed that after the anticipatory cue, their choice of button press would determine the reward outcome, the head of the caudate nucleus was activated. The authors also found that the magnitude of caudate activity was correlated with subjective ratings of control over the outcome. The action-outcome requirements for caudate nucleus involvement can be found in other work, even when no decision is made by the subjects (Knutson et al., 2001a,b, 2000). The outcome (obtaining the reward or avoiding punishment) in these studies is determined instead by the subject's response speed in a target detection task. Subjects were aware that the outcome was dependent on the speed of the response, and the task was difficult enough that correct performance was not guaranteed (thus the action is non-trivial). The activity of the caudate can therefore not be attributed to decision-making alone.

Tricomi et al., (2004) suggests that the action-contingency interpretation of caudate nucleus function may reconcile differences in caudate activity that has been observed in prior studies: studies in which subjects' decisions or reaction time determine the outcome generally find activity in the caudate (Delgado et al., 2000, 2004; Elliott et al., 2000; Knutson et al., 2001a,b, 2000). When responses do not determine the outcome (or only non-effortful responses are necessary) the caudate does not activate in response (Berns et al., 2001; Breiter et al., 2001; Elliott et al., 2003; McClure et al., 2003; O'Doherty et al., 2006; O'Doherty et al., 2003; Seymour et al., 2004). It seems that the caudate nucleus is sensitive to reinforcement of action, rather than to rewards in and of themselves.

It has also been noted that it does not appear to matter whether the rewards that reinforce the action are extrinsic or intrinsic, or whether they are merely imagined and not forthcoming. In a follow-up study of perceptual category learning (Tricomi et al., 2006), Japanese subjects for whom the English phonemes [r] and [l] are indistinct performed an identification task of the words ''road'' and ''load''. This task appears to induce learning, however only when there is performance feedback (McCandliss et al., 2002). Each subject performed alternating trials of training with and without feedback, followed by performance of a card-guessing task with monetary reward and punishment outcomes.

This allowed comparison of activity patterns elicited by an intrinsic reward (learning to distinguish two phonemes) and extrinsic reward (earning money). The feedback processing during the perceptual phoneme task demonstrated activation of the caudate nucleus bilaterally, as well as reward processing during the card- guessing task. Due to the within-subjects design, the authors could determine that the time course of activity in the caudate nucleus during the feedback processing was similar in both tasks. The caudate nucleus activity was better sustained in correct trials during perceptual learning, and monetary reward during the card guessing. It appears that, in motivated subjects, performance feedback was as rewarding as monetary gain, and the caudate seems to be sensitive to outcomes with either intrinsic or extrinsic value.

In a different study looking at food choices in hungry control subjects, caudate activity was noted when subjects were choosing preferred foods from a menu, even though they never received the actual tastes, but merely generated an expectation of what the foods would be like (Arana et al., 2003). The these studies suggest that the caudate is involved in a variety of executive, goal-directed behaviors, particularly where the outcome is perceived as desirable by the individual.

The activity of the caudate nucleus in goal-directed behavior can be observed in actions that occur in a social context (see Montague et al., 2006, for a review). For example, one study (King-Casas et al., 2005) used a 'trust' paradigm, in which pairs of players engaged in several rounds of monetary exchanges. On each round, one player (the investor) was endowed with a certain amount of money. The investor could keep the money, or invest it with the other player (the trustee). If invested, the amount was tripled, and the trustee then decided what fraction to send back to the investor. The authors used two MR scanners to measure neural activity in both players simultaneously (Montague et al., 2002). The results demonstrated that the caudate nucleus was the only structure with an increased response to benevolent reciprocity as opposed to malevolent reciprocity.

Correspondingly, increases in benevolent reciprocity, or trust, had a greater a effect on the behavior of the other person as opposed to decreases in trust. That is, increases in trust by the trustee correlated positively with changes in investment by the investor, whereas decreases did not show a behavioral correlate. A decrease in trust therefore has no predictive information for future behavior, and the caudate nucleus is not activated. An increase in trust does however change behavior, causing the investor to evaluate how much more to give next time. This condition also

involves an increase in the expectation that a subject has of the positive nature of their contingent interactions with the trustee. The caudate nucleus is again implicated in the evaluation of the action-outcome contingencies underlying goal-directed behavior in order to obtain a reward.

The role of the caudate nucleus in the complex series of interactions between social influences and reward which was further elaborated by two recent studies that examined modulation of caudate nucleus activity by perceptions of moral character, and altruistic punishment. In the first study, participants played an economic trust game with opponents portrayed as having praiseworthy, neutral, or suspect moral character. The perceived moral character influenced caudate nucleus activity during economic feedback. When participants had an expectation about their partner's moral character, the caudate nucleus response appeared diminished, as was the reliance on feedback of monetary outcome. The authors suggest that moral beliefs affect economic decision-making through modulations in the caudate nucleus.

These various modulations subsequently appear to influence the adjustment of choices based on trial-and-error feedback. A typical response to violations of trust is to punish the offender. In a study of altruistic punishment, participants could punish opponents (monetarily) who violated trust in an economic exchange game. The authors found that the caudate nucleus was activated when participants were able to punish opponents, and participants with the most profound activations in the caudate were willing to incur the greatest costs in order to punish. This finding can be interpreted as showing that higher punishment induces stronger satisfaction, resulting in greater caudate activation, or conversely, as indicating that higher caudate activation reflects a greater expected satisfaction from punishment, which then results in greater investments in punishment. The latter interpretation is consistent with goal-directed behavior resulting in actions that are motivated by anticipated rewards. As mentioned earlier, the anticipated reward need not be monetary, but can be as abstract as the satisfaction derived from punishment of trust violations.

Several imaging studies have implicated the caudate in set-shifting behavior such as work on the Wisconsin Card Sorting Task (Berg, 1948; Milner, 1963; Stewart et al., 2001). While at face value a task such as the WCST may not appear to involve goal-directed actions relative to other executive functions and behavioral processes, as the patient studies described above demonstrate, there is a clear conceptual similarity between making volitional shifts in behavioral strategy and choosing optimal goal-

directed actions. As such, ‘‘shifting’’ taps into the process by which actions are chosen based on the expectations of their consequences.

However, in neuroimaging, it is important to disentangle brain activity due to simple execution of the shift from brain activity due to the cognitive decision to shift. Monchi et al., (2006) did this in a functional imaging study using a similar card-sorting task to the WCST. Several conditions were included so that activity related to retrieving the sorting rule (the cue that indicated by what rule the cards should be sorted); the execution of a shift (done by including a ‘continuous shift’ condition, in which subjects shifted on every trial, and therefore no decision about whether or not to shift had to be made); and the cognitive decision to subsequently execute a shift. The results showed that the caudate nucleus is not activated by the simple execution of the shift, but rather the cognitive decision to shift. During blocks when subjects were continuously shifting, and no evaluation or decision to shift was required, just a new response, the caudate was not activated. However, when evaluation and a decision to change set are required, the caudate was activated.

These studies demonstrate how the caudate nucleus is in a central position to assist goal-directed learning, as this structure is sensitive to action contingencies and evaluation of subsequent outcomes. The data from neuroimaging studies propose that the following properties appear necessary to activate the caudate nucleus: some form of goal-directed action, with a perception that the outcome is contingent upon behavior; the knowledge of the outcome, or feedback; and incentive, which can be either extrinsically or intrinsically valuable, and can occur in individual and social contexts. In short, the caudate nucleus is ideally poised to guide behavior based on response-dependent feedback to obtain an outcome that is valued by the subject.

Considering the role of caudate nucleus in action contingencies and the evaluation of subsequent outcomes, it is possible that the preconceived negative evaluation by others in social situations seen in SAD has to do with aberrant caudate circuitry. The normal response-dependent feedback mediated by the caudate is somehow negatively biased in SAD, resulting in the phobic preconceived response to social stimuli.

ii. Nucleus Accumbens

The nucleus accumbens is thought to facilitate goal-directed behaviors by integrating information related to limbic drive and motor planning (Grace et al., 2000). The exact process by which the nucleus accumbens achieves this function is not yet clear, given that studies have revealed that the nucleus accumbens is involved in multiple distinct aspects of behavior such as “liking” and “wanting”. Some stimuli are ‘liked’ and produce pleasure and positive affect, and some are ‘disliked’. Some stimuli are ‘wanted’ and produce incentive motivation, yet others are avoided.

Usually we ‘want’ the stimuli that we ‘like’ and avoid the ones we don't ‘like’. But ‘liking’ and ‘wanting’ do not always go together and can contribute in different ways to behavior. Both ‘liking’ and ‘wanting’ have dissociable neural substrates in the nucleus accumbens (Peciña et al., 2008) and lesions in the nucleus accumbens are known to cause disruptions to an array of cognitive and affective processes, including operant and emotional learning, response inhibition and behavioral flexibility (Cassaday et al., 2005; Cardinal et al., 2001; Reading et al., 1991).

Electrophysiological studies in animals that are awake also support a role for the nucleus accumbens in these multiple functions (Lansink et al., 2008; Ishikawa et al., 2008). Such a diverse array of functional involvements might derive from the integration of inputs from multiple brain regions within the distinct subdivisions that comprise the nucleus accumbens. Therefore, the balance of drives from limbic, thalamic and cortical inputs might determine how the output guides behaviors with respect to specific aspects of cognitive and affective functions.

Such input interaction could be the basis of ensemble information processing (Buzsaki et al., 2004) in the nucleus accumbens. Indeed, electrophysiological recordings from multiple neurons simultaneously in behaving animals has shown correlated spike firing in sets of neurons of the nucleus accumbens (Lansink et al., 2008) that might reflect such ensemble-related activity. Considering the nucleus accumbens’ role in wanting and liking, it is possible that accumbens circuitry is involved in facilitating the avoidance seen in SAD, by “not liking” social situations and facilitating avoidance by not investing pleasure in social situations.

iii. Putamen

Functionally, the putamen is not easily differentiated from the caudate nucleus. These two structures are consequently considered as a functional unit, referred to in the

literature as the corpus striatum, since they are cytoarchitectonically and histochemically very similar. The functional neuroanatomy of the putamen is therefore difficult to isolate from that of the rest of the corpus striatum. The putamen is involved in a diverse array of functions and in the scope of the functional neuroanatomy of the basal ganglia, is seen as a "generalist" of sorts, not having any specialized role. However, considering the myriad of interconnections the putamen shares with other adjacent and distant brain structures, its functions can be classified as mainly motoric (De Long et al., 1990; Alexander et al., 1990) as well as having a role in reinforcement and implicit learning (Packard et al., 2002; Yamada et al., 2004). Both reinforcement and implicit learning play a significant role in the integration and processing of aversive stimuli, and may therefore have an important role to play in SAD pathogenesis.

iv. Globus Pallidus

The globus pallidus (GP) is involved in the extrapyramidal motor system and participates in the regulation of voluntary movement. The GP forms an integral part of the intrinsic and output nuclei of the basal ganglia. Striatal efferents collect into numerous bundles of myelinated fibers that converge topographically on the globus pallidus. Most of them are striopallidal fibers; some terminate in the internal segment of the globus pallidus, others in the external segment. Still others pass through the globus pallidus and reach both parts of the substantia nigra.

The two segments of the globus pallidus have similar inputs but distinctly different sets of outputs. The globus pallidus external segment (GPe) receives inhibitory inputs from the striatum and excitatory inputs from the subthalamic nucleus. It then distributes widespread inhibitory (GABA) outputs to most other parts of the basal ganglia. The functional map in the striatum continues into GPe, with different sectors dominated by inputs from the putamen, caudate nucleus, and ventral striatum. The functional significance of these diffusely projecting inhibitory connections is still unknown, but inactivating specific subareas of GPe can mimic the movement, cognitive, and behavioral disturbances characteristic of different basal ganglia disorders.

The globus pallidus internal segment (Gpi) and the substantia nigra pars reticulata (SNr), like the GPe, receive inhibitory inputs from the striatum and excitatory inputs from the subthalamic nucleus. They also receive inputs from GPe, however, and their efferents are separate and distinct from those of GPe. The internal pallidal segment projects mainly to the thalamus - an unusual example of seemingly specific inputs that use GABA - through two collections of fibers. One collection, the lenticular fasciculus , runs directly through the internal capsule and then passes medially as a sheet of fibers between the subthalamic nucleus and the zona incerta. At the medial edge of the zona incerta, the lenticular fasciculus makes a hairpin turn in a lateral and dorsal direction and enters the thalamus.

The second collection loops around the medial edge of the internal capsule as the ansa lenticularis, it joins the lenticular fasciculus and GABAergic fibers from SNr in the thalamic fasciculus, which then enters the thalamus. The thalamic fasciculus terminates in a variety of thalamic nuclei. Fibers related to movement control end in the ventral anterior nucleus of the thalamus (VA) and the ventral lateral nucleus of the thalamus (VL), those related to the caudate nucleus and prefrontal cortex end in the dorsomedial nucleus and in part of VA, and others end in the centromedian and parafascicular nuclei. VA/VL and the dorsomedial nucleus then project to frontal and other cortical areas, thus completing the principal circuit through the basal ganglia.
Most of these efferents from GPi-SNr to the thalamus also have a branch that descends to an area of the midbrain reticular formation adjacent to the decussation of the superior cerebellar peduncles (the pedunculopontine nucleus). Finally, a smaller number of GPi-SNr efferents reach the superior colliculus and the habenula. Those to the superior colliculus play a role in the control of eye movements; the function of the connections with the habenula is unknown.

The role that the globus pallidi play in essentially forming the principle output pathway for the basal ganglia as a whole is important to consider in the context of SAD, as fear circuitry, as well as other limbic circuits, are intimately interconnected with basal ganglia projections.

v. Amygdala

The amygdala influences a broad range of physiological and behavioral responses associated with emotion and is anatomically connected with several brain regions including the thalamus, anterior temporal lobes, prefrontal cortex (PFC), anterior

cingulate cortex (ACC), and ventral striatum (Aggleton et al., 1980). Functional magnetic resonance imaging (fMRI) studies of healthy adults have further shown that the amygdala, particularly the left amygdala, is responsive to negative emotional stimuli, with a preference for faces depicting negative emotional expressions (Sergerie et al., 2008).

During higher-order cognitive evaluation of these stimuli, such as when emotions are consciously suppressed (Ochsner et al., 2002; Beer et al., 2006; Urry et al., 2006; Delgado et al., 2008) or when labeling negative emotional facial expressions (Hariri et al., 2000, 2003; Lieberman et al., 2007; Foland et al., 2008), the ventral PFC also becomes active and correlations, typically negative, are observed between activation in these two regions (Hariri et al., 2000, 2003; Ochsner et al., 2004; Urry et al., 2006; Lieberman et al., 2007; Foland et al., 2008). It has been posited that this inverse relationship reflects a neural network whereby ventral PFC suppresses activation in the amygdala (Urry et al., 2006; Lieberman et al., 2007), thereby helping to potentially alleviate emotional distress (Ochsner et al., 2004; Urry et al., 2006; Berkman and Lieberman, 2009).

Amaral conceived the amygdala as a “protection device ... designed to detect and avoid danger” (Amaral et al., 2002). In a large meta-analysis conducted by Costafreda et al., (2008) reviewing 385 PETand fMRI studies, findings are consistent with an extension of this view towards a more general role of emotional evaluation of incoming stimuli, whereby meaning is attached to behaviorally relevant stimuli.
Negative stimuli may be privileged, perhaps due to their often direct survival value, but positive ones also generate amygdala activation. In accordance with this relevance detection role, they also found that external stimuli are prioritized over internally generated ones.

This detection function may also be facilitated by passive perception, and inhibited either by voluntary sup- pression or by co-occurring higher-level activity such as lan- guage. They found evidence of hemispheric specialisation, where the right amygdala may subserve a high-speed detection role for unconscious stimuli, while the left amygdala may be preferentially recruited when evaluation of language-related stimuli is required.

As noted previously by several authors (Etkin and Wager, 2007; Freitas-Ferrari et al., 2010) the amygdala and its connections play a key role in the attribution of emotional salience to stimuli and in the top-down modulation of associative,

attentional, and interpretative processes (de Carvalho et al., 2009). The abnormal functioning of this circuitry in SAD, resulting in impaired communication with prefrontal areas responsible for inhibitory responses, may lead to increased amygdala responsivity and a consequent sustained threat-related processing bias in SAD (Freitas-Ferrari et al., 2010)

vi. Hippocampus

The activation of the hippocampus involves a trisynaptic unidirectional circuit which originates in the entorhinal cortex (Donkelaar et al., 2011). The entorhinal cortex receives inputs from cortical association areas, subcortical structures, brain stem nuclei and other limbic structures, and projects to dentate granule cells via the perforant path. The next station of the circuit is a connection between the dentate granule cells and CA3 pyramidal cells via the mossy fibres. The CA3 pyramidal cells are in turn in synaptic contact via the Schaffer collaterals with CA1 pyramidal cells, which finally send their axons to the alveus and fimbria (Amaral et al., 1990). Glutamate is a key neurotransmitter at these three excitatory synapses.

The trisynaptic circuits seem to be organized in functional, thin parallel sections or lamellae, which are oriented perpendicular to the long axis of the hippocampus (Andersen et al., 1971, 2000). The mossy fibre projection from the dentate granule cells to the CA3 pyramidal cells has a strictly lamellar distribution (Blackstad 1956). Extensive longitudinal association pathways have been demonstrated between the horizontal sections (Amaral and Witter 1989; Kondo et al., 2008), although the GABAergic lateral inhibition from basket cells keeps these transverse hippocampal lamellae functionally separated (Sloviter 1994; Sloviter and Brisman 1995).

Numerous local hippocampal circuits regulate and inhibit the main excitatory trisynaptic circuit. One of these is formed by the basket cells, i.e. GABAergic interneurons found in the stratum oriens of the hippocampus proper and in the molecular and polymorph layers of the dentate gyrus (Lorente de Nó 1934; Amaral and Insausti 1990; Freund and Buzsaki 1996). In studies of human amnesia and of animal models in rodents and monkeys, the anatomical components of the neural system for memory have been identified in the medial temporal lobe (Markowitsch et al., 1985; Squire 1987; Squire et al., 1991). This system consists of the hippocampus and adjacent closely related cortices, including the entorhinal, perirhinal and

parahippocampal cortices. These structures, most likely by virtue of their widespread and reciprocal connections with neocortical structures, are essential for declarative memory. The medial temporal lobe memory system is needed to bind together the distributed storage sites in the neocortex that represent a whole memory.

The role of this system is only temporary: as time passes after learning, memory stored in the neocortex gradually becomes independent of medial temporal lobe structures (Squire 1987; Squire et al., 1991; Squire et al., 2007). The posterior parietal cortex is often activated during memory retrieval (Cabeza et al., 2008). Hyperactivation of limbic circuitry including the hippocampus may mediate the symptoms of SAD (Hattingh et al., 2013) by influencing behavioural inhibition, anxious temperament, and dispositional anxiety (Fox et al., 2014) which in turn may play a role in the avoidant behaviour seen in SAD.

C) Cortical Thickness:

The most consistent finding across brain imaging studies is that of increased activity in limbic and paralimbic regions in SAD (Freitas-Ferrari et al., 2010). While there are some studies addressing structural-anatomical brain changes in SAD, the results of these studies are mainly mixed. Cortical thickness and volume reports are not very consistent. Syal et al., (2012) reported bilateral decreased thinning in the fusiform and post central cortices, as well as right lateralized thinning in the rostral PFC, DLPFC, OFC, primary motor cortex, pre- and paracentral region, the temporal pole, inferior temporal cortex and the insular cortex. These regions are typically involved in social and emotional processing which suggests that thinning and the consequent loss in structural integrity might contribute to aberrant social and emotional processing in people with SAD.

Frick et al., (2013) reported increased cortical thickness in the left fusiform and lingual gyri. Both these areas are involved in the processing of emotional faces suggesting that dysfunction of this region may contribute to aberrant processing of socially valenced stimuli. Brühl et al (2014) found increased cortical thickness in the right temporal pole, ACC, DLPFC, parietal cortex and the left anterior insula. From a general functional perspective, these brain region fit into models of hyperactive neural circuits involved in the processing of emotional stimuli (temporal pole, anterior insula) and of frontoparietal networks particularly associated with executive, emotion regulating and attentional functions (DLPFC, ACC, parietal lobe) [e.g. Etkin et al.,

2009; Ochsner et al., 2012]. Increased thickness in the DLPFC and the superior parietal cortex in SAD are in line with models of disturbed, overactive and dysregulated attentional networks in anxiety disorders (Sylvester et al., 2012).

D) White Matter:

Global white matter volume did not differ in SAD from healthy controls in four studies, and only one study reported reduced global white matter (Baur et al., 2013a). However, one study reported globally reduced fractional anisotropy (FA), (Baur et al., 2013a). Significant FA changes were detected in the left uncinate fasciculus in three studies (Baur et al., 2013a; Qiu et al., 2014), with one study finding no difference in the left, but reduced FA in the right uncinate fasciculus (Phan et al., 2009). In the superior fasciculus, apparent diffusion coefficient (ADC) was reduced bilaterally in one study, which also reported reduced FA on the left side (Qiu et al., 2014), which is paralleled by another study (Baur et al., 2011). However, two studies found no difference in at least one side of the superior fasciculus (Baur et al., 2011; Phan et al., 2009) No changes in FA were reported for the inferior fronto-occipital fasciculus in two studies (Baur et al., 2013a; Phan et al., 2009), while one study showed reduced ADC (Qiu et al., 2014). There is no evidence for increased FA in white matter in most of the existing studies (Phan et al., 2009; Baur et al., 2013a; Qiu et al., 2014) except for increased FA and fibre density in one study (Liao et al., 2011).

E) Manual Tracing:

To date there has been only a single study utilizing manual methods of segmentation of subcortical volumes in SAD. Machado-de-Sousa et al., (2014) defined the hippocampus and amygdala as a priori regions of interest and used a manual tracing protocol described by Schummanet al., (2004). They found that bilateral amygdala and left hippocampus were enlarged in socially anxious individuals relative to controls. The volume of the right hippocampus was enlarged in sub-threshold social anxiety participants relative to controls.

No differences were found across groups in respect to total brain volume. Potential limitations to this study's approach include the fact that the protocol they used to manually segment these structures (Schumman et al. 2004) is quite out dated, considering advances in gradient and receiver coil technology and magnetic field strength, which has significantly increased imaging resolution and anatomical detail.

Another potential limitation is that the study population was small (n=11). The role of the other striatal structures and prominent subcortical gray matter structures in SAD pathogenesis are thus still not fully understood and as of yet, no detailed protocol exists which provides a comprehensive guide on how to identify the subcortical gray matter structures on MRI, how to separate them from one another considering their close proximity, and how to define their borders so that they may be traced and their volumes calculated.

6: Specific Aims

Extensive investigations utilizing functional neuroimaging techniques in SAD have advanced our understanding of SAD neurobiology significantly. Functional techniques however have limitations such as relatively low spatial resolution, dependence on automated data processing, and the fact that many of them are driven by a specific functional paradigm. Structural neuroimaging techniques are able to investigate the structural foundations of key brain regions, and when used in conjunction with one another on the same data set, these techniques such as manual tracing of subcortical gray matter volumes, cortical thickness analyses and white matter tractography can provide an integrated perspective of how the overall structure of the brain is altered in SAD.

In an attempt to answer the question regarding alterations in neuroanatomical structures in SAD, a manual tracing protocol (Chapter II) was developed to expertly segment, by hand, the major macroscopically visible subcortical gray matter structures in the human brain. This segmentation technique was then utilized to extract the volumes (Chapter III) of key structures implicated in the SAD neuroimaging literature. Cortical thickness analyses (Chapter IV) and white matter tractography (Chapter V) were utilized to complement and contextualize the manually segmented volumetric data, so that an integrated, overall perspective of SAD structural neurobiology (Chapter VI) can be achieved. The methodology of each technique is fully described in detail in each chapter.

Summary:

The neurobiological contributions to the pathogenesis of SAD are complex. A large body of functional neuroimaging work describes the functional neurobiological aspects of SAD, however the structural neuroimaging literature investigating the regions that underly these functional abnormalities is still relatively small. One previous study utilized manual segmentation to evaluate how the subcortical gray matter in SAD is altered. This study found increased volume in bilateral amygdalae, and in the left hippocampus. Limitations to this study include the relatively small sample size (n=12) and use of an older scanner. Advances in scanner quality in the last ten yearshave significantly improved the resolution of images and consequent visible anatomical detail.

This thesis will aim to overcome these limitations by including a larger sample size (n=18), and a clinical population that is as free from potential confounding factors such as psychiatric and medical co-morbidity and previous interventions. Additionally, the image acquisition will be done at high field strength (3T) with imaging parameters that maximize tissue contrast. Additionally, a highly detailed manual segmentation protocol will be developed to help the investigator reliably identify, and accurately trace the most prominent subcortical gray matter structures so that their volumes may be calculated. Previous segmentation protocols have not included all of the diencephalic and associated subcortical structures in a single approach.

White matter integrity has previously been investigated in five studies. All of them found decreased FA in a diversity of brain regions (discussed in detail above). However a potential limitation across all of these studies is the quality of the clinical sample. None of the previous studies utilizing DTI in SAD reported on a clinical sample that was free from psychiatric co-morbidity and that was also treatment naïve.

Three previous studies have investigated alterations in cortical thickness in SAD and the results were heterogenous regarding regional specificity and the quality of the observed changes: two studies demonstrated increased cortical thickness and one demonstrated reduced cortical thickness (discussed in detail above). Again, none of these studies reported that their clinical samples were treatment naïve and were free of any psychiatric comorbidity.

These factors may serve as potential important confounders on the data. Structural measures are extremely sensitive and can detect sub-millimeter changes in thickness in cortical thickness analyses, and in fractional changes in diffusivity in DTI measures. Structural measures have been previously reported to be sensitive to pharmacological intervention (Hafeman et al., 2012). Additionally, when co-morbidity is present, it might be unclear whether the observed changes are associated with SAD, or whether the co-morbidity is exerting a stronger influence on the neurobiology. To overcome these potential limitations, as previously stated, our sample population was free of any psychiatric comorbidity, and was psychopharmacologically and psychotherapeutically treatment naïve.

Overall, this thesis takes an integrated approach to the structural neurobiology of SAD. Differences in subcortical gray matter in SAD, are viewed in the context of changes in cortical thickness and white matter ultrastructure. This integrated approach will provide an overview of how brain architecture is altered in SAD, and with the manual tracing protocol, sets the ground for further manual investigations into brain structure.

Table: 1

Structural studies in SAD utilizing cortical thickness analyses, diffusion tensor imaging or manual tracing.

Study	SAD N (M/F)	Mean Age (SD)	HC N (M/F)	Mean Age (SD)	Approach
Syal et al., 2012	13 (8/5)	35.3 (11.8)	13 (8/5)	33.6 (11.2)	Cortical thickness
Frick et al., 2013	14 (14/0)	32.6 (8.7)	12(12/0)	27.9 (7.9)	Cortical thickness
Brühl et al., 2014	46 (29/17)	33.13 (10.61)	46 (29/17)	32.96 (8.87)	Cortical thickness
Phan et al., 2009	30(15/15)	27.20 (7.80)	30(10/20)	29.90 (8.13)	Diffusion tensor imaging
Bauer et al., 2011	25 (18/7)	32 (10.4)	25 (18/7)	23 (10.1)	Diffusion tensor imaging
Liao et al., 2011	18 (12/6)	22.67 (3.77)	18 (13/5)	21.89 (3.69)	Diffusion tensor imaging
Bauer et al., 2013	25 (18/7)	31.6 (10.4)	25 (18/7)	32.3 (10.1)	Diffusion tensor imaging
Qiu et al., 2014	18 (12/6)	22.72 (3.85)	18 (12/6)	21.78 (3.90)	Diffusion tensor imaging
Machado-de-Sousa et al., 2014	12 (7/5)	20.17	14 (11/13)	19.79	Manual tracing

Table: 2

Main findings of the studies listed in Table 1, and the structures implicated.

Study	Main findings and structures implicated
Syal et al., 2012	↓ **thickness**: **BT** fusiform & post central crtx; **R** rostral PFC, DLPFC, OFC, 1° motor crtx, pre & paracentral regions, temporal pole, inferior temporal crtx, insular crtx
Frick et al., 2013	↑ **thickness: L** fusiform & lingual gyri
Brühl et al., 2014	↑ **thickness: R** temporal pole, ACC, DLPFC, parietal crtx; **L** anterior insula
Phan et al., 2009	↓ **FA: R** uncinate fasciculus near the OFC
Bauer et al., 2011	↓ **FA: L** uncinate fasciculus, superior longitudinal fasciculus
Liao et al., 2011	↓ **FA: R** arcuate fasciculus; ↑ **FA: L** fronto-occipital fasciculus; ↑ **FA:** Genu of the CC
Bauer et al., 2013	↓ **Vol: L** uncinate fasciculus; ↓ **Mean fibre length: L** uncinate fasciculus
Qiu et al., 2014	↓ **FA: L**: insula, inferior frontal gyrus, middle temporal gyrus, & inferior parietal gyrus ↑ **ADC: BT** inferior frontal gyrus, middle temporal gyrus; **L** inferior parietal gyrus, & insula
Machado-de-Sousa et al., 2014	↑ **Vol: BT** amygdala; **L** hippocampus

↓ denotes decreased; ↑ denotes increased

crtx: cortex; L: left; R: right; BT: bilateral; 1°: primary; FA: fractional anisotropy; Vol: volume; ADC: apparent diffusion coefficient; PFC: prefrontal cortex; DLPFC: dorsolateral prefrontal cortex; OFC: orbitofrontal cortex; ACC: anterior cingulate cortex

References:

1. Alonso, J., Angermeyer, M. C., Bernert, S., Bruffaerts, R., Brugha, T. S., Bryson, H., et al. (2004). Disability and quality of life impact of mental disorders in Europe: results from the European Study of the Epidemiology of Men- tal Disorders (ESEMeD) project. Acta Psychiatrica Scandinavica, 109, 38–46.
2. American Psychiatric Association, 2013. Diagnostic and Statistical Manual of Mental Disorders, Fifth Edition (DSM-5). American Psychiatric Association, Washington, DC.
3. Baur, V., Bruhl, A.B., Herwig, U., Eberle, T., Rufer, M., Delsignore, A., Jancke, L., Hanggi, J., 2013a. Evidence of frontotemporal structural hypoconnectivity in social anx- iety disorder: a quantitative fiber tractography study. Hum. Brain Mapp. 34, 437–446.
4. Baur, V., Hänggi, J., Rufer, M., Delsignore, A., Jäncke, L., Herwig, U., Bruhl, A.B., 2011. White matter alterations in social anxiety disorder. J. Psychiatry Res. 45, 1366–1372.
5. Baxter, A.J., Scott, K.M., Vos, T., Whiteford, H.A., 2013. Global prevalence of anxiety disorders: a systematic review and meta-regression. Psychol. Med. 43, 897–910.
6. Beck, A.T., Clark, D.A., 1997. An information processing model of anxiety: automatic and strategic processes. Behav. Res. Ther. 35, 49–58.
7. Bruhl, A.B., Hanggi, J., Baur, V., Rufer, M., Delsignore, A., Weidt, S., Jancke, L., Her- wig, U., 2014. Increased cortical thickness in a frontoparietal network in social anxiety disorder. Hum. Brain Mapp. 35, 2966–2977.
8. Buckner, R.L., Krienen, F.M., Yeo, B.T.T., 2013. Opportunities and limitations of intrin- sic functional connectivity MRI. Nat. Neurosci. 16, 832–837.
9. Buhle, J.T., Silvers, J.A., Wager, T.D., Lopez, R., Onyemekwu, C., Kober, H., Weber, J., Ochsner, K.N., 2014. Cognitive reappraisal of emotion: a meta-analysis of human neuroimaging studies. Cereb. Cortex, in press.

10. Carlson, J.M., Greenberg, T., Rubin, D., Mujica-Parodi, L.R., 2010. Feeling anxious: anticipatory amygdalo-insular response predicts the feeling of anxious antici- pation. Soc. Cogn. Affect. Neurosci.
11. Cavanna, A.E., Trimble, M.R., 2006. The precuneus: a review of its functional anatomy and behavioural correlates. Brain 129, 564–583.
12. Chang, L.J., Yarkoni, T., Khaw, M.W., Sanfey, A.G., 2013. Decoding the role of the insula in human cognition: functional parcellation and large-scale reverse inference. Cereb. Cortex 23, 739–749.
13. Cisler, J.M., Koster, E.H.W., 2010. Mechanisms of attentional biases towards threat in anxiety disorders: an integrative review. Clin. Psychol. Rev. 30, 203–216.
14. Cisler, J.M., Olatunji, B.O., 2012. Emotion regulation and anxiety disorders. Curr. Psychiatry Rep. 14, 182–187.
15. Corbetta, M., Patel, G., Shulman, G.L., 2008. The reorienting system of the human brain: from environment to theory of mind. Neuron 58, 306–324.
16. Corbetta, M., Shulman, G.L., 2002. Control of goal-directed and stimulus-driven attention in the brain. Nat. Rev. Neurosci. 3, 201–215.
17. Costello EJ, Mustillo S, Erkanli A, et al: Prevalence and development of psychiatric disorders in childhood and adolescence. Arch Gen Psychiatry 60(8):837–844, 2003
18. Costello EJ, Mustillo S, Erkanli A, et al: Prevalence and development of psychiatric disorders in childhood and adolescence. Arch Gen Psychiatry 60(8):837–844, 2003
19. Craig, A.D., 2009. How do you feel—now? The anterior insula and human awareness. Nat. Rev. Neurosci. 10, 59–70.
20. Davila, J., & Beck, J. G. (2002). Is social anxiety associated with impairment in close relationships? A preliminary investigation. Behavior Therapy, 33, 427–446.
21. de Wit, S.J., Alonso, P., Schweren, L., Mataix-Cols, D., Lochner, C., Menchon, J.M., Stein, D.J., Fouche, J.P., Soriano-Mas, C., Sato, J.R., Hoexter, M.Q., Denys, D., Nakamae, T., Nishida, S., Kwon, J.S., Jang, J.H., Busatto, G.F., Cardoner, N., Cath, D.C., Fukui, K., Jung, W.H., Kim, S.N., Miguel, E.C., Narumoto, J., Phillips, M.L., Pujol, J., Remijnse, P.L., Sakai, Y., Shin, N.Y., Yamada, K., Veltman, D.J., van den Heuvel, O.A., 2014. Multicenter

voxel-based morphometry mega-analysis of structural brain scans in obsessive–compulsive disorder. Am. J. Psychiatry 171, 340–349.

22. Dennis, E.L., Gotlib, I.H., Thompson, P.M., Thomason, M.E., 2011. Anxiety modulates insula recruitment in resting-state functional magnetic resonance imaging in youth and adults. Brain Connect. 1, 245–254.
23. Dewey, J., Hana, G., Russell, T., Price, J., McCaffrey, D., Harezlak, J., et al. (2010). Reliability and validity of MRI-based automated volumetry software relative to auto-assisted manual measurement of subcortical structures in HIV-infected patients from a multisite study. NeuroImage, 51(4), 1334–1344. doi:10.1016/j.neuroimage.2010.03.033
24. Diekhof, E.K., Geier, K., Falkai, P., Gruber, O., 2011. Fear is only as deep as the mind allows: a coordinate-based meta-analysis of neuroimaging studies on the regu- lation of negative affect. NeuroImage 58, 275–285.
25. Etkin, A., 2012. Neurobiology of anxiety disorders: from neural circuits to novel solutions? Depress. Anxiety 29, 355–358.
26. Etkin, A., Wager, T.D., 2007. Functional neuroimaging of anxiety: a meta-analysis of 1105 emotional processing in PTSD, social anxiety disorder, and specific phobia. Am. 1106 J. Psychiatry 164, 1476–1488.
27. Fehm L, Pelissolo A, Furmark T, Wittchen HU: Size and burden of social phobia in Europe. Eur Neuropsychopharmacol 15(4):453–462, 2005
28. Fehm L, Pelissolo A, Furmark T, Wittchen HU: Size and burden of social phobia in Europe. Eur Neuropsychopharmacol 15(4):453–462, 2005
29. Fehm, L., Pelissolo, A., Furmark, T., Wittchen, H.U., 2005. Size and burden of social phobia in Europe. Eur. Neuropsychopharmacol.: J. Eur. Coll. Neuropsychophar- macol. 15, 453–462.
30. Freitas-Ferrari, M. C., Hallak, J. E. C., Trzesniak, C., Filho, A. S., Machado-de-Sousa, J. P., Chagas, M. H. N., et al. (2010). Neuroimaging in social anxiety disorder: a sys- tematic review of the literature. Prog. Neuropsychopharmacol. Biol. Psychiatry 34, 565–580.
31. Goldin, P.R., McRae, K., Ramel, W., Gross, J.J., 2008. The neural bases of emotion 1173 regulation: reappraisal and suppression of negative emotion. Biol. Psychiatry 1174 63, 577–586.

32. Grahn, J. A., Parkinson, J. A., & Owen, A. M. (2008). The cognitive functions of the caudate nucleus. *Progress in Neurobiology*, *86*(3), 141–155. doi:10.1016/j.pneurobio.2008.09.004
33. Greicius, M.D., Krasnow, B., Reiss, A.L., Menon, V., 2003. Functional connectivity in 1176 the resting brain: a network analysis of the default mode hypothesis. Proc. Natl. 1177 Acad. Sci. 100, 253–258.
34. Hayes, J.P., Hayes, S.M., Mikedis, A.M., 2012. Quantitative meta-analysis of neural activity in posttraumatic stress disorder. Biol. Mood Anxiety Disord. 2, 9.
35. Herman, A. A., Stein, D. J., SEEDAT, S., & Heeringa, S. G. (2009). The South African Stress and Health (SASH) study: 12-month and lifetime prevalence of common mental disorders. SAMJ
36. Hutchinson, J.B., Uncapher, M.R., Wagner, A.D., 2009. Posterior parietal cortex and episodic retrieval: convergent and divergent effects of attention and memory. Learn. Mem. 16, 343–356.
37. Ipser, J.C., Singh, L., Stein, D.J., 2013. Meta-analysis of functional brain imaging in specific phobia. Psychiatry Clin. Neurosci. 67, 311–322.
38. Kalisch, R., 2009. The functional neuroanatomy of reappraisal: time matters. Neu- rosci. Biobehav. Rev. 33, 1215–1226.
39. Kessler R, Petukhova M, Samson NA, et al: Twelve-month and lifetime prevalence and lifetime morbid risk of anxiety and mood disorders in the United States.. Int J Methods Psychiatr Res 21(3):169–184, 2012 10.1002/mpr.1359
40. Kessler, R. C. (2003). The impairments caused by social phobia in the general popu- lation: implications for intervention. Acta Psychiatrica Scandinavica, 108, 19–27. doi:10.1034/j.1600-0447.108.s417.2.x
41. Kessler, R.C., Berglund, P., Demler, O., Jin, R., Merikangas, K.R., Walters, E.E., 2005. Lifetime prevalence and age-of-onset distributions of DSM-IV disor- ders in the National Comorbidity Survey Replication. Arch. Gen. Psychiatry 62, 593–602.
42. Kim, M.J., Whalen, P.J., 2009. The structural integrity of an amygdala-prefrontal pathway predicts trait anxiety. J. Neurosci. 29, 11614–11618.

43. Klumpp, H., Angstadt, M., Phan, K.L., 2012. Insula reactivity and connectivity to anterior cingulate cortex when processing threat in generalized social anxiety disorder. Biol. Psychol. 89, 273–276.
44. Kohn, N., Eickhoff, S.B., Scheller, M., Laird, A.R., Fox, P.T., Habel, U., 2014a. Neu- ral network of cognitive emotion regulation—an ALE meta-analysis and MACM analysis. NeuroImage 87, 345–355.
45. Kohn, N., Falkenberg, I., Kellermann, T., Eickhoff, S.B., Gur, R.C., Habel, U., 2014. Neural correlates of effective and ineffective mood induction. Soc. Cogn. Affect. Neurosci., in press.
46. Langner, R., Eickhoff, S.B., 2012. Sustaining attention to simple tasks: a meta- analytic review of the neural mechanisms of vigilant attention. Psychol. Bull. 139, 870–900.
47. LeDoux, J.E., 2000. Emotion circuits in the brain. Annu. Rev. Neurosci. 23, 155–184.
48. Lerner, A., Bagic, A., Hanakawa, T., Boudreau, E.A., Pagan, F., Mari, Z., Bara-Jimenez, W., Aksu, M., Sato, S., Murphy, D.L., Hallett, M., 2009. Involvement of insula and cingulate cortices in control and suppression of natural urges. Cereb. Cortex 19, 218–223.
49. Lewis-Fernández R, Hinton DE, Laria AJ, et al: Culture and the anxiety disorders: recommendations for DSM-V. Depress Anxiety 27(2):212–229, 2010
50. Lewis-Fernández R, Hinton DE, Laria AJ, et al: Culture and the anxiety disorders: recommendations for DSM-V. Depress Anxiety 27(2):212–229, 2010
51. Lewis-Fernández R, Hinton DE, Laria AJ, et al: Culture and the anxiety disorders: recommendations for DSM-V. Depress Anxiety 27(2):212–229, 2010
52. Liao, W., Xu, Q., Mantini, D., Ding, J., Machado-de-Sousa, J.O.P., Hallak, J.E.C., Trzesniak, C., Qiu, C., Zeng, L., Zhang, W., Crippa, J.A.S., Gong, Q., Chen, H., 2011. Altered gray matter morphometry and resting-state functional and structural connectivity in social anxiety disorder. Brain Res. 1388, 167–177.
53. Lipsitz, J.D., Schneier, F.R., 2000. Social phobia. Epidemiology and cost of illness. PharmacoEconomics 18, 23–32.

54. Lipsitz, J.D., Schneier, F.R., 2000. Social phobia. Epidemiology and cost of illness. PharmacoEconomics 18, 23–32.
55. Lochner, C., Mogotsi, M., du Toit, P. L., Kaminer, D., Niehaus, D. J., & Stein, D. J. (2003). Quality of life in anxiety disorders: a comparison of obsessive–compulsive dis- order, social anxiety disorder, and panic disorder. Psychopathology, 36, 255–262. doi:10.1159/000073451
56. Machado-de-Sousa, J.P., Osorio Fde, L., Jackowski, A.P., Bressan, R.A., Chagas, M.H., Torro-Alves, N., Depaula, A.L., Crippa, J.A., Hallak, J.E., 2014. Increased amyg- dalar and hippocampal volumes in young adults with social anxiety. PLoS One 9, e88523.
57. Marek, R., Strobel, C., Bredy, T.W., Sah, P., 2013. The amygdala and medial prefrontal cortex: partners in the fear circuit. J. Physiol.
58. Mendlowicz, M. V., & Stein, M. B. (2000). Quality of life in individuals with anxiety disorders. The American Journal of Psychiatry, 157, 669–682. doi:10.1176/appi.ajp.157.5.669
59. Menon, V., Uddin, L., 2010. Saliency, switching, attention and control: a network model of insula function. Brain Struct. Funct. 214, 655–667.
60. Mohlman J, Bryant C, Lenze EJ, et al: Improving recognition of late life anxiety disorders in Diagnostic and Statistical Manual of Mental Disorders, Fifth Edition: observations and recommendations of the Advisory Committee to the Lifespan Disorders Work Group. Int J Geriatr Psychiatry 27(6):549–556, 2012 10.1002/gps.2752
61. Mohlman J, Bryant C, Lenze EJ, et al: Improving recognition of late life anxiety disorders in Diagnostic and Statistical Manual of Mental Disorders, Fifth Edition: observations and recommendations of the Advisory Committee to the Lifespan Disorders Work Group. Int J Geriatr Psychiatry 27(6):549–556, 2012 10.1002/gps.2752
62. Ochsner, K.N., Silvers, J.A., Buhle, J.T., 2012. Functional imaging studies of emotion regulation: a synthetic review and evolving model of the cognitive control of emotion. Ann. N.Y. Acad. Sci. 1251, E1–E24.
63. Paulus, M.P., Stein, M.B., 2006. An insular view of anxiety. Biol. Psychiatry 60, 383–387.

64. Phan, K.L., Fitzgerald, D.A., Nathan, P.J., Moore, G.J., Uhde, T.W., Tancer, M.E., 2005. Neural substrates for voluntary suppression of negative affect: a functional mag- netic resonance imaging study. Biol. Psychiatry 57, 210–219.
65. Phan, K.L., Orlichenko, A., Boyd, E., Angstadt, M., Coccaro, E.F., Liberzon, I., Arfanakis, K., 2009. Preliminary evidence of white matter abnormality in the uncinate fasciculus in generalized social anxiety disorder. Biol. Psychiatry 66, 691–694.
66. Piras, F., Piras, F., Caltagirone, C., Spalletta, G., 2013. Brain circuitries of obsessive compulsive disorder: a systematic review and meta-analysis of diffusion tensor imaging studies. Neurosci. Biobehav. Rev. 37, 2856–2877.
67. Qiu, C., Zhu, C., Zhang, J., Nie, X., Feng, Y., Meng, Y., Wu, R., Huang, X., Zhang, W., Gong, Q., 2014. Diffusion tensor imaging studies on Chinese patients with social anxiety disorder. Biomed. Res. Int. 2014, 860658.
68. Quilty, L. C., Ameringen, M. V., Mancini, C., Oakman, J., & Farvolden, P. (2003). Qual- ity of life and the anxiety disorders. Journal of Anxiety Disorders, 17, 405–426. doi:10.1016/s0887-6185(02)00225-6
69. Radua, J., Grau, M., van den Heuvel, O.A., Thiebaut de Schotten, M., Stein, D.J., Canales-Rodriguez, E.J., Catani, M., Mataix-Cols, D., 2014. Multimodal voxel- based meta-analysis of white matter abnormalities in obsessive–compulsive disorder. Neuropsychopharmacology 39, 1547–1557.
70. Radua, J., van den Heuvel, O.A., Surguladze, S., Mataix-Cols, D., 2010. Meta-analytical comparison of voxel-based morphometry studies in obsessive–compulsive dis- order vs other anxiety disorders. Arch. Gen. Psychiatry 67, 701–711.
71. Raichle, M.E., MacLeod, A.M., Snyder, A.Z., Powers, W.J., Gusnard, D.A., Shul- man, G.L., 2001. A default mode of brain function. Proc. Natl. Acad. Sci. 98, 676–682.
72. Robinson, J.L., Laird, A.R., Glahn, D.C., Lovallo, W.R., Fox, P.T., 2010. Metaanalytic connectivity modeling: delineating the functional connectivity of the human amygdala. Hum. Brain Mapp. 31, 173–184.
73. Robinson, O.J., Charney, D.R., Overstreet, C., Vytal, K., Grillon, C., 2012. The adaptive threat bias in anxiety: amygdalaâD dorsomedial prefrontal cortex coupling and aversive amplification. NeuroImage 60, 523–529.

74. Rotge, J.Y., Langbour, N., Guehl, D., Bioulac, B., Jaafari, N., Allard, M., Aouizerate, B., Burbaud, P., 2010. Gray matter alterations in obsessive–compulsive disorder: an anatomic likelihood estimation meta-analysis. Neuropsychopharmacology 35, 686–691.
75. Ruscio AM, Brown TA, Chiu WT, et al: Social fears and social phobia in the USA: results from the National Comorbidity Survey Replication. Psychol Med 38(1):15–28, 2008
76. Sabatinelli, D., Fortune, E.E., Li, Q., Siddiqui, A., Krafft, C., Oliver, W.T., Beck, S., Jef- fries, J., 2011. Emotional perception: meta-analyses of face and natural scene processing. NeuroImage 54, 2524–2533.
77. Sartory, G., Cwik, J., Knuppertz, H., Schürholt, B., Lebens, M., Seitz, R.J., Schulze, R., 2013. In search of the trauma memory: a meta-analysis of functional neuroimag- ing studies of symptom Provocation in Posttraumatic Stress Disorder (PTSD). PLoS ONE 8, e58150.
78. Schneier, F. R., Heckelman, L. R., Garfinkel, R., Campeas, R., Fallon, B. A., Gitow, A., et al. (1994). Functional impairment in social phobia. Journal of Clinical Psychiatry, 55, 322–331.
79. Schneier, F. R., Heckelman, L. R., Garfinkel, R., Campeas, R., Fallon, B. A., Gitow, A., et al. (1994). Functional impairment in social phobia. Journal of Clinical Psychiatry, 55, 322–331.
80. Schneier, F. R., Johnson, J., Hornig, C. D., Liebowitz, M. R., & Weissman, M. M. (1992). Social phobia: comorbidity and morbidity in an epidemiologic sample. Archives of General Psychiatry, 49, 282–288.
81. Schumann CM, Hamstra J, Goodlin-Jones BL, Lotspeich LJ, Kwon H, et al. (2004) The amygdala is enlarged in children but not adolescents with autism; the hippocampus is enlarged at all ages. J Neurosci 24: 6392–6401.
82. Sergerie, K., Chochol, C., Armony, J.L., 2008. The role of the amygdala in emotional processing: a quantitative meta-analysis of functional neuroimaging studies. Neurosci. Biobehav. Rev. 32, 811–830.
83. Shulman, G.L., Fiez, J.A., Corbetta, M., Buckner, R.L., Miezin, F.M., Raichle, M.E., Petersen, S.E., 1997. Common blood flow changes across visual tasks: II. Decreases in cerebral cortex. J. Cogn. Neurosci. 9, 648–663.

84. Simmons, A.N., Matthews, S.C., 2012. Neural circuitry of PTSD with or without mild traumatic brain injury: a meta-analysis. Neuropharmacology 62, 598–606.
85. Sparrevohn, R. M., & Rapee, R. M. (2009). Self-disclosure, emotional expression and intimacy within romantic relationships of people with social phobia. Behaviour Research and Therapy, 47, 1074–1078. doi:10.1016/j.brat.2009.07.016
86. Sridharan, D., Levitin, D.J., Menon, V., 2008. A critical role for the right fronto-insular cortex in switching between central-executive and default-mode networks. Proc. Natl. Acad. Sci. U.S.A. 105, 12569–12574.
87. Stein, J.L., Wiedholz, L.M., Bassett, D.S., Weinberger, D.R., Zink, C.F., Mattay, V.S., Meyer-Lindenberg, A., 2007a. A validated network of effective amygdala connectivity. Neuroimage 36, 736–745.
88. Stein, M. B., & Kean, Y. M. (2000). Disability and quality of life in social phobia: epidemiologic findings. The American Journal of Psychiatry, 157, 1606–1613. doi:10.1176/appi.ajp.157.10.1606
89. Stein, M. B., & Kean, Y. M. (2000). Disability and quality of life in social phobia: epidemiologic findings. The American Journal of Psychiatry, 157, 1606–1613. doi:10.1176/appi.ajp.157.10.1606
90. Stein, M. B., Torgrud, L. J., & Walker, J. R. (2000). Social phobia symptoms, subtypes, and severity: findings from a community survey. Archives of General Psychiatry, 57, 1046–1052. doi:10.1001/archpsyc.57.11.1046
91. Stein, M.B., Simmons, A.N., Feinstein, J.S., Paulus, M.P., 2007b. Increased amygdala and insula activation during emotion processing in anxiety-prone subjects. Am. J. Psychiatry 164, 318–327.
92. Steinert, C., Hofmann, M., Leichsenring, F., Kruse, J., 2013. What do we know today about the prospective long-term course of social anxiety disorder? A systematic literature review. J. Anxiety Disord. 27, 692–702.
93. Steinert, C., Hofmann, M., Leichsenring, F., Kruse, J., 2013. What do we know today about the prospective long-term course of social anxiety disorder? A systematic literature review. J. Anxiety Disord. 27, 692–702.
94. Syal, S., Hattingh, C.J., Fouche, J.P., Spottiswoode, B., Carey, P.D., Lochner, C., Stein, D.J., 2012. Grey matter abnormalities in social anxiety disorder: a pilot study. Metab. Brain Dis. 27, 299–309.

95. Sylvester, C.M., Corbetta, M., Raichle, M.E., Rodebaugh, T.L., Schlaggar, B.L., Sheline, Y.I., Zorumski, C.F., Lenze, E.J., 2012. Functional network dysfunction in anxiety and anxiety disorders. Trends Neurosci. 35, 527–535.
96. Talati, A., Pantazatos, S.P., Schneier, F.R., Weissman, M.M., Hirsch, J., 2013. Gray mat- ter abnormalities in social anxiety disorder: primary, replication, and specificity studies. Biol. Psychiatry 73, 75–84.
97. Tomasi, D., Volkow, N.D., 2011. Association between functional connectivity hubs and brain networks. Cereb. Cortex.
98. Weiner, K.S., Grill-Spector, K., 2012. The improbable simplicity of the fusiform face area. Trends Cogn. Sci. 16, 251–254.
99. Wittchen HU, Jacobi F: Size and burden of mental disorders in Europe—a critical review and appraisal of 27 studies. Eur Neuropsychopharmacol 15(4):357–376, 2005
100. Wittchen HU, Stein MB, Kessler RC: Social fears and social phobia in a community sample of adolescents and young adults: prevalence, risk factors and co-morbidity. Psychol Med 29(2):309–323, 1999
101. Wittchen HU, Stein MB, Kessler RC: Social fears and social phobia in a community sample of adolescents and young adults: prevalence, risk factors and co-morbidity. Psychol Med 29(2):309–323, 1999
102. Wittchen, H.U., Jacobi, F., Rehm, J., Gustavsson, A., Svensson, M., Jonsson, B., Olesen, J., Allgulander, C., Alonso, J., Faravelli, C., Fratiglioni, L., Jennum, P., Lieb, R., Maercker, A., van Os, J., Preisig, M., Salvador-Carulla, L., Simon, R., Steinhausen, H.C., 2011. The size and burden of mental disorders and other disorders of the brain in Europe 2010. Eur. Neuropsychopharmacol. 21, 655–679.
103. Wolitzky-Taylor KB, Castriotta N, Lenze EJL, et al: Anxiety disorders in older adults: a comprehensive review. Depress Anxiety 27(2):190–211, 2010
104. Wolitzky-Taylor KB, Castriotta N, Lenze EJL, et al: Anxiety disorders in older adults: a comprehensive review. Depress Anxiety 27(2):190–211, 2010
105. Yeo, B.T.T., Krienen, F.M., Sepulcre, J., Sabuncu, M.R., Lashkari, D., Hollinshead, M., Roffman, J.L., Smoller, J.W., Zöllei, L., Polimeni, J.R., Fischl, B., Liu, H., Buckner, R.L., 2011. The organization of the human cerebral cortex estimated by intrinsic functional connectivity. J. Neurophysiol. 106, 1125–1165.

106. Ziv, M., Goldin, P.R., Jazaieri, H., Hahn, K.S., Gross, J.J., 2013b. Emotion regulation 1532 in social anxiety disorder: behavioral and neural responses to three socio- 1533 emotional tasks. Biol. Mood Anxiety Disord. 3, 20.
107. King-Kallimanis BL, Gum AM, Kohn R: Comorbidity of depressive and anxiety disorders for older Americans in the national comorbidity survey-replication. Am J Geriatr Psychiatry 17(9):782–792, 2009
108. Beesdo K, Bittner A, Pine DS, et al: Incidence of social anxiety disorder and the consistent risk for secondary depression in the first three decades of life. Arch Gen Psychiatry 64(8):903–912, 2007

CHAPTER II

Manual Tracing of Subcortical Gray Matter:

A Protocol

Introduction

Magnetic resonance imaging (MRI) based brain volumetry is a valuable technique for identifying subcortical morphometric changes in vivo and determining the regional neurological impact of psychopathology, disease progression, and advancing therapeutic regimens (Dewey et al., 2010). Volumetric MR imaging was the first noninvasive in vivo technique to assess the volume of the intracranial structures accurately (Condon et al., 1986; Kohn et al., 1991). Today, the techniques of MR imaging volume quantification utelize manual, semiautomatic or fully automated techniques. Manual segmentation is performed by an observer tracing the outer contour of a region of interest on each section. The semi-automatic techniques also require input and feedback from the observer, which can introduce unwelcome bias into the calculations. Both manual and semiautomatic techniques are time-consuming and thus expensive, therefore stimulating the proliferation of fully automated techniques.

Fully automated techniques for structural brain measurement, such as voxel-based morphometry, generally employ an atlas-based segmentation approach to generate an individualized anatomical label map for a spatially normalized patient image. The segmentation utelizes either a Bayesian probabilistic approach in which the shape and appearance models are constructed from a library of manually segmented images, or an affine rigid linear transformation which combines information about voxel intensity relative to a probability distribution for tissue classes. These are then combined with information about the spatial relationship of the voxel to the location of neighboring structures obtained from a manually labeled atlas.

Advancements in automated techniques have contributed significantly to the neuroimaging literature, however manual delineation by trained experts remain the “gold standard” of accuracy in volumetric analyses (Dewey et al., 2010). The advantage of manual tracing lies within the neuroanatomist being able to interpret variations in normal anatomy on a case by case basis. This minimises incorrect segmentation of structures, and mazimises accuracy. Several authors have saught to develop specific stepwise manual tracing protocols for the volumetric analysis of subcortical structures. Looi et al (2008) was one of the first to publish a step wise

tracing protocol for the caudate nucleus (Looi et al., 2008). In this study, the caudate nucleus was traced in the axial plane from inferior to superior. The summation of the volume of each slice traced was reconstructed, yielding the total caudate volume for each respective side. Limitations of this approach, which can impact the accuracy of volumetric measurements include; the field strength of the magnet used in the image acquisition which was 1.5T offering lower resolution images when compared to higher field strengths; the slice thickness which was greater than 1mm further reducing resolution of the images; the use of multiple tracers which may be a potential source bias (Cherbuin, Anstey, Réglade-Meslin, & Sachdev, 2009); and insufficient detail regarding the tracing process.

Morey et al (2009) conducted manual tracing of the hippocampus and amygdala, however the tracing protocol was only a subsection of a larger study and the discussion of their actual tracing protocol was included in a short appendix to the study (Morey et al., 2009). The hippocampus and amygdala were traced in the coronal plane from most posterior to most anterior aspects. The volumes of each respective structure where then calculated. Limitations of this approach were insufficient detail outlining the anatomical delineation of each structure and the insufficient detail describing the stepwise progression in tracing a structure from its proximal and distal aspects. Another limitation was that the tracing was voxel based, which is possibly less accurate than outline tracing. This is because outline tracing follows the contour of the structure which adheres more accurately to anatomical uniformity as opposed to voxel based segmentation, which potentially loses volumetric data between voxels.

In the existing literature, there has yet been no work on a detailed step-wise manual tracing protocol for the most prominent macroscopically visible subcortical gray matter structures that take advantage of current advancements in image imaging technology resulting in exquisitely detailed high resolution images.

Methods:

I. Image Acquisition

Magnetic resonance imaging was conducted on the 3T Siemens system (MAGNETOM Allegra, Erlangen, Germany) at the Cape Universities Brain Imaging Centre. Whole brain T1- weighted 3D magnetization-prepared rapid

gradient echo (MPRAGE) images were acquired using the following parameters: spatial resolution 0 1.0 × 1.0 × 1.0 mm3; slices 0 160; matrix 0 179×256; TR 0 2,300 ms; TE 0 3.93 ms; TI 0 1,100 ms and flip angle 0 12°.

II. Software

OsiriX is developed as a stand-alone application for the MacOSX operating system. The program is an image processing software dedicated to DICOM images (".dcm" / ".DCM" extension) produced by imaging equipment (MRI, CT, PET, PET-CT, SPECT-CT, Ultrasounds, ...). It is fully compliant with the DICOM standard for image communication and image file formats. OsiriX is able to receive images transferred by DICOM communication protocol from any PACS or imaging modality (C-STORE SCP/SCU, and Query/Retrieve : C-MOVE SCU/SCP, C-FIND SCU/SCP, C-GET SCU/SCP, WADO) .

OsiriX has been specifically designed for navigation and visualisation of multi-modality and multidimensional images: 2D Viewer, 3D Viewer, 4D Viewer (3D series with temporal dimension) and 5D Viewer (3D series with temporal and functional dimensions). The 3D Viewer offers all modern rendering modes: Multiplanar reconstruction (MPR), Surface Rendering, Volume Rendering and Maximum Intensity Projection (MIP). All these modes support 4D data and are able to produce image fusion between two different series (PET-CT and SPECT-CT display support). OsiriX is at the same time a DICOM PACS workstation for imaging and an image processing software for medical research, functional imaging, 3D imaging, confocal microscopy and molecular imaging.

The OsiriX software was developed based on an open architecture built on existing open-source components and offers all the basic image manipulation functions of zoom, pan, intensity adjustment, and filtering with real-time performance. Additional functions such as multiplanar projection, convolution filters, variable slice thickness adjustments, volume rendering, minimum and maximum intensity projections, and surface rendering are also accessible in quasi-real-time.

The program enables the rapid review of very large sets of images and does not rely on pre-loading of the images from the disk to memory before review. As soon as an images series is selected, images will automatically be displayed on the

screen in a cine loop using a‘‘streaming’’ technique, enabling direct display of the images at a very rapid pace.

Regions of Interest:

The animal literature concerning anxiety overlaps with what is found in the functional human neuroimaging literature, and implicates the amygdala, nucleus accumbens, and other striatal structures (Le Doux et al., 2000; Davis et al., 2006; Panksepp et al., 2011). The vast functional neuroimaging literature regarding SAD implicates several subcortical structures, such as the amygdala, nucleus accumbens, lentiform nuclear complex, and hippocampus (Freitas-Ferrari et al., 2010).

The Amygdala:

The amygdala lies in the dorsomedial temporal pole, anterior to the hippocampus, close to the tail of the caudate nucleus and partly deep to the gyrus semilunaris, gyrus ambiens and uncinate gyrus. The amygdala forms the ventral, superior and medial walls of the tip of the inferior horn of the lateral ventricle. The amygdala is partly continuous above with the inferomedial margin of the claustrum. Fibres of the external capsule and substriatal grey matter, including the cholinergic magnocellular nucleus basalis (of Meynert), incompletely separate it from the putamen and globus pallidus. Laterally, it is close to the optic tract. The Amygdala has been extensively implicated in social anxiety in the functional imaging literature (Evans et al., 2008; Shah, Klumpp, Angstadt, Nathan, & Phan, 2009).

The Caudate Nucleus:

The caudate nucleus is a curved, comet-shaped mass. It has a large anterior head, which tapers to a body, and an inferiorly-curving tail. Its head is covered with ependyma and lies in the floor and lateral wall of the anterior horn of the lateral ventricle, in front of the interventricular foramen. The tapering body is in the floor of the body of the ventricle, and the narrow tail follows the curve of the inferior horn, and so lies in the ventricular roof, in the temporal lobe. Medially, the greater part of the caudate nucleus abuts the thalamus, along a junction that is marked by a groove, the sulcus terminalis. The sulcus contains the stria terminalis, lying deep to the ependyma. The sulcus terminalis is especially prominent anterosuperiorly (because of the large size of the head and body of the caudate nucleus relative to the tail), and here

the stria terminalis is accompanied by the thalamostriate vein. The caudate nucleus has previously been implicated in the social anxiety functional literature (Sareen et al., 2007), but no volumetric data relating to social anxiety disorder has been published to date.

The Lentiform Complex:

The lentiform complex lies deep to the insular cortex, with which it is roughly coextensive, although they are separated by a thin layer of white matter and by the claustrum. The latter splits the insular subcortical white matter to create the extreme and external capsules; the external capsule separates the claustrum from the putamen. The internal capsule separates the lentiform complex from the caudate nucleus. The lentiform complex consists of the laterally placed putamen and the more medial globus pallidus, which are separated by a thin layer of fibres: the lateral or external medullary lamina. The globus pallidus is itself divided into two segments, a lateral (or external) segment and a medial (or internal) segment, separated by an internal (or medial) medullary lamina. The various components of the lentiform nuclear complex have previously been implicated in the social anxiety literature (Warwick, Carey, Jordaan, Dupont, & Stein, 2008), but no volumetric data relating to social anxiety disorder has been published to date.

The Nucleus Accumbens:

The ventral striatum consists of the nucleus accumbens and the olfactory tubercle. In front of the anterior commissure, much of the grey matter of the anterior perforated substance, and especially the olfactory tubercle, is indistinguishable from, and continuous with, the fundus striati in terms of cellular composition, histochemistry and interconnections. The caudate nucleus is continuous medially with the nucleus accumbens, which abuts the nuclei of the septum, close to the paraolfactory area, the diagonal band of Broca and the fornix. The nucleus accumbens receives mainly glutamatergic projections from the amygdala, hippocampus, thalamus and prefrontal cortex, and dopaminergic projections from the mesencephalon. Although not directly implicated in SAD, both dopamine (Tiihonen, Kuikka, Bergström, & Lepola, 1997) and glutamate (Phan et al., 2005) have been implicated in social anxiety pathophysiology. Due to its difficult neuroanatomical location, this region may

benefit from being segmented manually in social anxiety – here, segmentation has previously been accomplished (Mavridis, Boviatsis, & Anagnostopoulou, 2011).

The Hippocampus:

The hippocampus lies above the subiculum and medial parahippocampal gyrus, forming a curved elevation (approximately 5 cm long) along the floor of the inferior horn of the lateral ventricle. Its anterior end is expanded, and here its margin may present two or three shallow grooves that give a paw-like appearance, the pes hippocampi. The ventricular aspect is convex. It is covered by ependyma, beneath which fibres of the alveus converge medially on a longitudinal bundle of fibres, the fimbria of the fornix. Passing medially from the collateral sulcus, the neocortex of the parahippocampal gyrus merges with the transitional juxtallocortex of the subiculum. The latter curves superomedially to the inferior surface of the dentate gyrus, then laterally to the laminae of the hippocampus. This curvature continues, first superiorly, then medially above the dentate gyrus, and ends pointing towards the centre of the superior surface of the dentate gyrus.

The dentate gyrus is a crenated strip of cortex related inferiorly to the subiculum, laterally to the hippocampus, and more medially to the fimbria of the fornix. The form of the fimbria is quite variable, but medially it is separated from the crenated medial margin of the dentate gyrus by the fimbriodentate sulcus. The hippocampal sulcus, of variable depth, lies between the dentate gyrus and the subicular extension of the parahippocampal gyrus. Posteriorly, the dentate gyrus is continuous with the gyrus fasciolaris and thus with the indusium griseum. Anteriorly, it is continued into the notch of the uncus, turning medially across its inferior surface, as the tail of the dentate gyrus (band of Giacomini), and vanishes on the medial aspect of the uncus. The various components of the hippocampus have previously been implicated in the social anxiety literature (Lorberbaum et al., 2004), but no manually traced volumetric data relating to social anxiety disorder has been published to date.

A Note on Neural Plasticity

Over the past two decades, our understanding of how the brain is changed by experience, referred to as *neural plasticity*, has developed and evolved considerably. Once believed to be fairly constant in its organisation and function, it has become clear that the brain is inherently capable of changing after stress and injury to enable a variable degree of behavioral restitution (Kolb et al., 2014). Neural plasticity is therefore an important theoretical underpinning when relating structure to function, i.e. how certain measurable parameters change in conjunction with altered function, as with neurobiological alterations associated with psychopathology.

What follows in this chapter is a detailed procedure which aims to describe in sufficient detail, the manual tracing of those macroscopically visible subcortical gray matter structures which includes the caudate nucleus, the nucleus accumbens, the putamen, globus pallidus, hippocampus and amygdala. The aims of the manual segmentation is to provide an accurate estimation of the volume of these subcortical structures which are widely implicated in most neuroscientific neuroimaging literature on psychopathology. This will enable the researcher to reliably associate structural changes, with those observable functional alterations seen in the psychopathology which cause the patient distress and suffering. This will include an overview of the functional anatomy of the region of interest, followed by an overview of the regional anatomy, then a detailed subsection on how to delineate the neuroanatomical boundaries of each of the six structures, and a step wise process outlining the plane of the section, enhancing the contrast between gray and white matter, volumetric reconstruction and shape inspection.

The Caudate Nucleus

Regional Anatomy

The caudate nucleus is an elongated and arched grey mass, which lies just ventrolateral to the lateral ventricle and can be subdivided into a large anterior portion, the head or caput, a smaller middle portion, the corpus, and a caudal portion, the tail or cauda. The head is covered with ependyma and lies in the floor and lateral wall of the anterior horn of the lateral ventricle, in front of the interventricular foramen. The tapering body is in the floor of the body of the

ventricle, and the narrow tail follows the curve of the inferior horn, and so lies in the ventricular roof, in the temporal lobe.

Medially, the greater part of the caudate nucleus abuts the thalamus, along a junction that is marked by a groove, the sulcus terminalis. The sulcus contains the stria terminalis, lying deep to the ependyma. The sulcus terminalis is especially prominent anterosuperiorly (because of the large size of the head and body of the caudate nucleus relative to the tail), and here the stria terminalis is accompanied by the thalamostriate vein. The corpus callosum lies above the head and body of the caudate nucleus. The two are separated laterally by the fronto-occipital fasciculus, and medially by the subcallosal fasciculus which caps the nucleus. The caudate nucleus is largely separated from the lentiform complex by the anterior limb of the internal capsule. However, the inferior part of the head of the caudate becomes continuous with the most inferior part of the putamen immediately above the anterior perforated substance; this junctional region is sometimes known as the fundus striati. Variable bridges of cells connect the putamen to the caudate nucleus for most of its length. They are most prominent anteriorly, in the region of the fundus striati and the head and body of the caudate nucleus, where they break up the anterior limb of the internal capsule.

In the temporal lobe, the anterior part of the tail of the caudate nucleus becomes continuous with the posteroinferior part of the putamen. The vast bulk of the caudate nucleus and putamen are often referred to as the dorsal striatum. A smaller inferomedial part of the rostral striatum is referred to as the ventral striatum, and includes the nucleus accumbens.

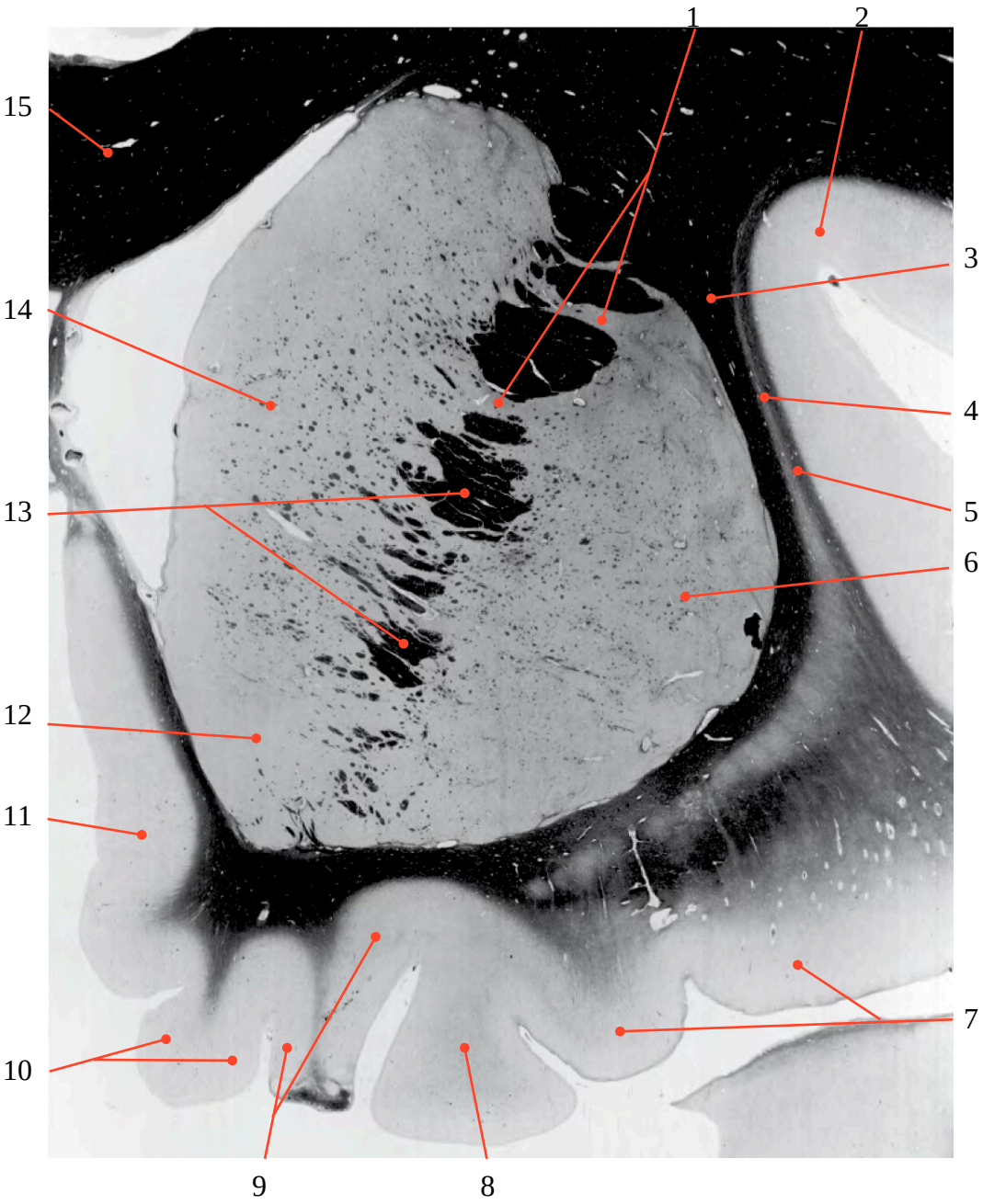

Figure 1:

Coronal myelin stained micrograph demonstrating the caudate nucleus and surrounding structures: 1. gray matter bridges; 2. insular cortex; 3. external capsule; 4. claustrum; 5. extreme capsule; 6. anterior aspect of the putamen; 7. piriform cortex; 8. posteromedial orbital lobule; 9. olfactory area; 10. straight gyrus; 11. subcallosal area; 12. nucleus accumbens; 13. internal capsule; 14. caudate nucleus; 15. body of the corpus callosum

Micrograph from Atlas of the Human Brain, 3rd ed by Mai et al., (2008)

Caudate Tracing Protocol

The specific tracing technique was developed to firstly maximize the differentiation between gray and white matter, which allows for better edge detection of the structure; secondly to effectively delineate the neuroanatomical boundaries in the first and last tracing slice defining the anterior and posterior dimensions of the caudate nucleus, and finally provide a detailed stepwise instruction so that this protocol can be reliably duplicated in further manual tracing research.

Step I

The first task is to determine the anterior most boundary so that the first tracing of the nuclear outline of the caudate nucleus can be preformed. This is achieved by opening two simultaneous windows (fig. 2.). The first containing the coronal T1WI and the second the sagittal T1WI. The sagittal view is then navigated to demonstrate the midline. The midline in the sagittal plane is defined when the cerebral aqueduct of Sylvius is visualized draining the third ventricle and opening up into the fourth ventricle. The median aperture of Magendie should also be visible, along with other midline structures such as the arbor vitae of the cerebellum, massa intermedia, the anterior and posterior commisures, the pineal gland, optic chiasm, fornix and the corpus callosum.

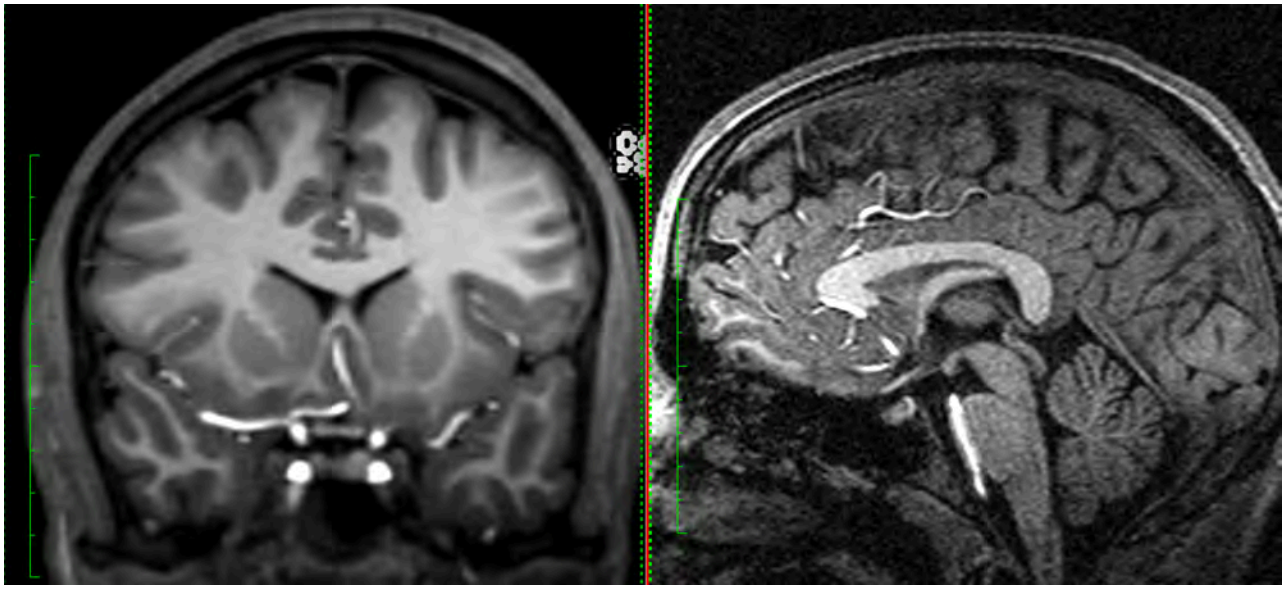

Figure: 2
Simultaneous display of two orthogonal planes. Left demonstrates the coronal plane where right demonstrates the mid-sagittal plane.

Once the midline is ascertained, the sagittal plane is navigated laterally to demonstrate the head of the caudate nucleus. The head of the caudate nucleus forms the most anterior aspect of the structure.

In OsiriX, guidelines appear to demonstrate the slice position of one window relative to the other open window (fig. 3.). This is helpful in aligning the slice position and to determine the relative slice position from one plane to another orthogonal plane.

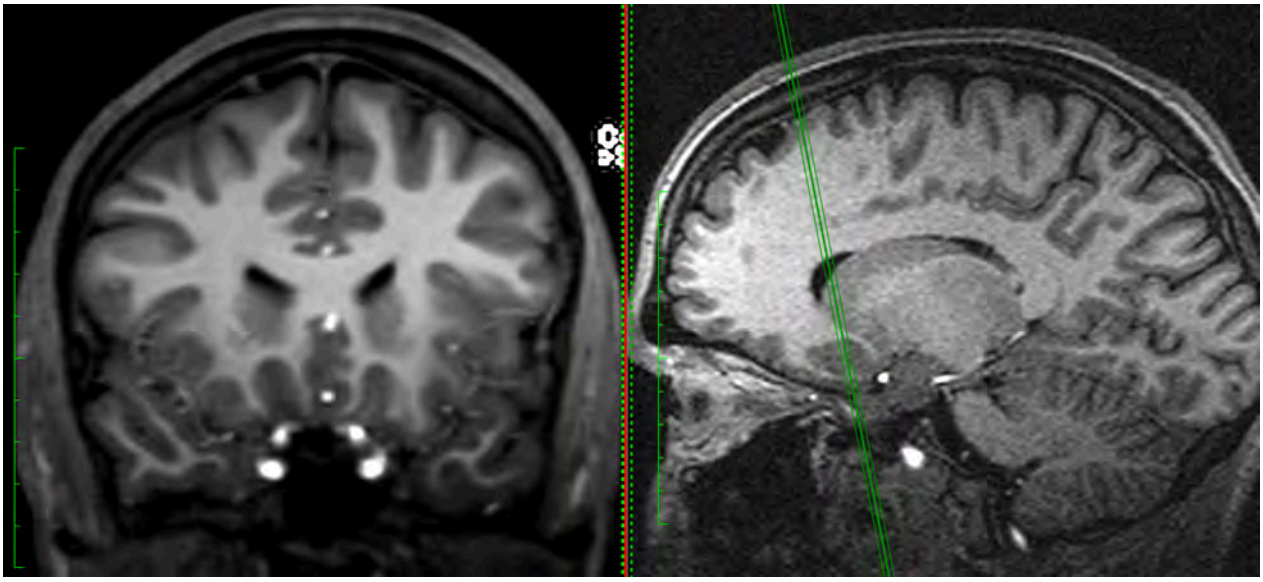

Figure: 3

Guidelines seen here as three parallel green lines intersecting the anterior aspect of the caudate nucleus in the sagittal plane, represent the relative slice position in the coronal plane on the left.

Once a side is selected to begin the tracing, the coronal section is navigated until the alignment guide visible on the sagittal window intersects the anterior most aspect of the caudate nucleus (fig. 4.).

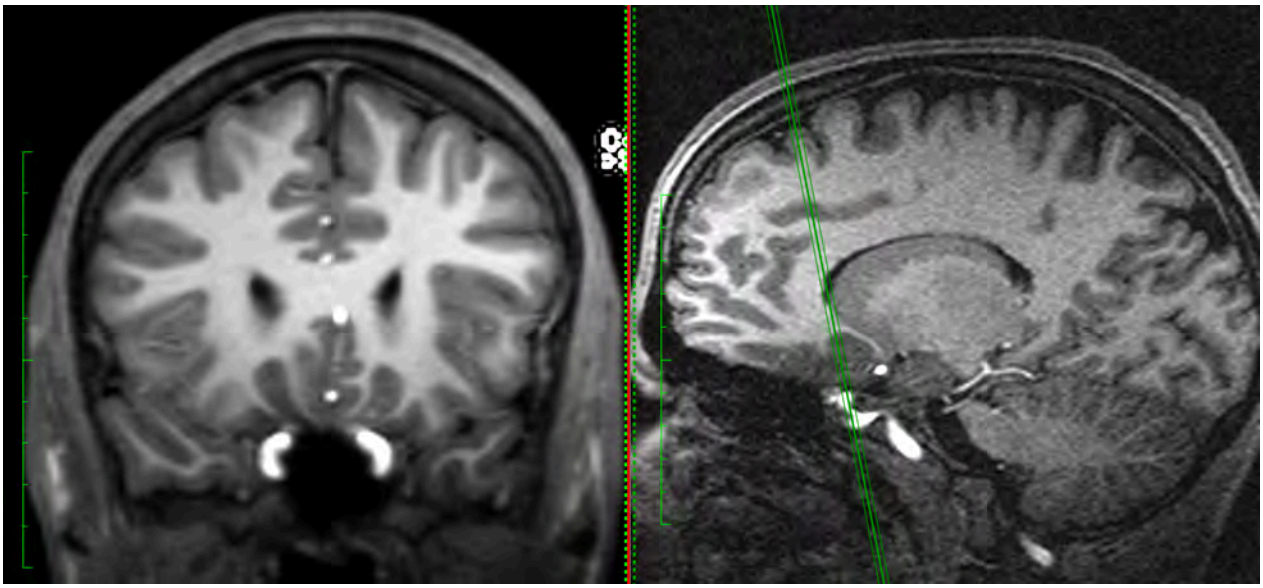

Figure: 4

The alignment guide seen in Fig 3 now intersects the anterior most aspect of the caudate nucleus in the sagittal plane. The coronal view demonstrates the relative slice position indicated by the alignment guide in the sagittal plane.

Step II

To maximize edge detection the contrast between gray and white matter must be optimized. In OsiriX, this is easily accomplished by applying a colour look-up table (CLUT) filter to the scans. A CLUT filter is a mechanism used to transform a range of input colours into another range of colours. The result is an enhanced differentiation between white and gray matter, which serves to enhance the detection of the physical edge of the nucleus by the human eye facilitating more accurate tracing of the outline (fig. 5a, 5b.).

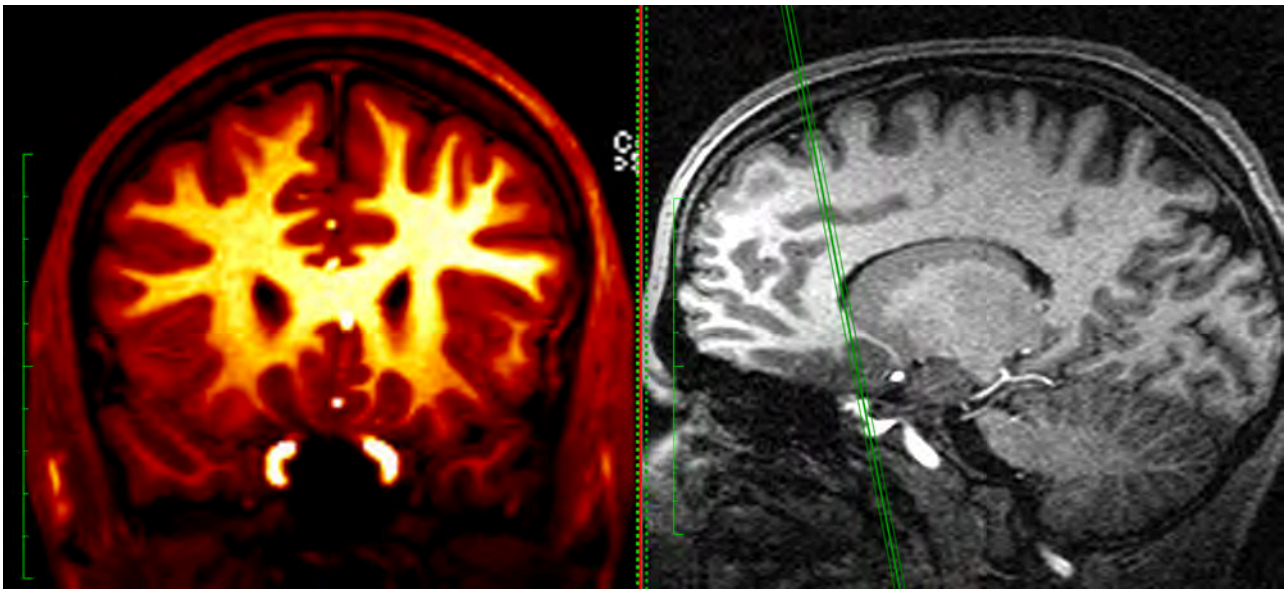

Figure: 5a

Application of the CLUT filter maximizes the contrast between gray and white matter by transforming the colours without distorting the anatomical boundaries.

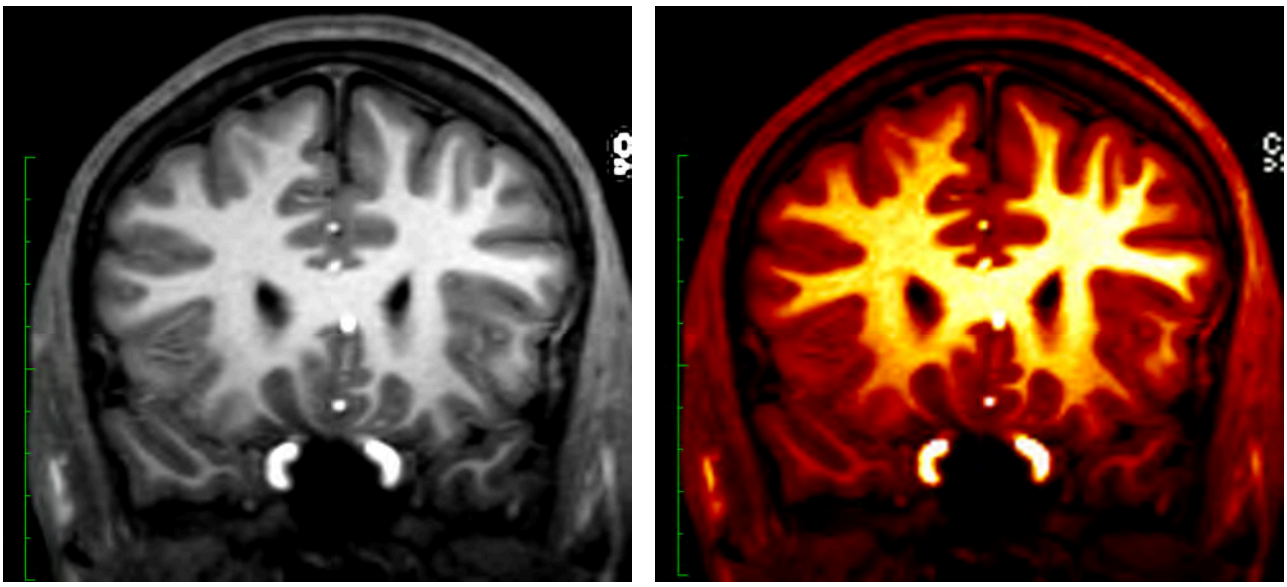

Figure: 5b

Side by side comparison without (left) and with (right) the CLUT filter applied.

Step III

Once alignment is achieved, the orthogonal planes calibrated correctly, CLUT filter applied, the first trace of the caudate outline can be made. This is accomplished with a tracing tablet – a piece of hardware that uses a pen and tablet interface, translating the movement of the pen to the screen. When the tip of the pen touches the tablet, an action command is performed, and in the case of the tracing of a structure, the action command is that of an outline function in OsiriX. The outline of the region of interest (ROI) can then be traced along the gray white border of the nucleus from anterior to posterior (Fig. 6a – d.).

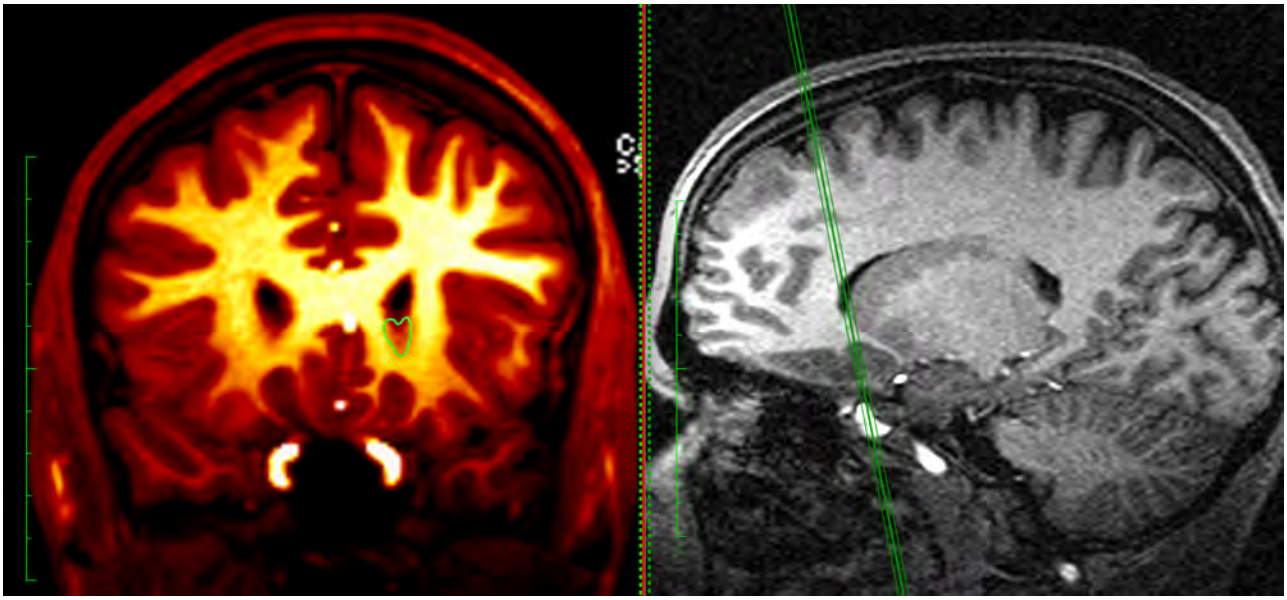

Figure: 6a
First tracing of the most anterior aspect of the caudate head.

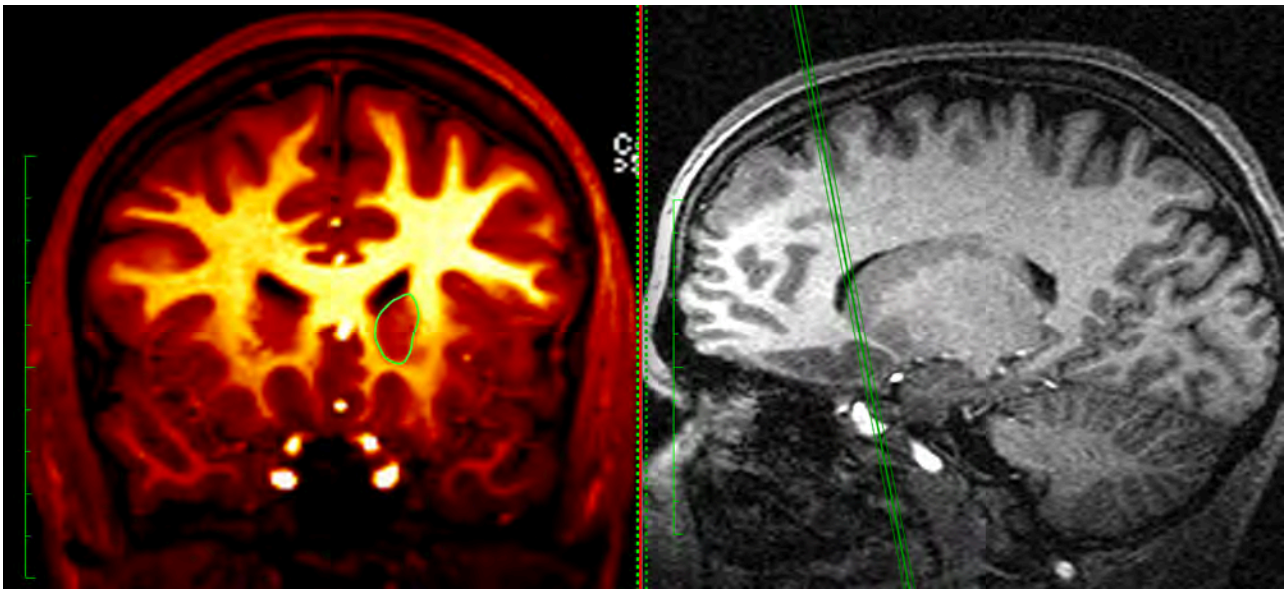

Figure: 6b

Consecutive tracing of the caudate head.

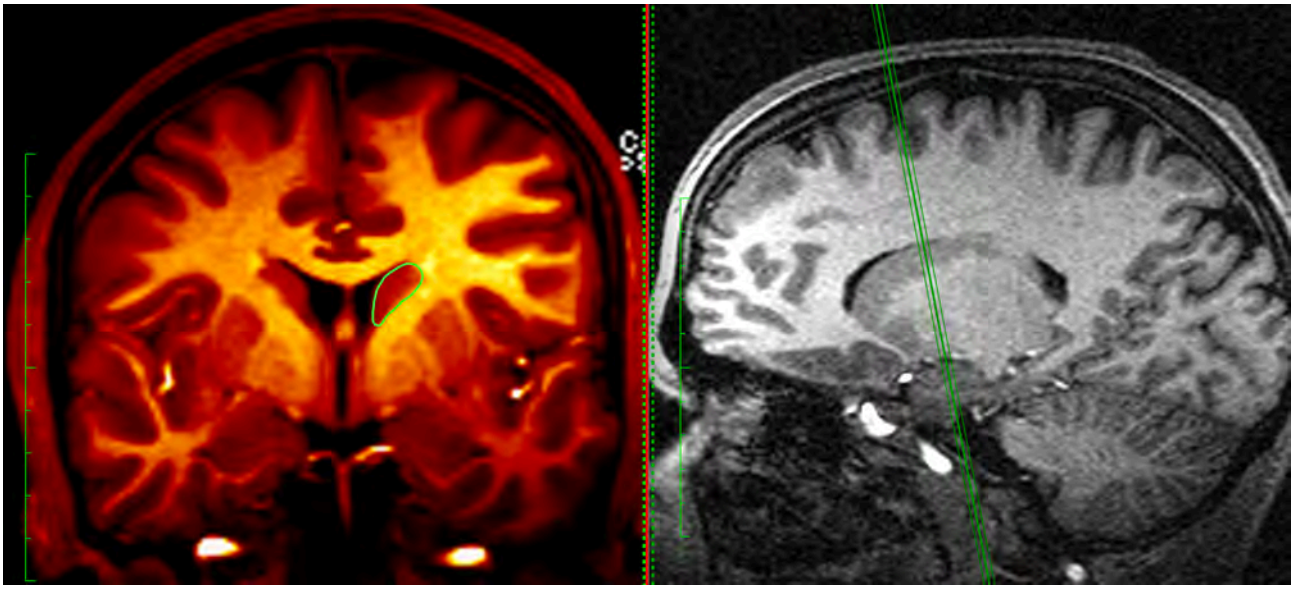

Figure: 6c

Tracing of the body of the caudate

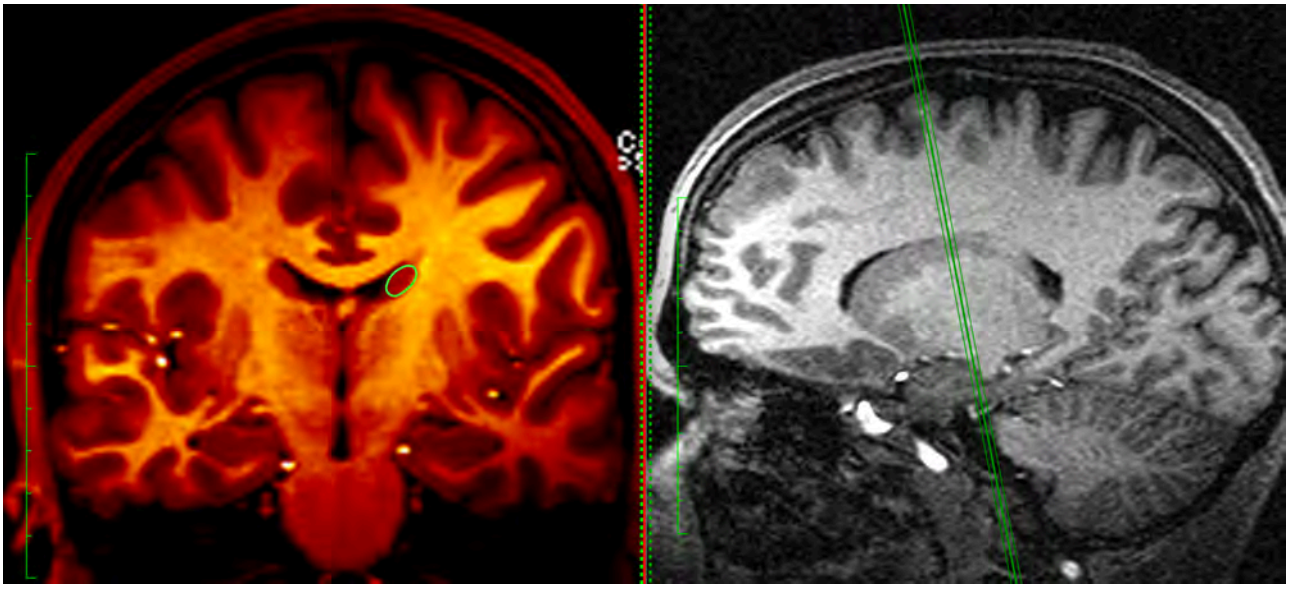

Figure: 6d

Tracing of the tail of the caudate.

Step IV

Once the entire extent of the nucleus has been traced in its anterior and posterior dimensions, a volumetric reconstruction is preformed. The volumetric reconstruction calculates the volume of the structure that has been traced and also provides an opportunity for anatomical inspection. The volumetric reconstruction is inspected to confirm that there are no irregularities in the shape of the

nucleus, and that the tracing conforms to what one would expect the structure to look like when dissected in a cadaveric specimen (Fig. 6e.).

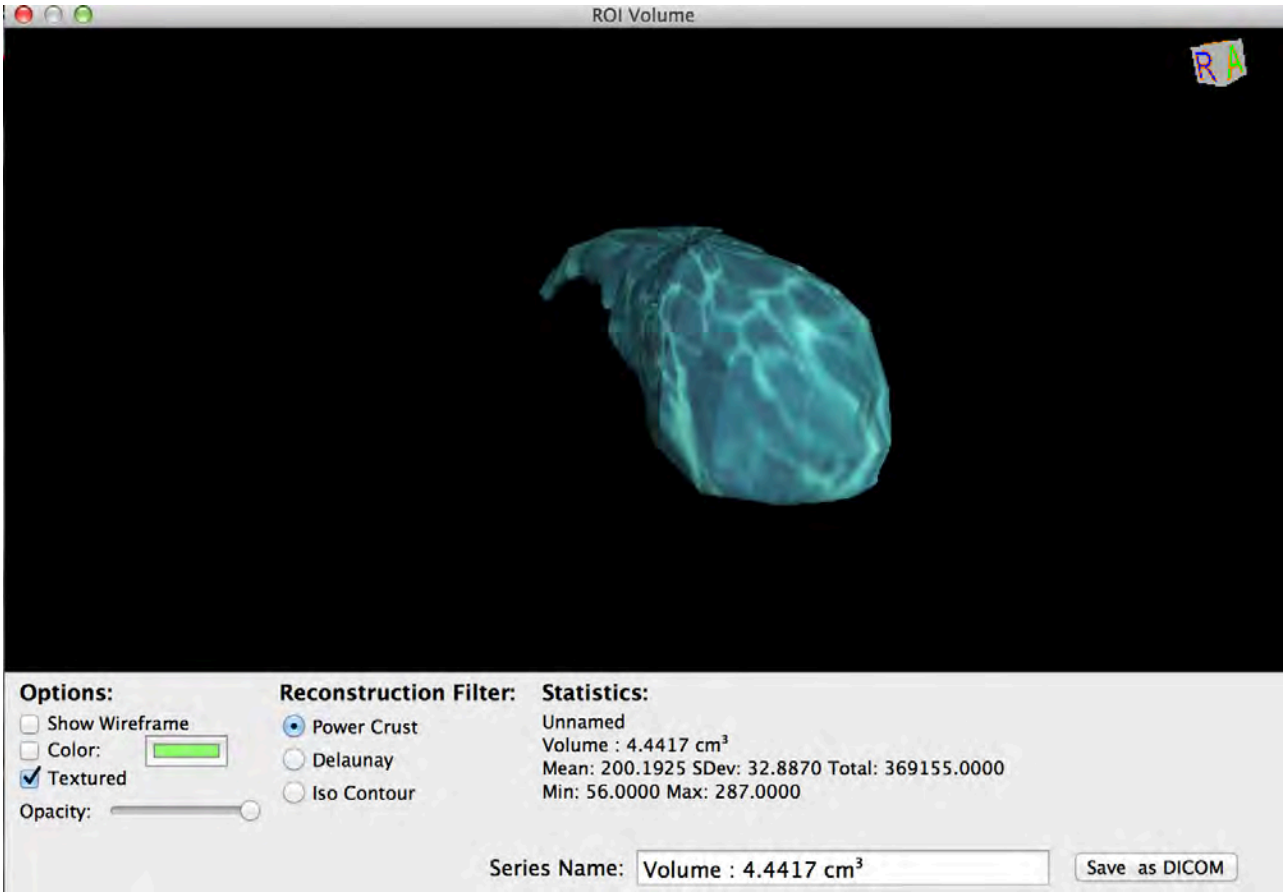

Figure: 6e

Volumetric reconstruction of the tracings demonstrating the three-dimensional rendering of the caudate nucleus. This rendering can be rotated to observe all aspects of the nucleus. The volume is also calculated and displayed at the bottom of the window.

Special Considerations:

The nucleus accumbens, cytoarchitectonically and histochemically closely resembles the caudate nucleus and the putamen. The nucleus accumbens lies closely apposed to the most rostroventromedial part of the caudate–putamen complex. The caudate nucleus is flanked laterally by the internal capsule, which cleaves the striatum into the caudate nucleus medially and the putamen laterally. The superolateral boundary of the caudate nucleus is thus easy to distinguish, however, this cleavage is incomplete: ventrally, the caudate nucleus and the putamen meet each other in the nucleus accumbens. This presents a challenge for the delineation of the most inferolateral aspect of the caudate head and the anteromedial aspect of the nucleus accumbens.

The anterior and posterior dimensions of the nucleus accumbens can be best appreciated in the sagittal plane. The superior boundary of the nucleus accumbens can be determined by

visualizing the most inferior aspect of the anterior limb of the internal capsule. The medial and lateral boundaries of the nucleus accumbens are the most difficult to define. Using “The Atlas of the Human Brain” by Mai et al (2008), the medial relationship of the nucleus accumbens with the caudate head can be discerned on myelin stained micrographs (Fig. 7.).

The most reliable technique to define the inferolateral boundary of the caudate head from the accumbens is by navigating to the most anterior aspect of the nucleus accumbens on the sagittal plane (Fig. 8a.). On the coronal, the inferior limit for the tracing of the caudate head is a line drawn from the most inferior tip of the anterior horn of the lateral ventricle to the inferior edge of the anterior limb of the internal capsule (Fig. 8.b.). Using this plane, the caudate can reliably be separated from the nucleus accumbens on imaging.

Figure: 7

Myelin stained micrograph (left) and annotated diagram (right) demonstrating the boundaries of the caudate head, nucleus accumbens and putamen. Red circle indicates the inferior most boundary of the anterior limb of the internal capsule, representing the superior aspect of the nucleus accumbens. Blue circle indicates the anteroinferior most corner of the anterior horn of the lateral ventricle. Micrograph and diagram from Atlas of the Human Brain, 3rd ed by Mai et al., (2008)

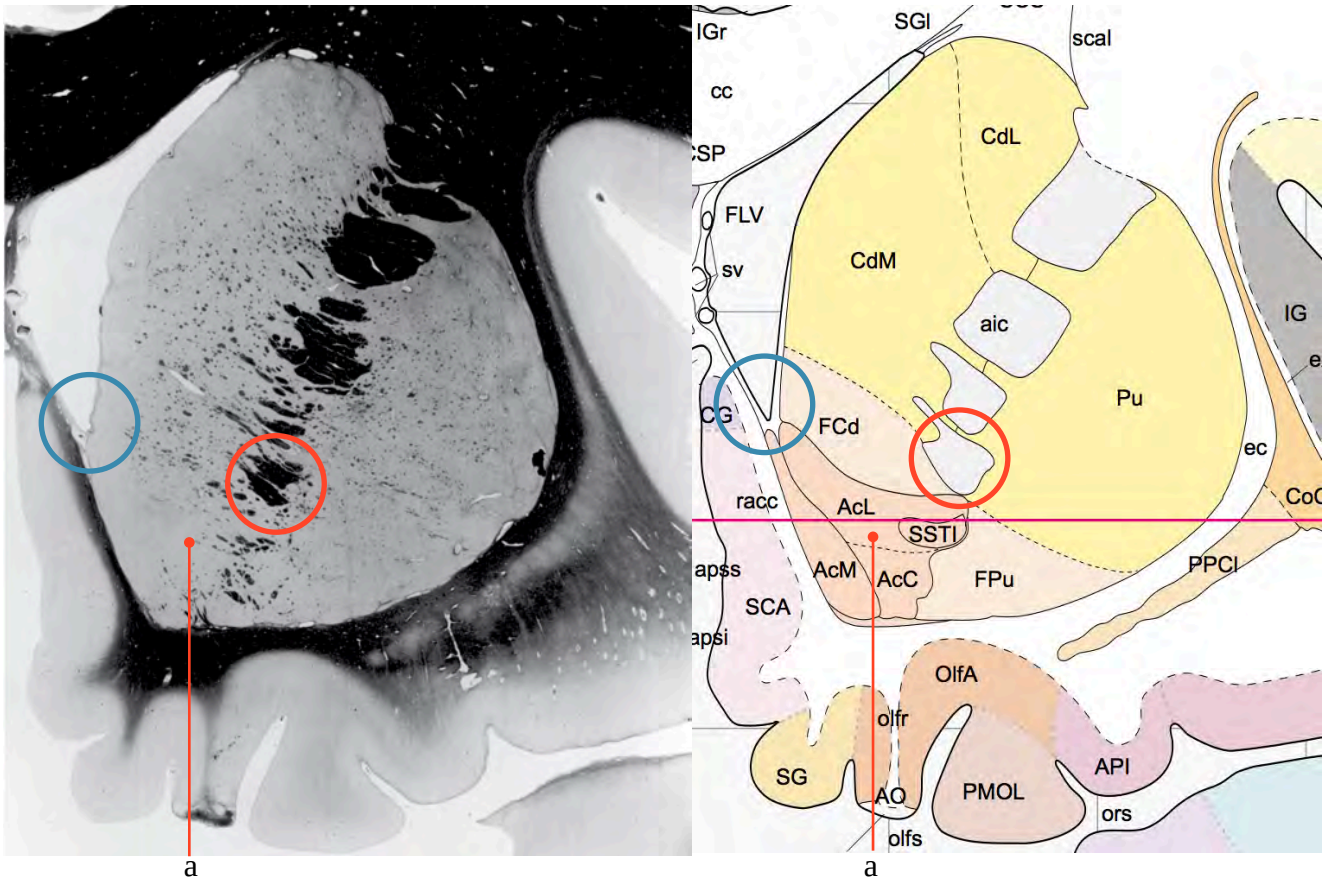

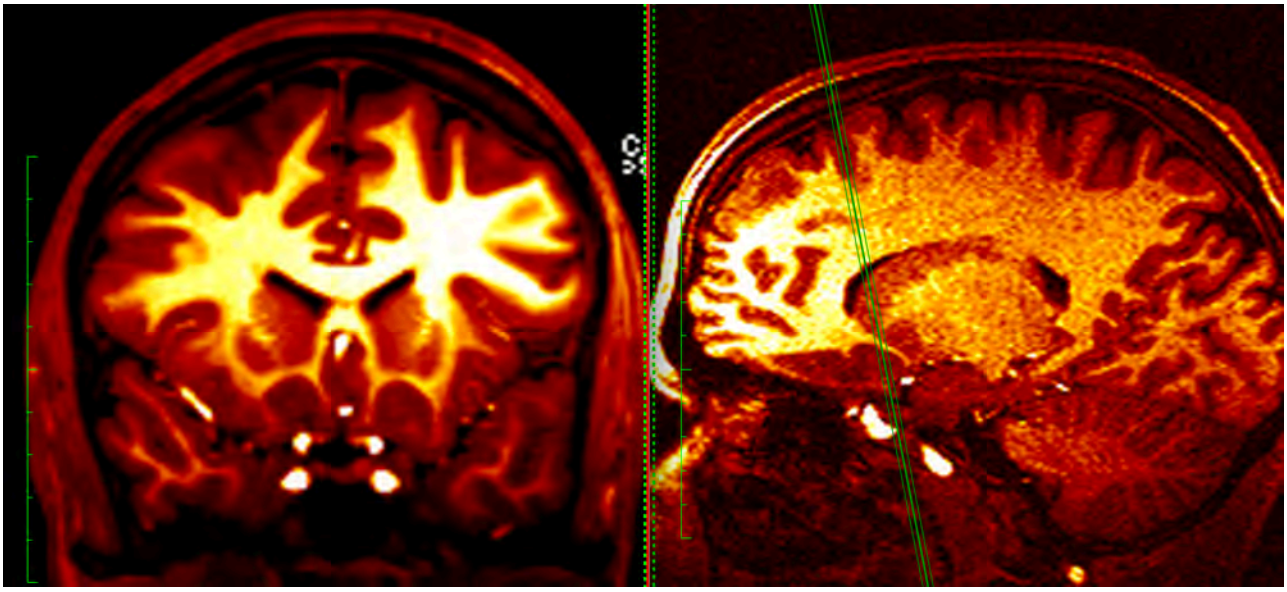

Figure: 8a

Side by side display of coronal and sagittal views. The CLUT filter is applied to both views so that the gray-white interface is more easily visualized. The green guideline in the sagittal view demonstrates the anterior most tip of the nucleus accumbens and its superior extent, limited by the inferior edge of the anterior limb of the internal capsule.

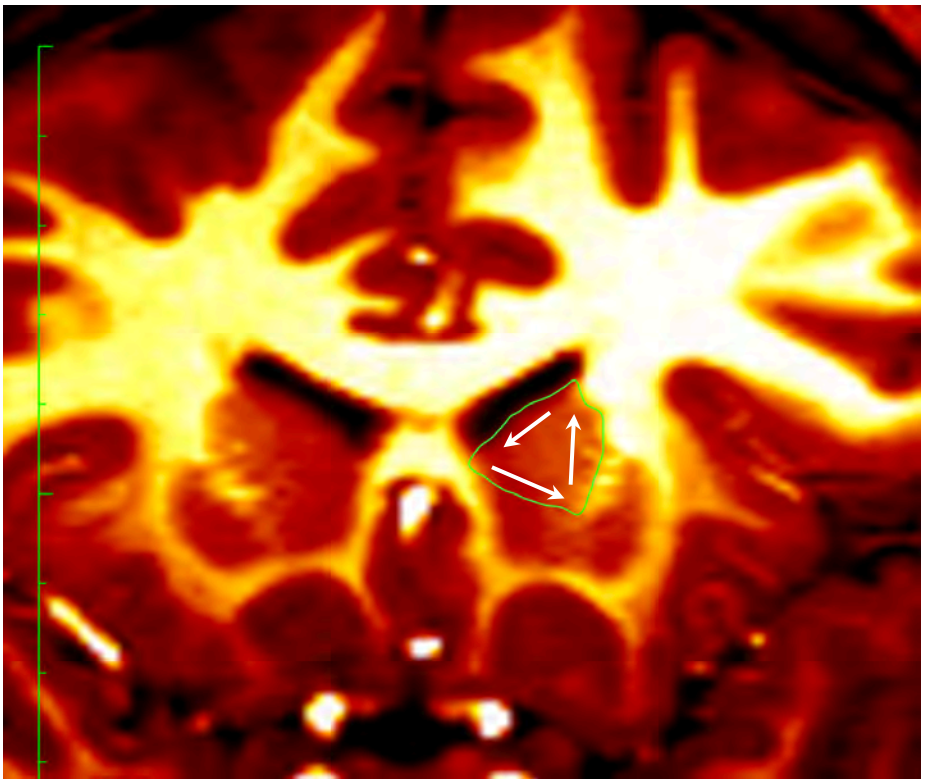

Figure: 8b

Coronal view of the anterior most aspect of the nucleus accumbens. Green outline demonstrates the tracing of the caudate head. Arrows indicate direction of the lines traced from the superior tip of the caudate head to the interior tip of the anterior horn of the lateral ventricle, laterally to meet the lateral, inferior edge of the caudate head as it abuts the medial edge of the anterior limb of the internal capsule.

The Nucleus Accumbens

Regional Anatomy

The ventral striatum consists of the nucleus accumbens and the olfactory tubercle. In front of the anterior commissure, much of the grey matter of the anterior perforated substance, and especially the olfactory tubercle, is indistinguishable from, and continuous with, the fundus striati, in terms of cellular composition, histochemistry and interconnections. The caudate nucleus is continuous medially with the nucleus accumbens, which abuts the nuclei of the septum, close by the paraolfactory area, diagonal band of Broca and the fornix.

The nucleus accumbens receives a dopaminergic innervation from the midbrain ventral tegmental area (cell group A10) of the mesencephalon which projects its dopamine terminals in the nucleus accumbens, via the medial forebrain bundle. It is believed to represent the neural substrate for the rewarding effects of several classes of drugs of abuse and is, therefore, a major determinant of their addictive potential. The experimental observation that the locomotor activating effects of psychomotor stimulant drugs such as amphetamine and cocaine (which act presynaptically on dopaminergic neurones to enhance dopamine release or block its reuptake, respectively) are dependent on dopamine transmission in the nucleus accumbens, led to the hypothesis that the reinforcing or rewarding properties of these drugs are mediated by the mesolimbic dopamine system.

In most animal studies the nucleus accumbens is divided into two distinct parts: a shell, confined to the ventromedial margin of the nucleus, and a central core. The shell of the nucleus is associated with the limbic system and the core with the extrapyramidal motor system, and the information is mainly transmitted from shell to core. Although this dichotomy is well established in rodents, it is not clearly seen in humans (Haber et al., 1999; Lauer et al., 1996; Neto et al., 1998).

Nucleus Accumbens Tracing Protocol

Step I

The anterior and posterior dimensions of the nucleus accumbens must be defined so that the first tracing in the coronal plane can be made. The anterior and posterior extent of the nucleus accumbens is best appreciated in the sagittal plane (Fig: 9.). Once the sagittal plane is navigated so that these dimensions are appreciated, the coronal plane is navigated so that it intersects the anterior most aspect of the nucleus accumbens, seen in the sagittal plane.

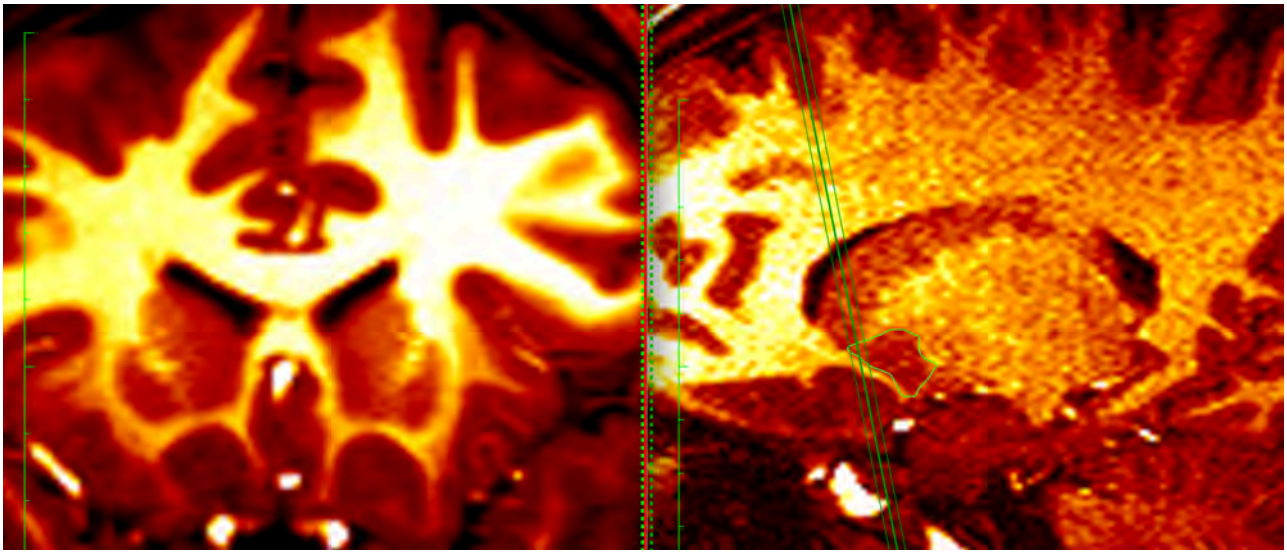

Figure: 9

The anterior and posterior extent of the nucleus accumbens is seen on the sagittal plane (right) with the green guideline intersecting the most anterior aspect of the accumbens. The coronal image (left) displays the corresponding location.

Step II

The first tracing is made in the coronal plane by drawing a line from the inferior corner of the anterior horn of the lateral ventricle, laterally, towards the medial edge of the putamen as it abuts the inferior aspect of the anterior limb of the internal capsule. A second line at the end of the first, is drawn inferiorly towards the edge of the gray white interface of the accumbens inferiorly.

From there the outline is followed superomedially towards the inferior corner of the anterior horn of the lateral ventricle (Fig: 10.).

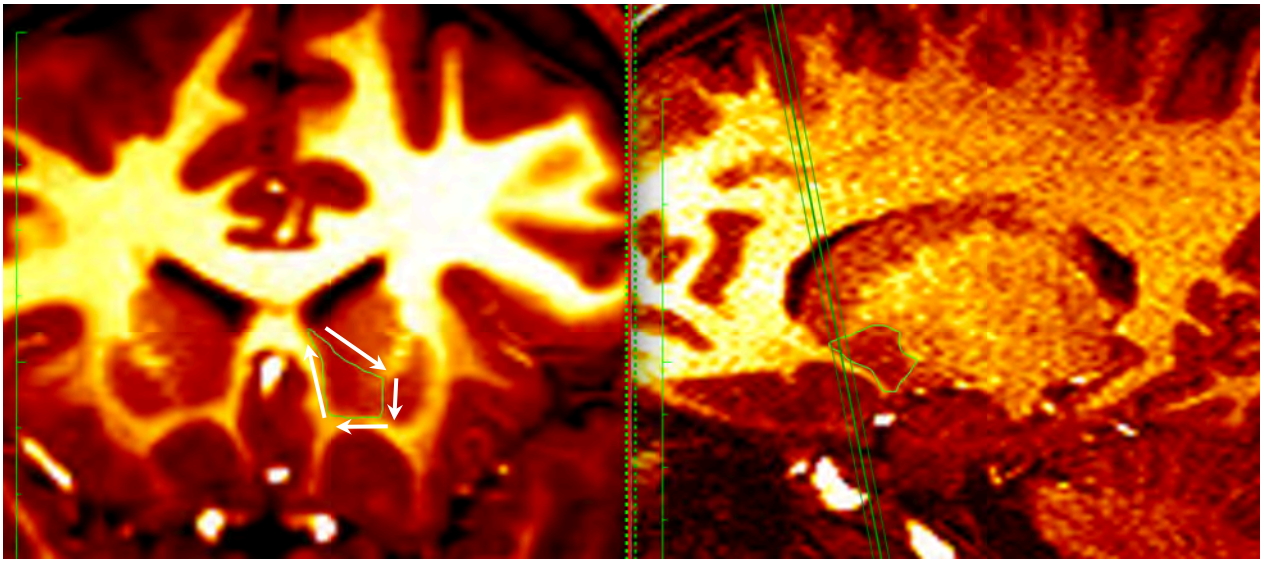

Figure: 10

Tracing of the anterior most aspect of the accumbens in the coronal plane (left). Sagittal section (right) demonstrates the relative position of the coronal plane, seen here intersecting the most anterior aspect of the accumbens. The arrows on the coronal image demonstrate the direction of the tracing, with the uppermost arrow marking the first line.

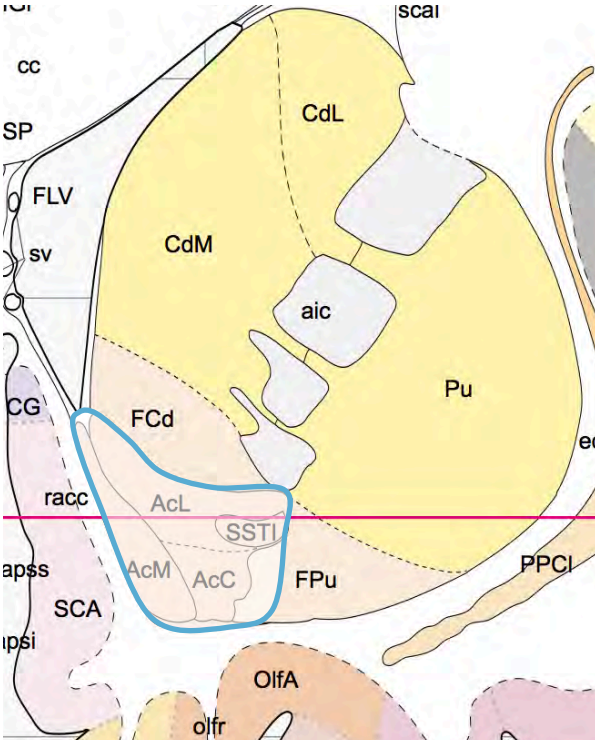

Figure: 11

Diagram demonstrating the tracing outline of the accumbens, and the inclusion of all the nuclear subgroups. The method of anatomical delineation described in Step II above reliably correlates with the known spatial arrangement of the nucleus accumbens from histological studies.

Step III

The same process as that described in Step II is followed while tracing from anterior to posterior. The last tracing in the series is done when the posterior boundary is being intersected by the guidelines in the sagittal plane.

Step IV

The tracings are reconstructed so that the volume may be calculated and the three-dimensional rendering can be inspected for anatomical continuity (Fig. 12.).

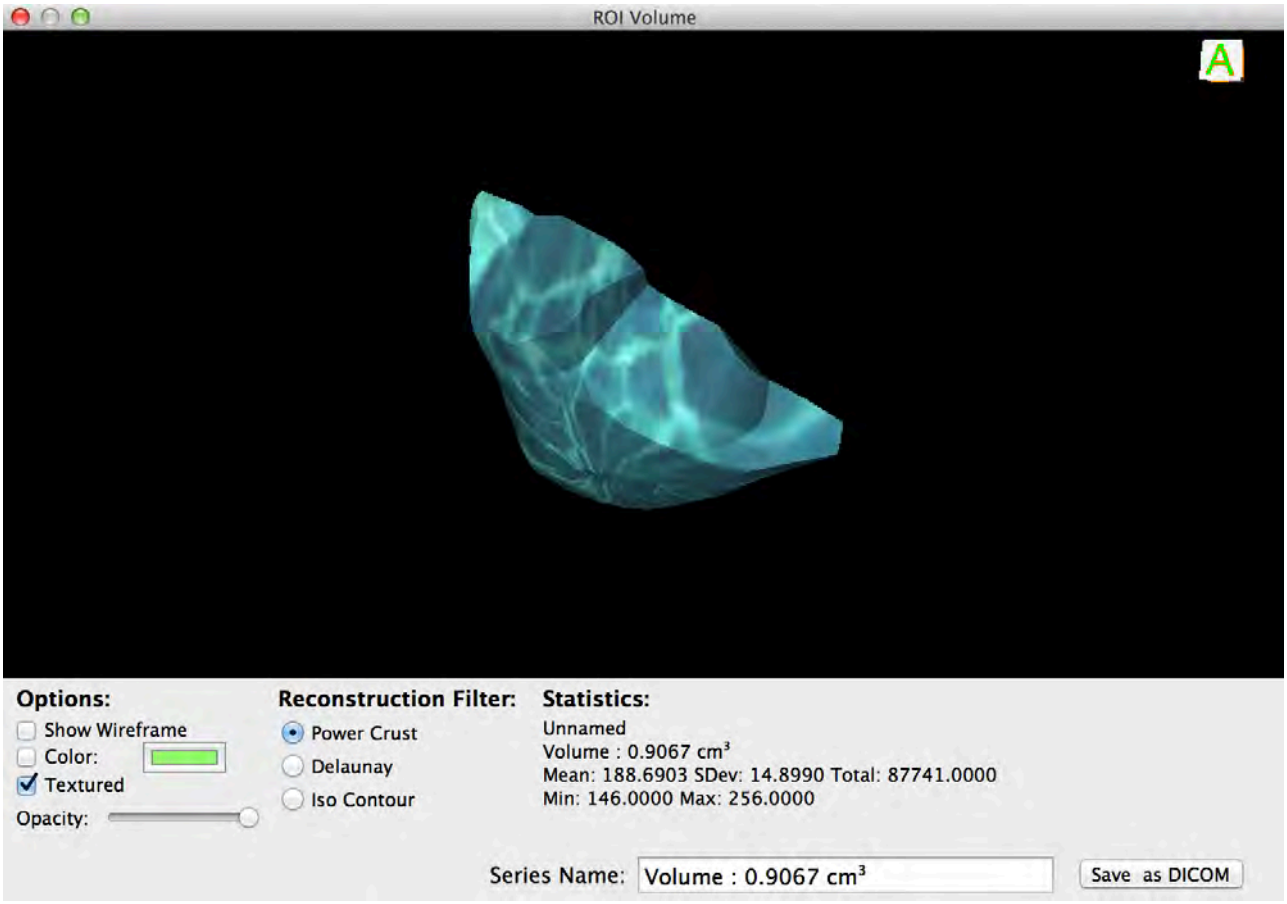

Figure: 12

Volumetric reconstruction of the accumbens demonstrating its anterior aspect. The volume of the tracing is shown in the bottom of the window.

The Putamen

Regional Anatomy

As mentioned above, the dorsal part of the striatum is composed of the caudate nucleus and the putamen. These two nuclear groups have the same origin, the same structure and also the same afferent fibre connections. They are largely separated by the internal capsule. The putamen forms together with the medially adjacent globus pallidus, the lentiform nucleus. The lentiform complex has the form of a Brasil nut and lies in the bottom of the insula. Between the lentiform nucleus and the insular cortex are situated, successively, the external capsule, the claustrum which is a thin sheet of grey matter, and the extreme capsule. The globus pallidus can be easily distinguished from the putamen by its pale colour in unstained sections (and signal intensity characteristics on imaging), which reflects the presence of a large number of myelinated fibres, and its relative darkness in Weigert-stained sections.

The caudate and putamen are traversed by numerous small bundles of thinly-myelinated small-diameter axons, which are mostly striatal afferents and efferents. The somatosensory and motor cortices project predominantly to the putamen. Their afferents establish a somatotopic pattern, in which the lower body is represented laterally and the upper body is represented medially. The motor cortex is unique in sending axons through the corpus callosum to the contralateral putamen, where they end with the same spatial ordering. The occipital and temporal cortices project to the tail of the caudate nucleus and to the inferior putamen.

The striatum also receives afferents, which are more crudely spatially organized, from the polysensory intralaminar thalamus. The cerebello-receptive nucleus centralis lateralis and the cerebello- and pallidoreceptive centromedian nucleus projects to the putamen. The aminergic inputs to the putamen are derived from the substantia nigra pars compacta, the retrorubral nucleus, the dorsal raphe nucleus and the locus coeruleus.

Putamen Tracing Protocol

Step I

As before with the caudate nucleus and nucleus accumbens, the boundaries of the nucleus must first be ascertained before the tracing of the nuclear outline can begin. The superior and inferior boundaries of the putamen can be easily defined on the coronal plane. The anterior and posterior boundaries can be demonstrated on the axial plane. The putamen is traced in the axial plane from superior to inferior. The first step is to align the coronal view with the medial aspect of the putamen just anterior to the genu of the internal capsule seen on the axial view, so that the superior limit of

the putamen can be visualized on the coronal plane (Fig. 13a.). The axial image is then navigated so that the green guidelines transect the anterior most aspect of the putamen (Fig. 13b.).

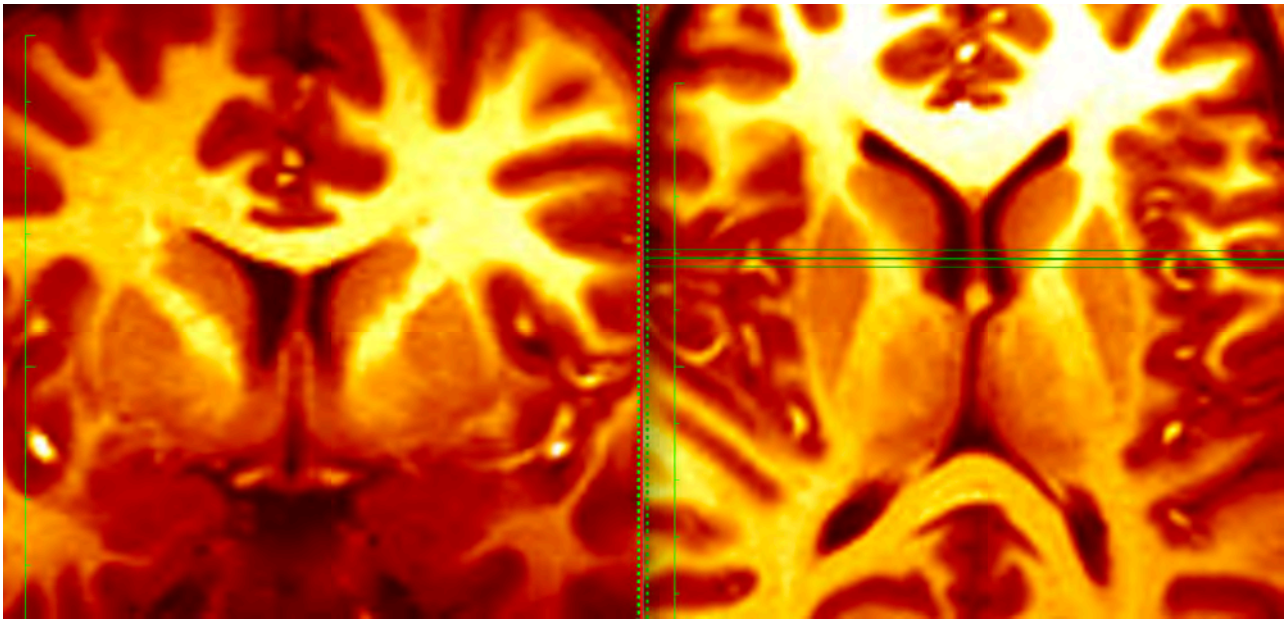

Figure: 13a

Simultaneous display of the coronal (left) and axial (right) views at the level of the diencephalon. The green guidelines are positioned just anterior to the genu of the internal capsule. This defines the most superior edge of the putamen on the coronal view.

Step II

The first tracing is made of the superior aspect of the putamen (Fig. 14a - d.). Consecutive tracings are then preformed, tracing the outline of the putamen from superior to inferior. The anterior boundary of the putamen is clearly defined by the anterior limb of the internal capsule. The medial aspect of the putamen is less clearly defined due to the close proximity of the globus pallidus, however the signal intensity differences between the putamen and the globus pallidus, accentuated with the CLUT filter, makes delineation of the medial boundary relatively simple.

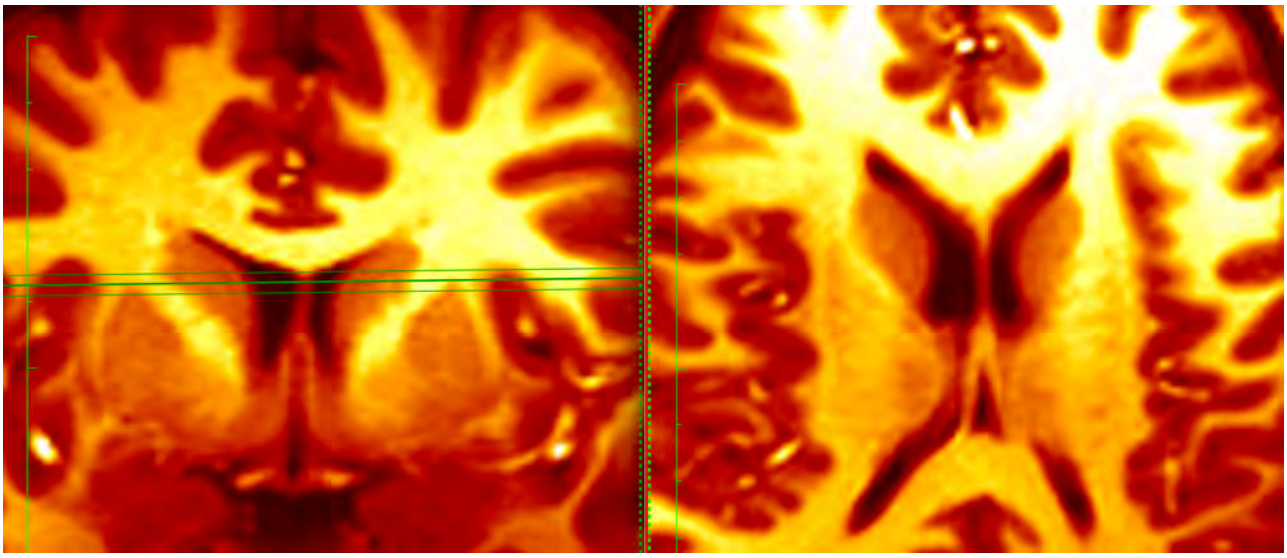

Figure: 13b

The axial view is now representative of the most tuperior aspect of the putamen. The green guidelines in the coronal view are seen transecting the superior tip of the putaminae.

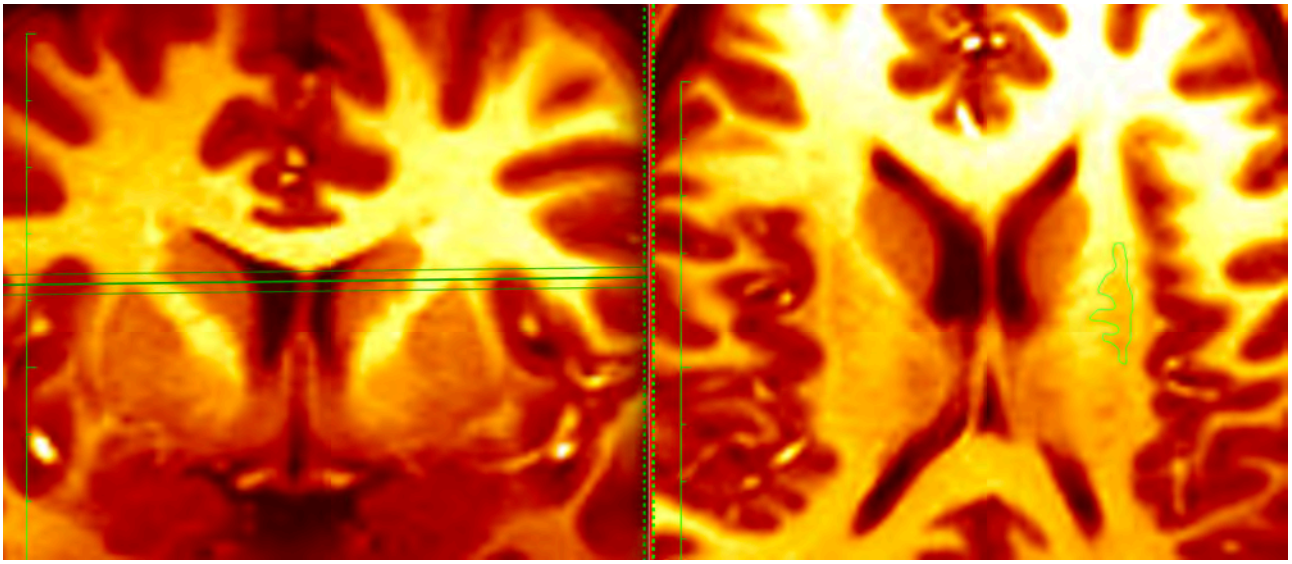

Figure: 14a

The first tracing of the superior aspect of the putamen is made (right).

Step III

Once the entire putamen has been traced, the volume is reconstructed for volume calculation and the inspection of anaotmical continuity (Fig. 15.). The putamen should appear as a “c-shaped” structure in the axial plane with a lateral convex border and medial concave border, with a large anterior aspect and a gradually tapering smaller posterior aspect.

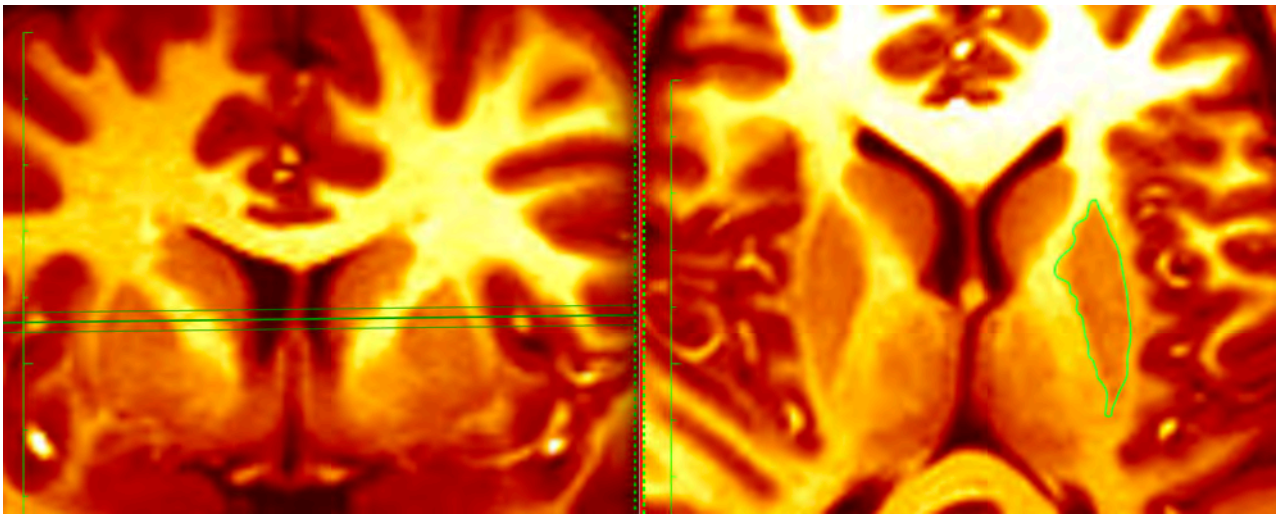

Figure: 14b

Consecutive tracing of the putamen.

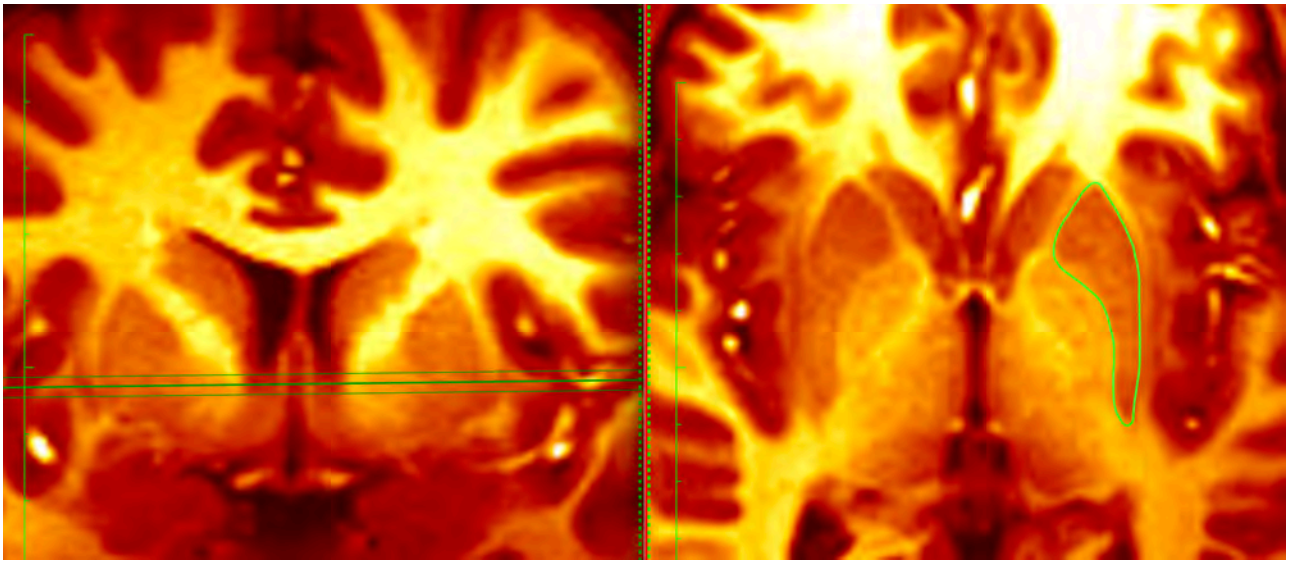

Figure: 14c

The lateral aspect of the globus pallidus as it abuts the medial aspect of the putamen becomes evident as the tracing continues inferiorly. The signal intensity cahrateristic clearly distinguish the relatively hyperintnese globus pallidus from the relatiely hypointnese putamen.

Special Considerations

The inferior edge of the putamen is seen far more posteriorly on the coronal image. It is therefore necessary to navigate posteriorly on the coronal view to guide the inferior depth of the tracing in the axial view. Once the guideline intersects the inferior most point of the putamen, the final tracing can be made.

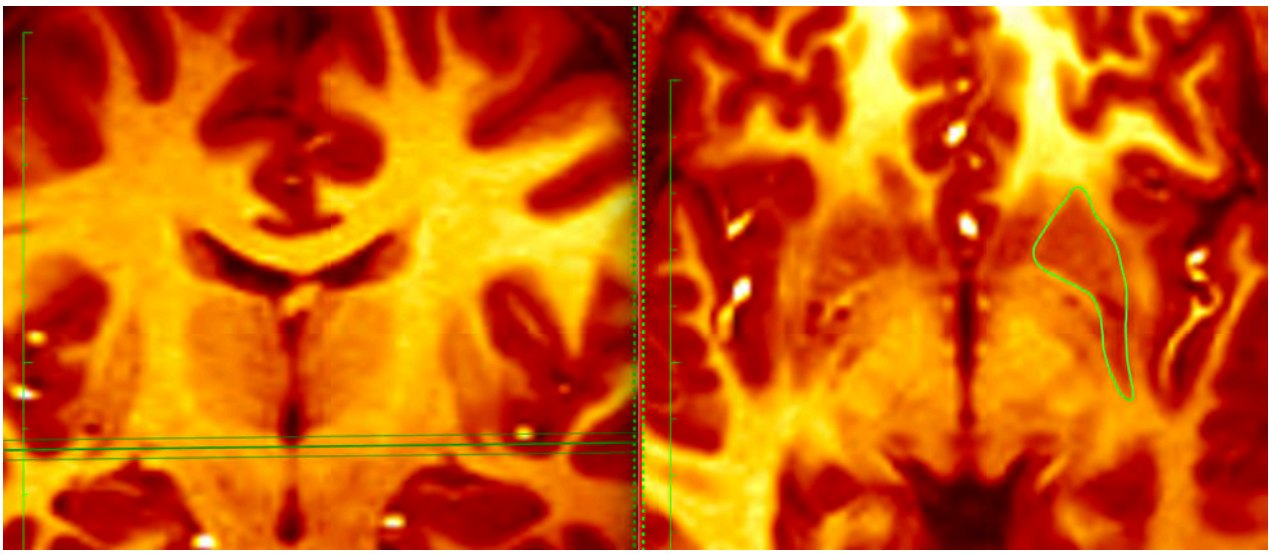

Figure: 14d

The inferior most aspect of the putamen is visualised on the coronal plane far more posteriorly. The coronal plane is therefore navigated as nescessary to obtain continued visualisation of the nuclear outline.

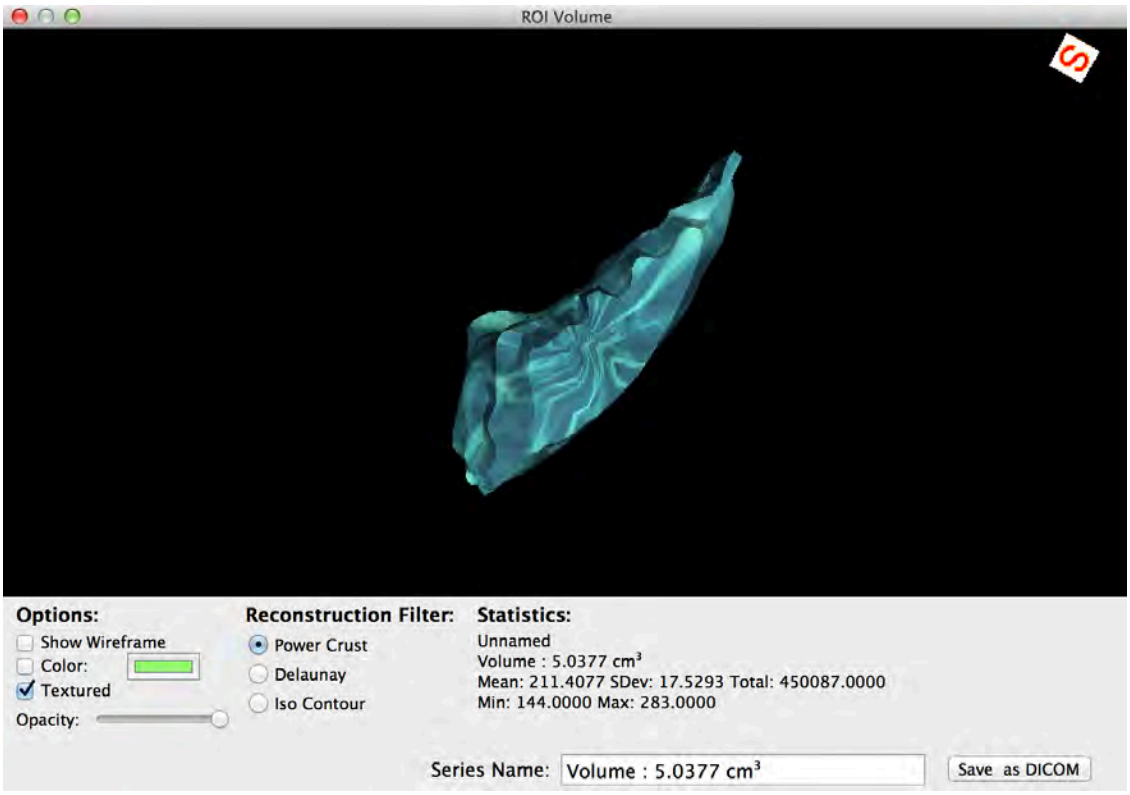

Figure: 15

Vomutric reconstruction demonstrating suprior view of the putamen. The three-dimensional model deomstrates the prototypical concave lateral border and convex medial border, confirming anatomical continuity. Volume is demonstrated in the bottom corner of the display.

The Globus Pallidus / Pallidal Complex

Regional Anatomy

The globus pallidus lies medial to the putamen and lateral to the internal capsule. It consists of two segments, lateral (external) and medial (internal), which are separated by an internal medullary lamina, and which have substantially different connections. Both segments receive large numbers of fibres from the striatum and subthalamic nucleus. The lateral segment projects reciprocally to the subthalamic nucleus as part of the ‘indirect pathway’. The medial segment is considered to be a homologue of the pars reticulata of the substantia nigra, with which it shares similar cellular and connectional properties. Together, these segments constitute the main output of the basal ganglia to other levels of the neuraxis, principally to the thalamus and superior colliculus.

The cell density of the globus pallidus is less than one-twentieth of that of the striatum. The morphology of the majority of cells is identical in the two segments. They are large multipolar GABAergic neurones that closely resemble those of the substantia nigra pars reticulata. The dendritic fields are discoid, with planes at right angles to incoming striatopallidal axons, each of which, therefore, potentially contacts many pallidal dendrites en passant. This arrangement, coupled with the diameters of the dendritic fields (500 μm), suggests that a precise topographical organization is unlikely within the pallidum.

Striatopallidal fibres are of two main types. They project either to the lateral or the medial pallidal segment. Those projecting to the lateral segment constitute the beginning of the so-called ‘indirect pathway’. They utilize GABA as their primary transmitter and also contain enkephalin. Efferent axons from neurones in the lateral segment pass through the internal capsule in the subthalamic fasciculus, and travel to the subthalamic nucleus. Striatopallidal axons destined for the medial pallidum constitute the so-called ‘direct pathway’. Like the indirect projection, these also utilize GABA as their primary transmitter but they also contain substance P and dynorphin, rather than enkephalin. Efferent axons from the medial pallidal segment project through the ansa lenticularis and fasciculus lenticularis.

The former runs round the anterior border of the internal capsule and the latter penetrates the capsule directly. Having traversed the internal capsule, both pathways unite in the subthalamic region, where they follow a horizontal hairpin trajectory, and turn upwards to enter the thalamus as

the thalamic fasciculus. The trajectory circumnavigates the zona incerta and creates the so-called ‘H’ fields of Forel. Within the thalamus, pallidothalamic fibres end in the ventral anterior and ventral lateral nuclei and in the intralaminar centromedian nucleus. These in turn project excitatory (presumed glutamatergic) fibres primarily to the frontal cortex, including the primary and supplementary motor areas. The medial pallidum also projects fibres caudally to the pedunculopontine nucleus. This lies at the junction of the midbrain and the pons, close to the superior cerebellar peduncle, and corresponds approximately to the physiologically identified ‘mesencephalic locomotor region’.

Globus Pallidus Tracing Protocol

Step I

The superoinferior and anteroposterior dimensions of the GP is readily defined in the coronal and axial planes. The medial boundary is defined by the lateral aspect of the internal capsule, and the lateral boundary by the medial edge of the putamen. The GP appears more hyprintense when compared to the putamen, and is thus easily distinguished. To conduct the first tracing, the coronal plane is navigated until the internal and external segments of the GP can be visualized (Fig. 16a. & b). The axial plane is the navigated to intersect the most superior boundary of the GP. The first tracing can then be made in the axial plane.

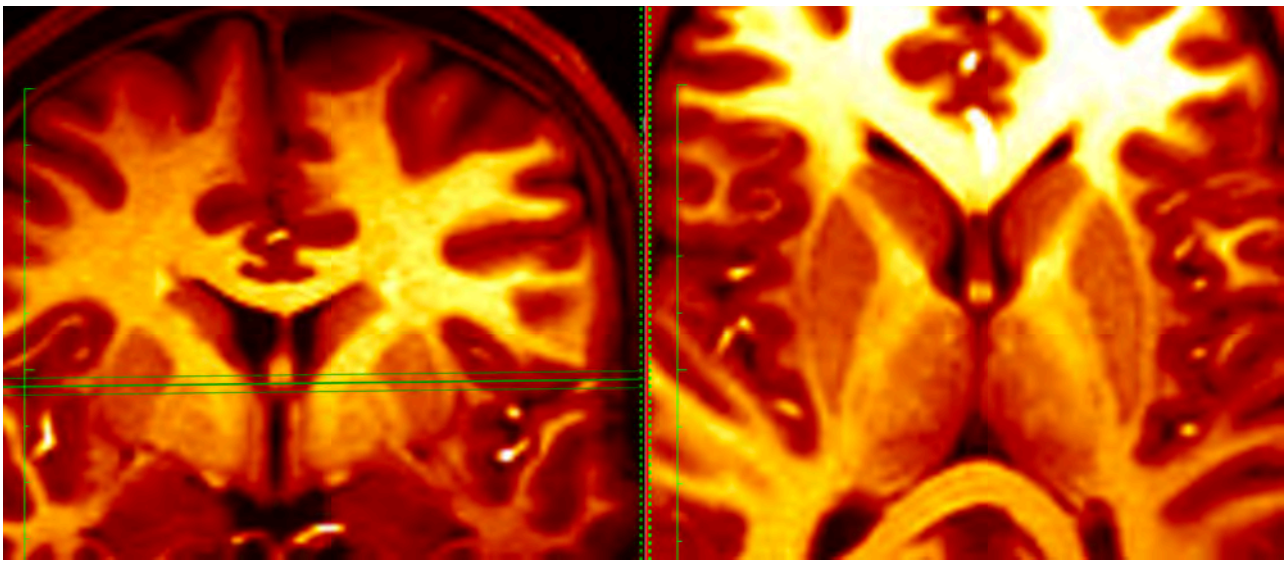

Figure: 16a

Simultaneous display of the coronal (left) and axial (right) sections through the basal ganglia. The green guidelines are seen intersecting the most superior aspect of the globus pallidus. The axial sectoin corresponds to the level indicated in the coronal plane. The internal and external segments are visible in the coronal plane.

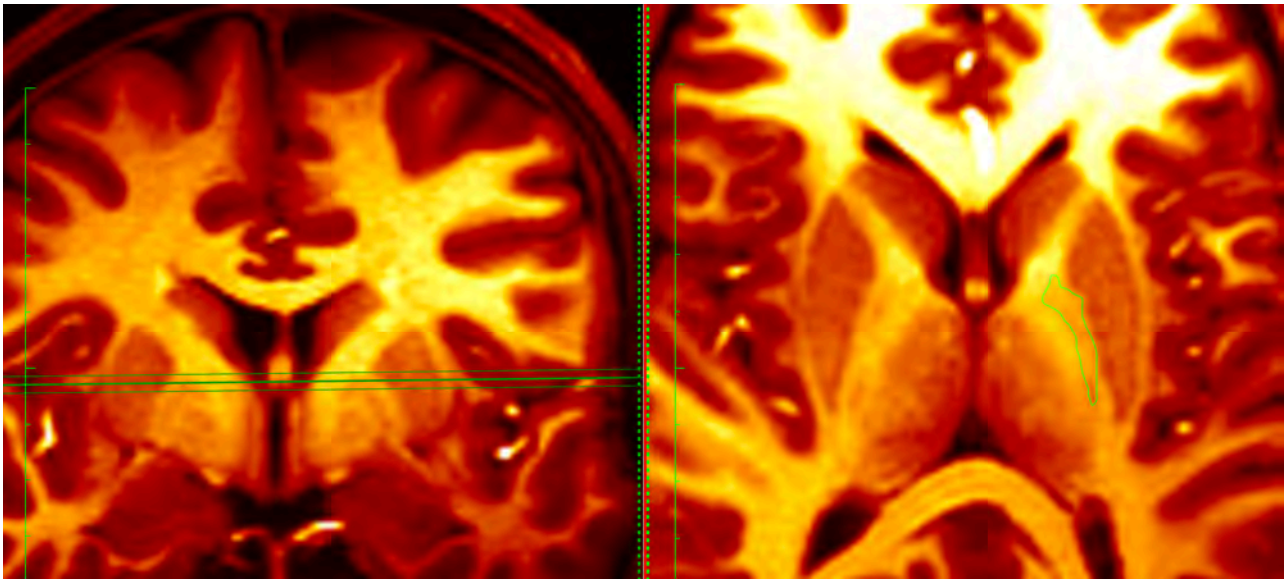

Figure: 16b

The first tracing of the superior most aspect of the globus pallidus is made.

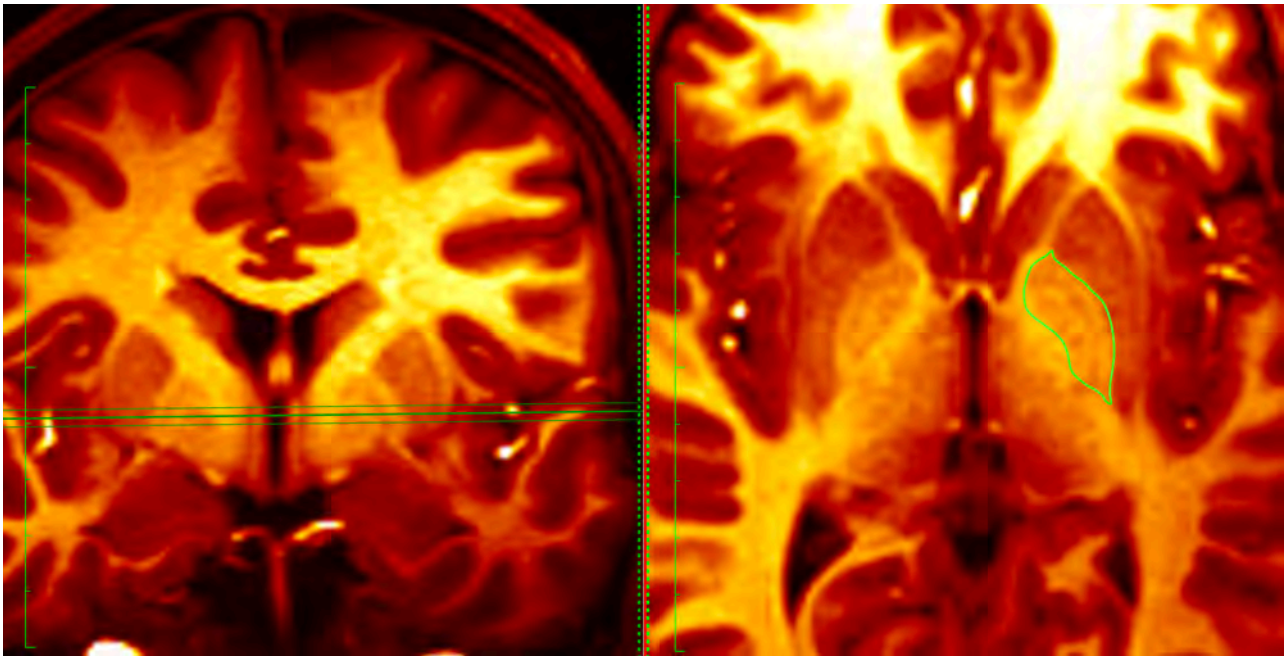

Figure: 17

Consecutive tracing

Step II

Once the tracing is complete, the volume is reconstructed for inspection of anatomical continuity and volume calculation (Fig. 18).

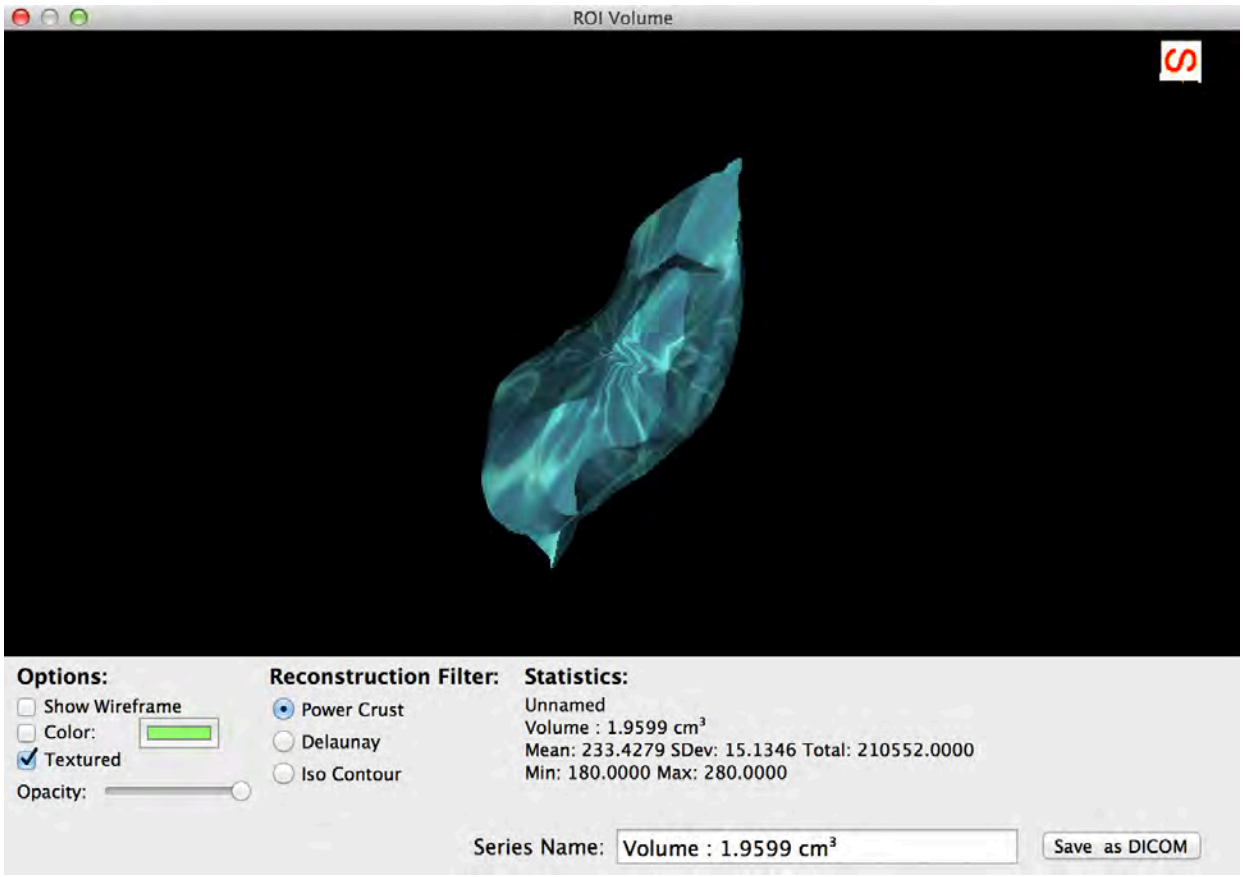

Figure: 18

Volumetric reconstruction of the globus pallidus. The classical lateral convex and medial concave morphology of the structure is observed. The volume is shown in the bottow right of the window.

Special Considerations

At 3T, the respective internal and external segments of the GP can be visualized, however it would be practically impossible to trace these segments individually with any measure of accuracy. Therefore it is advisable that the entire pallidal complex is traced as a whole.

The Amygdala

Regional Anatomy

The amygdala is a highly differentiated and heterogeneous structure located in the medial part of the temporal lobe (Fig 19). The amygdala is neither a structural nor a functional unit (Swanson et al., 1998) but rather a region where distinct structures belonging to different systems are in close contact to each other. Amygdaloid nuclei can be classified into four functional systems: accessory olfactory, main olfactory, autonomic and frontotemporal cortical.

Subdivisions:

Donkelaar et al., (2011) summarizes the subdivisions of the amygdala by noting that in most mammals, the amygdala or amygdaloid complex forms the floor of the telencephalon between the olfactory tubercle and the hippocampus. The amygdaloid complex comprises several irregularly shaped subdivisions, which gives it a thalamic appearance (Amaral 1987). The cytoarchitectonic organization of the amygdaloid complex has been extensively studied, beginning with the studies of Volsch et al., (1906, 1910) on insectivores and primates. Brockhaus et al., (1938) subdivided the human amygdala into numerous small subdivisions. Most recent studies follow the American school of comparative neurology (Johnston et al., 1923; Crosby et al., 1941; Lauer et al., 1945), according to which the amygdaloid complex is divided into a few nuclei only, including a corticomedial (the cortical, central and medial nuclei) and a basolateral (the basal and lateral nuclei) group. In contrast, extensive quantitative comparative studies led Stephan et al., (1977) to separate the cortical amygdaloid nucleus from the corticomedial group and to assign it to the basolateral group.

[^{3}H]-Thymidine data on the time of neuron origin in rodents and rhesus monkeys support such a subdivision of the amygdala (Donkelaar et al., 1979; Bayer et al., 1980; McConnell et al., 1983; Bayer et al., 1987; Kordower et al., 1992). Braak and Braak (1983) studied the neuronal types in the human basolateral amygdala. The amygdala is composed of pallial and subpallial parts (Lammers et al., 1972; Stephan et al., 1977; Amaral et al., 1987; Heimer et al., 1991; de Olmos et al., 2004). The basolateral part and the associated cortical amygdala form the pallial part, whereas the central and medial amygdaloid nuclei form the subpallial part. The centromedial amygdala forms a continuum with the bed nucleus of the stria terminalis, known as the extended amygdala (Alheid et al., 1988; Heimer et al., 1997b; de Olmos et al., 2004). The centromedial amygdala and the rest of the extended amygdala contain a rich assortment of peptides and neurotransmitters (Price et al., 1987; Amaral et al., 1992; de Olmos et al., 2004). The basolateral group lacks the dense innervation by peptidergic fibres of the centromedial amygdala. The amygdala has a role in emotions through participation in two key functions: (1) processing signals

about the emotional significance of the environment, and (2) interfacing with autonomic motor systems for the expression of emotions (LeDoux et al., 2000a). These functions are processed along distinct pathways, linking the amygdala with orbitofrontal, medial prefrontal and anterior temporal cortices, and central autonomic structures.

Johnston (1923) argued that the bed nucleus of the stria terminalis forms a continuum with the central and medial amygdaloid nuclei. Much later, the similarities between the bed nucleus of the stria terminalis and the centromedial amygdala were rediscovered in tract-tracing studies by José de Olmos (de Olmos et al., 1972; de Olmos and Ingram 1972) and in immunohistochemical studies (see de Olmos 2004). Cell columns accompany the stria terminalis along its dorsal course. De Olmos and collaborators appreciated that such cell columns also accompany the ventral amygdalofugal pathway along its course through the sublenticular part of the substantia innominata into the ventral forebrain. The whole continuum, i.e. the centromedial amygdala with its extensions both alongside the stria terminalis and through ventrally located cell columns in the substantia innominata, has been labelled the extended amygdala. The extended amygdala has been further subdivided into the central extended amygdala and the medial extended amygdala (Alheid et al., 1995; Heimer et al., 1997b; de Olmos et al., 2004).

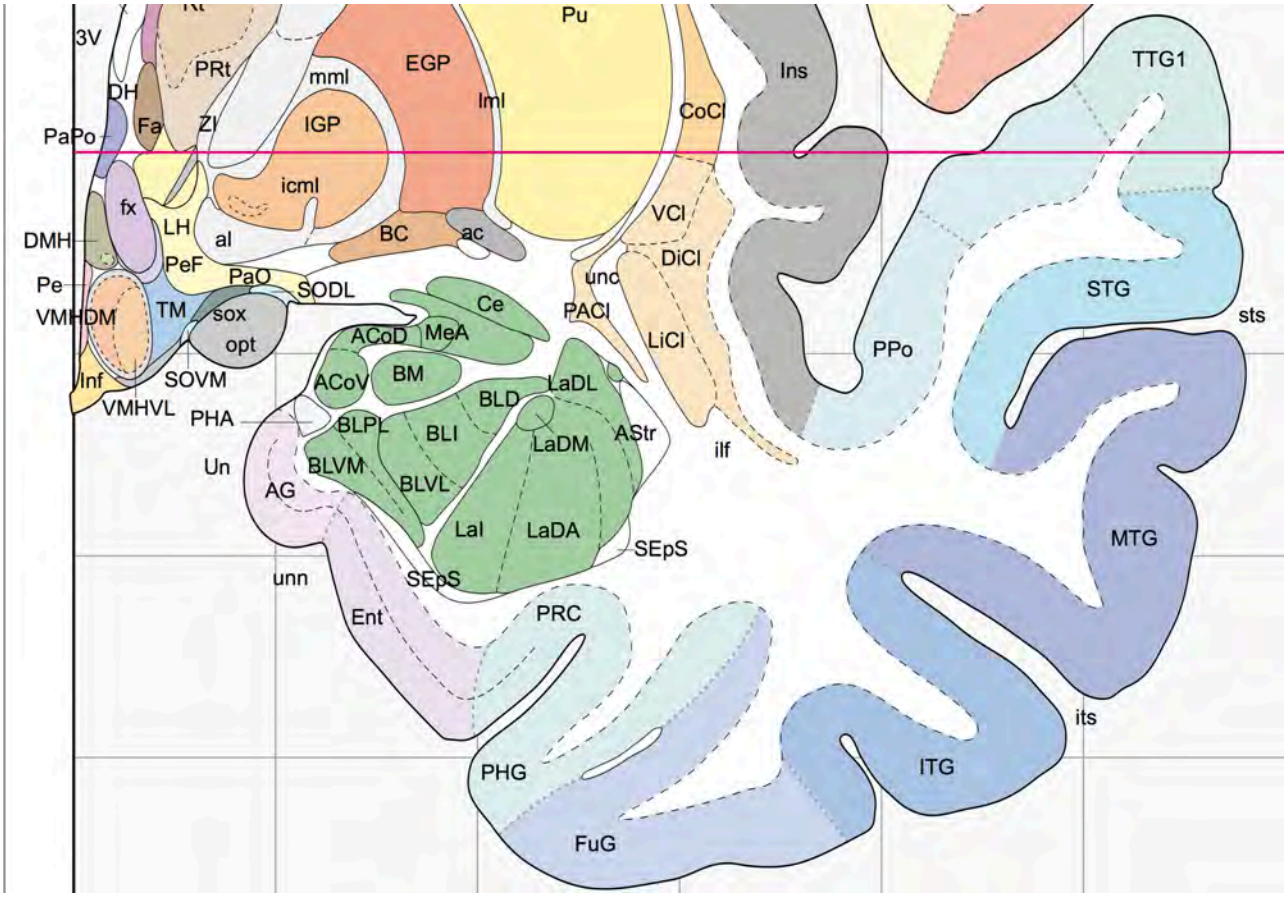

Figure: 19

Illustration of a coronal section through the body of the amygdala (green) demonstrating all the nuclear subdivisions: ACoD: anterior cortical amygdaloid nucleus dorsal part; ACoV: anterior cortical amygdaloid nucleus ventral part; AStr: amygdalostriatal transit area; BLD: basolateral amygdaloid nucleus, dorsal (magnocellular) part; BLI: basolateral amygdaloid nucleus, intermediate part; BLPL: basolateral amygdaloid nucleus, paralaminar part; BLVL: basolateral amygdaloid nucleus, ventrolateral part; BLVM: basolateral amygdaloid nucleus ventromedial part; BM: basomedial amygdloid nucleus; Ce: central amygdaloid nucleus; LaDA: lateral amygdaloid nucleus, dorsal anterior part; LaDL: lateral amygdaloid nucleus, dorsolateral part; Lal: lateral amygdaloid nucleus intermediate part; LaDM: lateral amygdaloid nucleus dorsomedial part; MeA: medial amygdaloid nucleus, anterior part

Amygdala Tracing Protocol

Step I

The amygdala is orientated in a slope starting inferiorly in its anterior aspect and sloping superiorly towards its posterior aspect. The amygdala is essentially encapsulated in the white matter anterior and superior to the hippocampus proper, separated from it by the slit like space of the temporal horn of the lateral ventricle (Fig. 20.). The first tracing is made by determining the most anterior aspect of the amygdala in the sagittal plane. The contrast of the amygdala is lighter than the overlying gray matter, but darker than the white matter in which it is encapsulated. It is thus possible to distinguish the most anterior aspect of the amygdala in the coronal plane (Fig. 21.).

Step II

The second tracing of the amygdala is the easiest to preform. The entire nucleus can easily be discerned from the overlying entorhinal cortex, as this section is usually through the bulk of the body of the amygdala (Fig. 22.).

Step III

Consecutive tracings of the amygdala are difficult because the nucleus begins to slope superiorly, changing orientation, and also because various structures with different signal intensity characteristics such as the CSF in the temporal horn of the lateral ventricle, the ventricular ependyma, the thin white matter covering of the hippocampus proper the alveus, must now be distinguished from the amygdala (Fig. 23 – 25.).

Step IV

As the amygdala slopes superiorly, it becomes isolated in the white matter forming the roof of the temporal horn of the lateral ventricle, clearly distinguishable from the starkly hypointnese CSF below it. Once the tracing is complete, the volume is reconstructed for inspection of anatomical continuity and volume calculation.

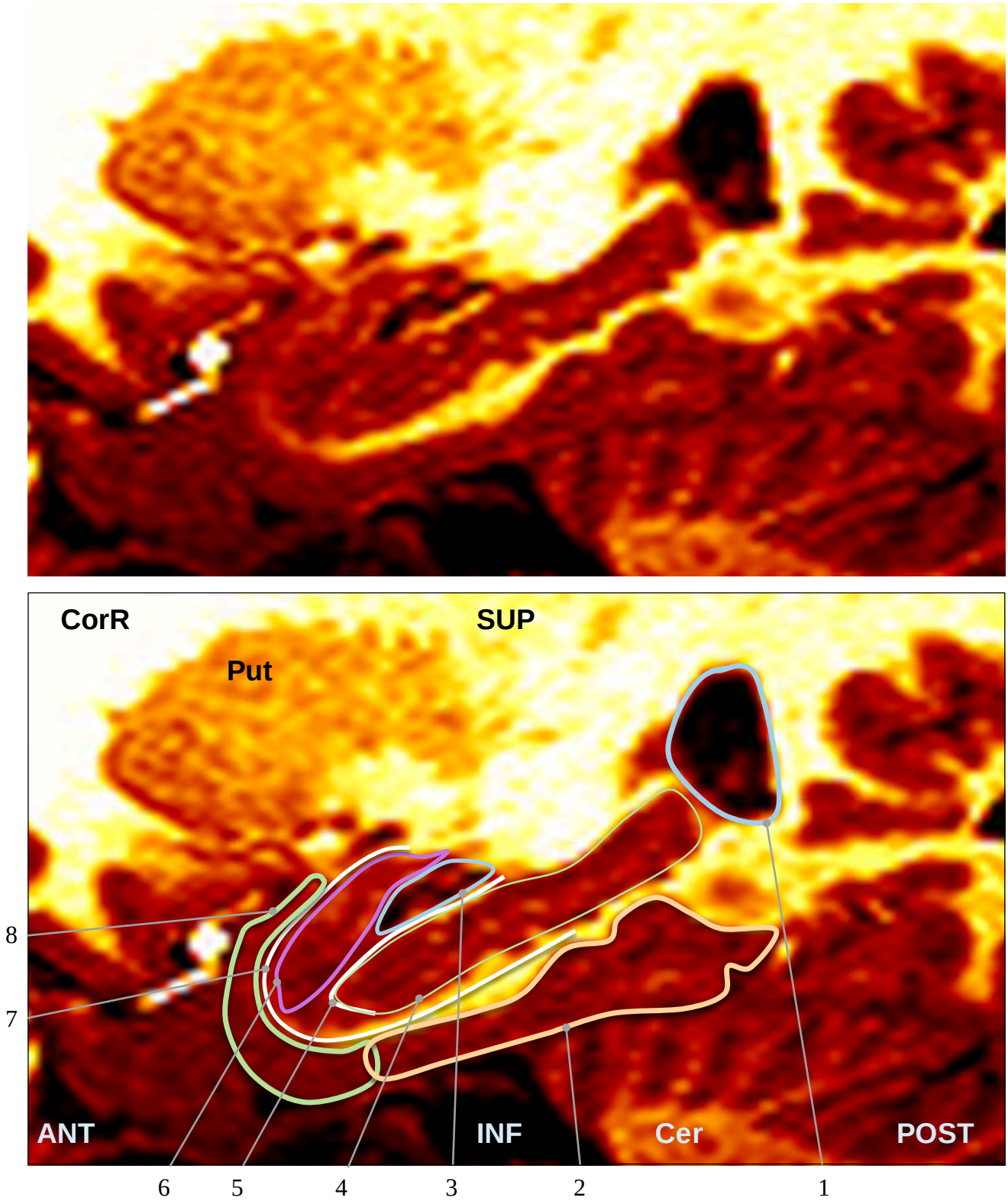

Figure: 20

Sagittal section through the temporal lobe demonstrating the anteroposterior relationships of the temporal limbic structures.

CorR: corona radiata; Put: putamen; SUP: superior; ANT: anterior; INF: inferior; POST: posterior; Cer: cerebellum; 1: atrium of the lateral ventricle; 2: entorhinal cortex of the parahippocampal gyrus; 3: CSF cleft between the inferior aspect of the amygdala and the superior aspect of the pes hippocampi; 4: hippocampal formation; 5: alveus; 6: amygdala; 7: white matter of the temporal lobe interposing the uncus and the amygdala; 8: gray matter of the uncus

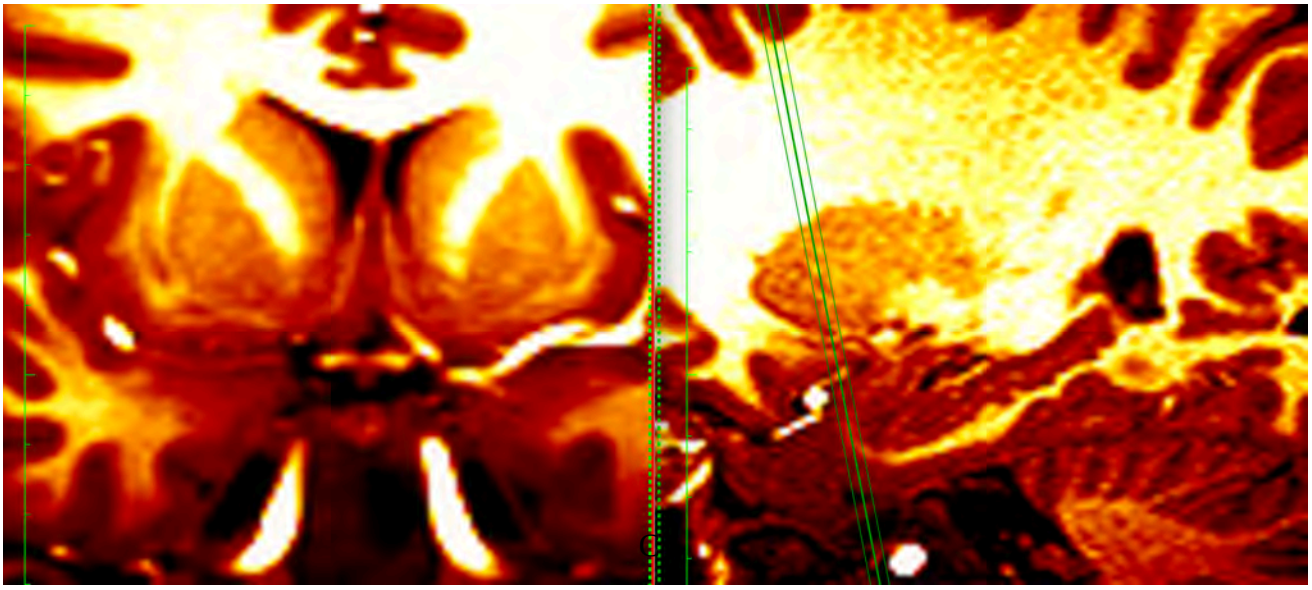

A B

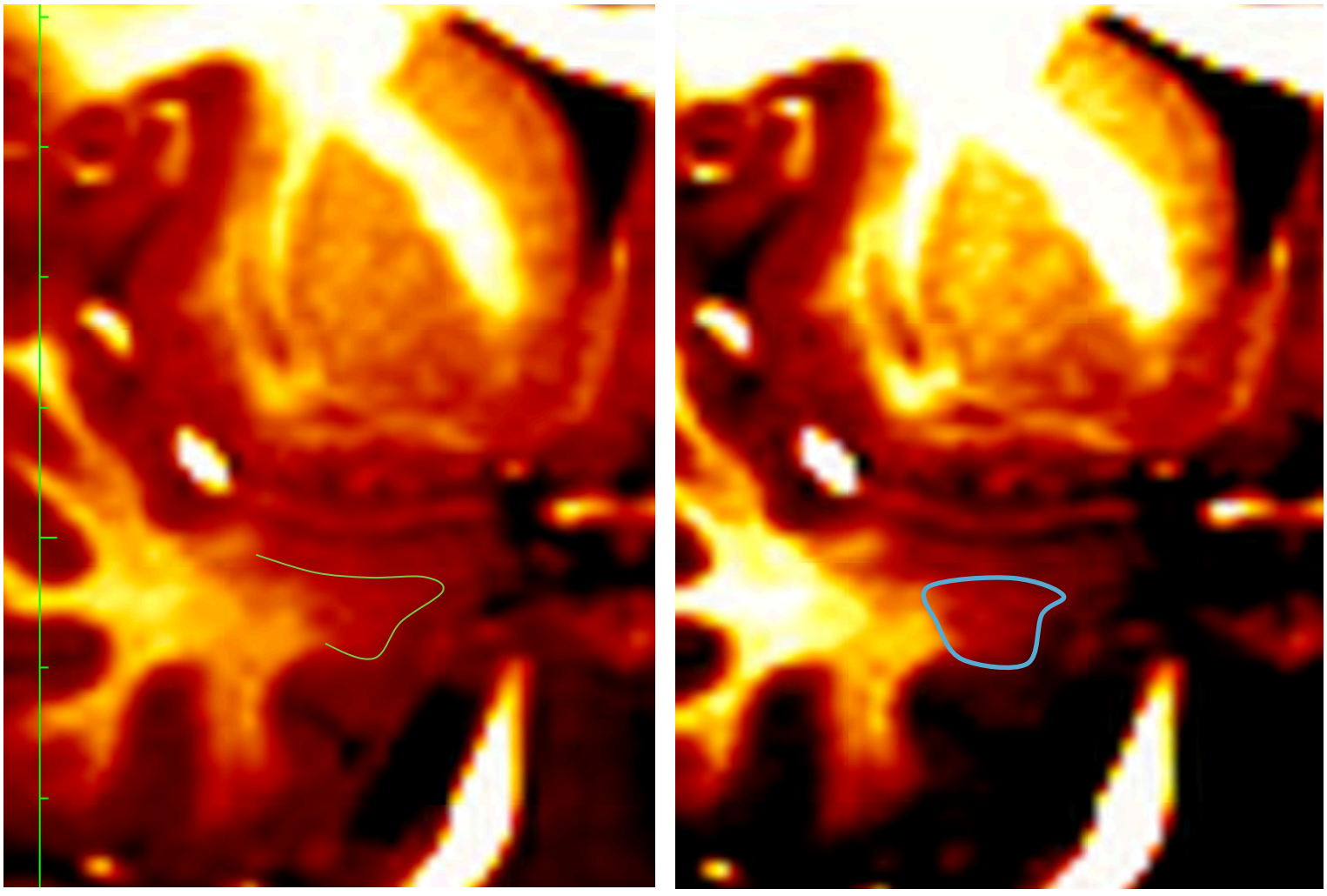

C D

Figure: 21

A) Coronal, B) Sagittal viw through the anterior most aspect of the amygdala indicated by the green guidelines in (B). C) magnified view of the uncus, green line indicating the interface between entorhinal cortex and amygdala (which is more hyperintnese due to the vast amount of white matter running into the amygdala). D) contrast exaggerated view revealing the amygdaloid nucelus as a separate entity.

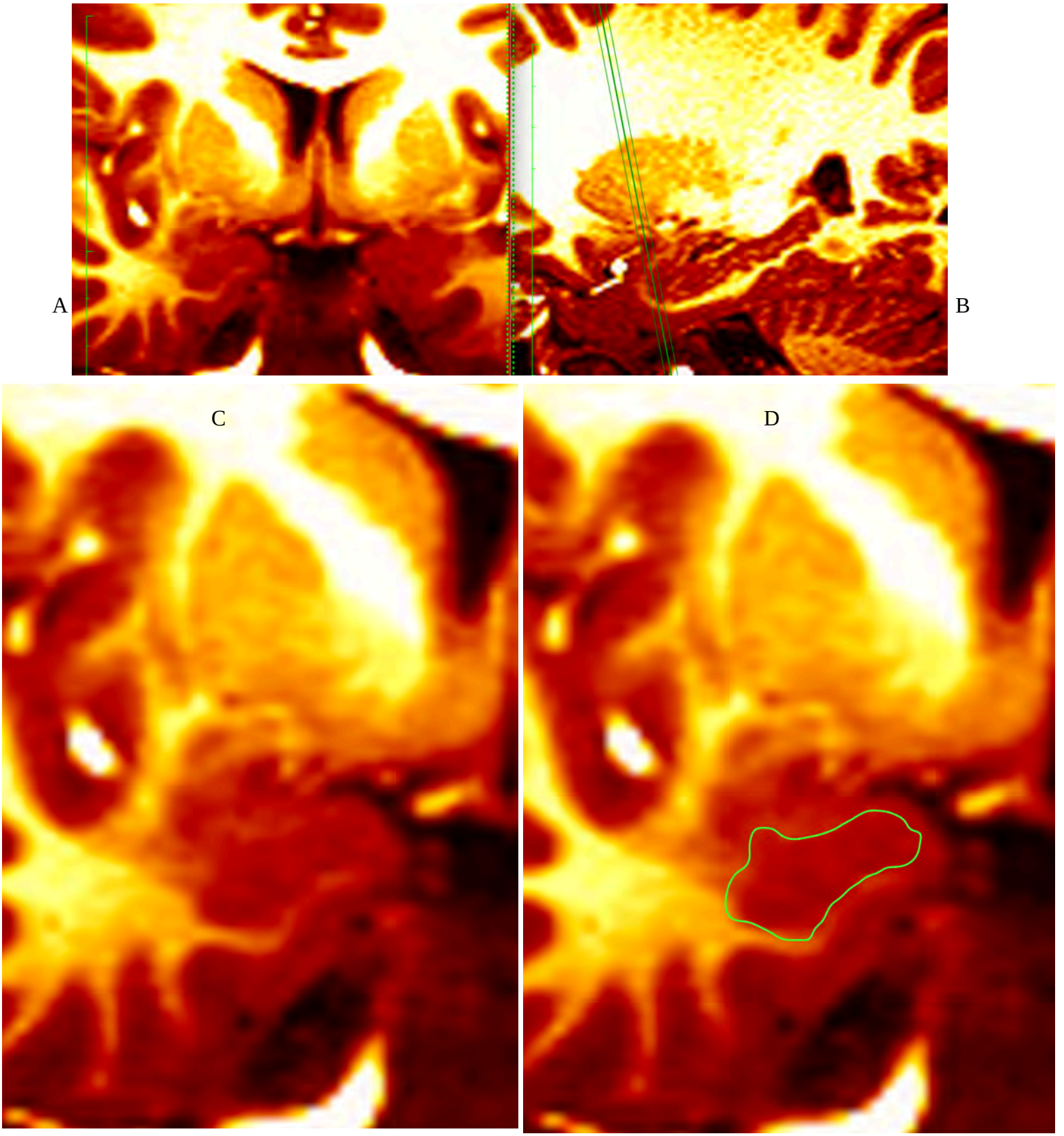

Figure: 22

Coronal section through the body of the amygdaloid nucleus (A, C & D). B demonstrates the relative position of the the coronal section. Close-up sections (C & D) demonstrate the amygdala encapusulated in the white matter of uncus, with the entorhinal cortex overlying it. D, demonstrates the second tracing.

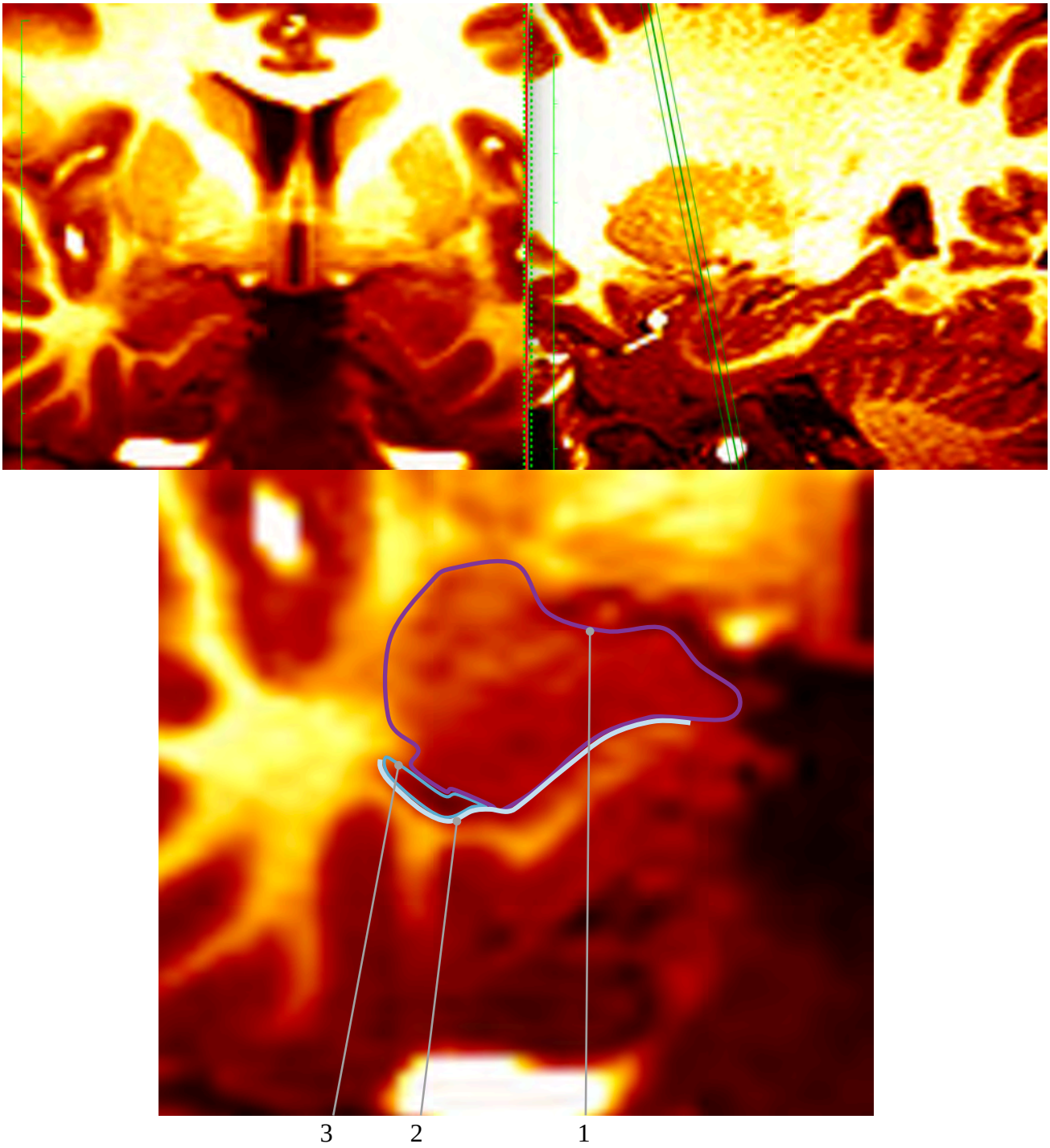

Figure: 23

Consecutive tracing of the amygdala demonstrate its complex spatial organisation relative to the temporal horn of the lateral ventricle, and the hippocampal fomration. 1: outline of the amygdala; 2: ventricular ependyma; 3: Outline of the anterior most aspect of the temporal horn of the lateral ventricle.

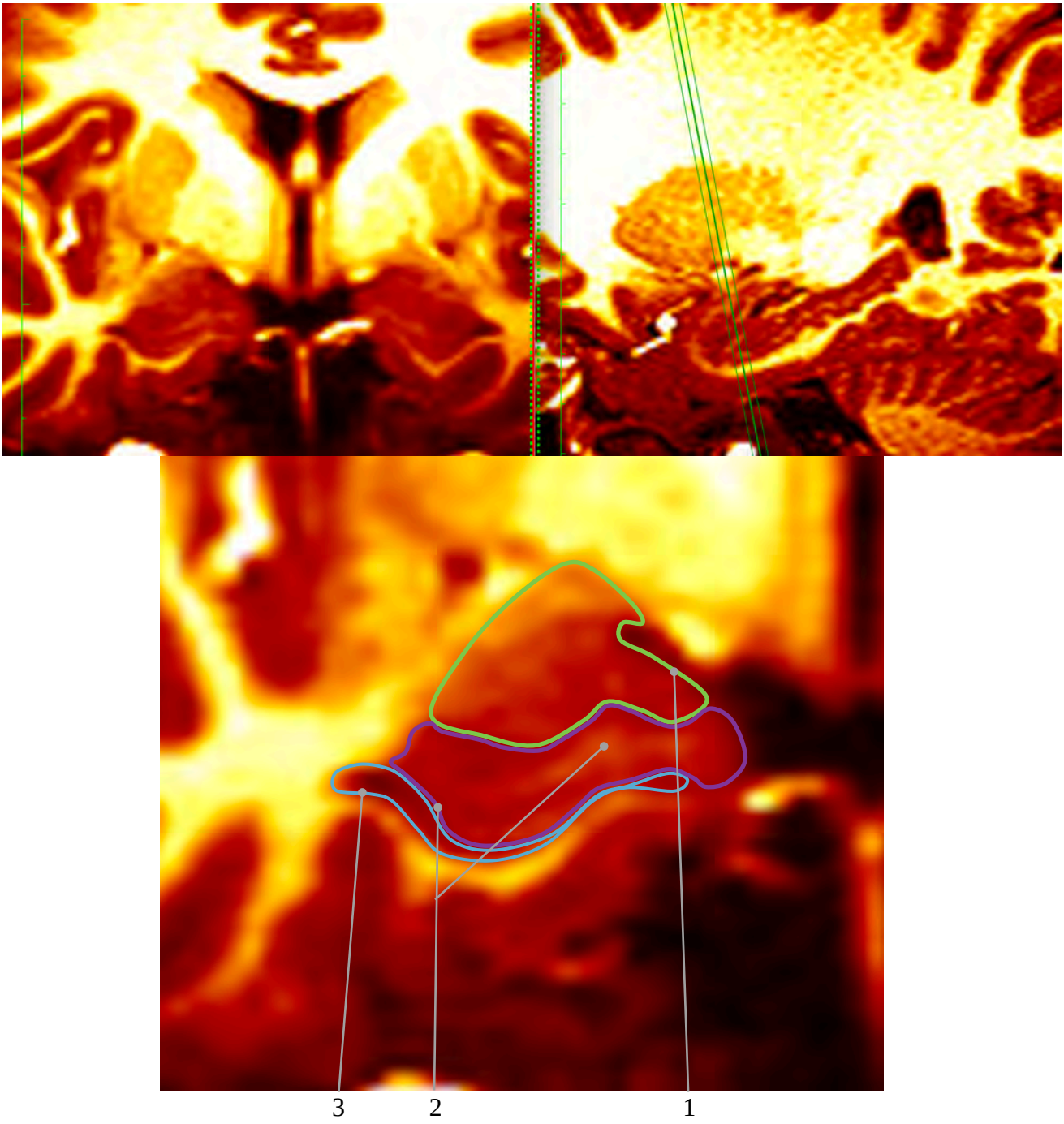

Figure: 24

Consecutive tracing of the amygdala. The coronal plane now intersects the pes hippocampi (2), the temporal horn of the lateral ventricle (3) and the amygdala (1). It become more difficult to differentiate the amygdala from the hippocampus below. Fortunately, due to the extensive white matter connectivity of the amygdala, its contrast is lighter than that of the underlying hippocampus, thus wit exaggerating the contrast slightly, these boundaries are discernable.

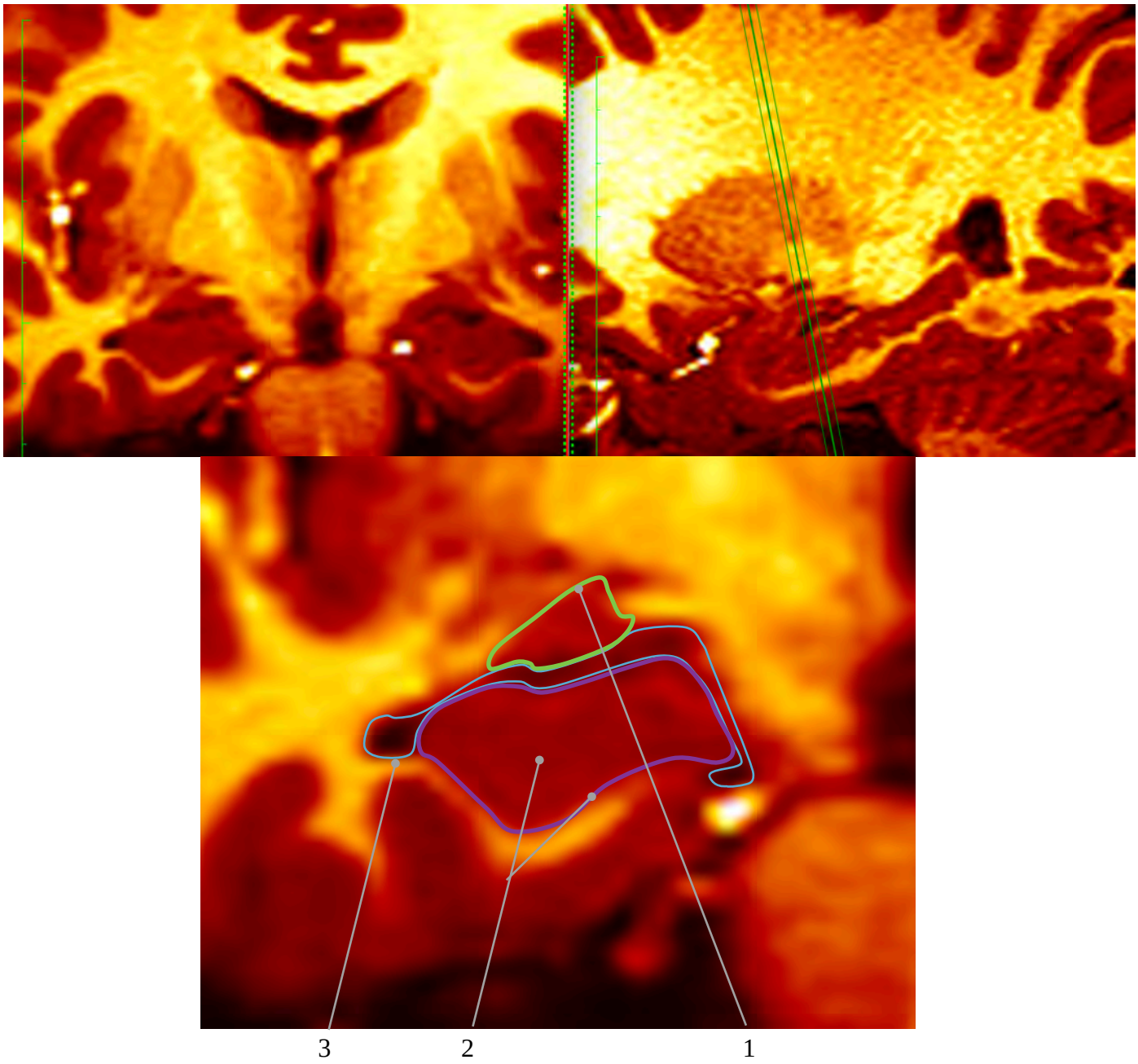

Figure: 25

Posterior most tracing of the amygdala. As the postrior aspect of the amygdala (1) slopes superiorly into the roof of the temporal horn of the lateral ventricle, it tapers down. The temporal horn of the lateral ventricle (3) is clearly visible separating the hippocampus (2) which occupies the floor of the temporal horn, with the tail of the amygdala.

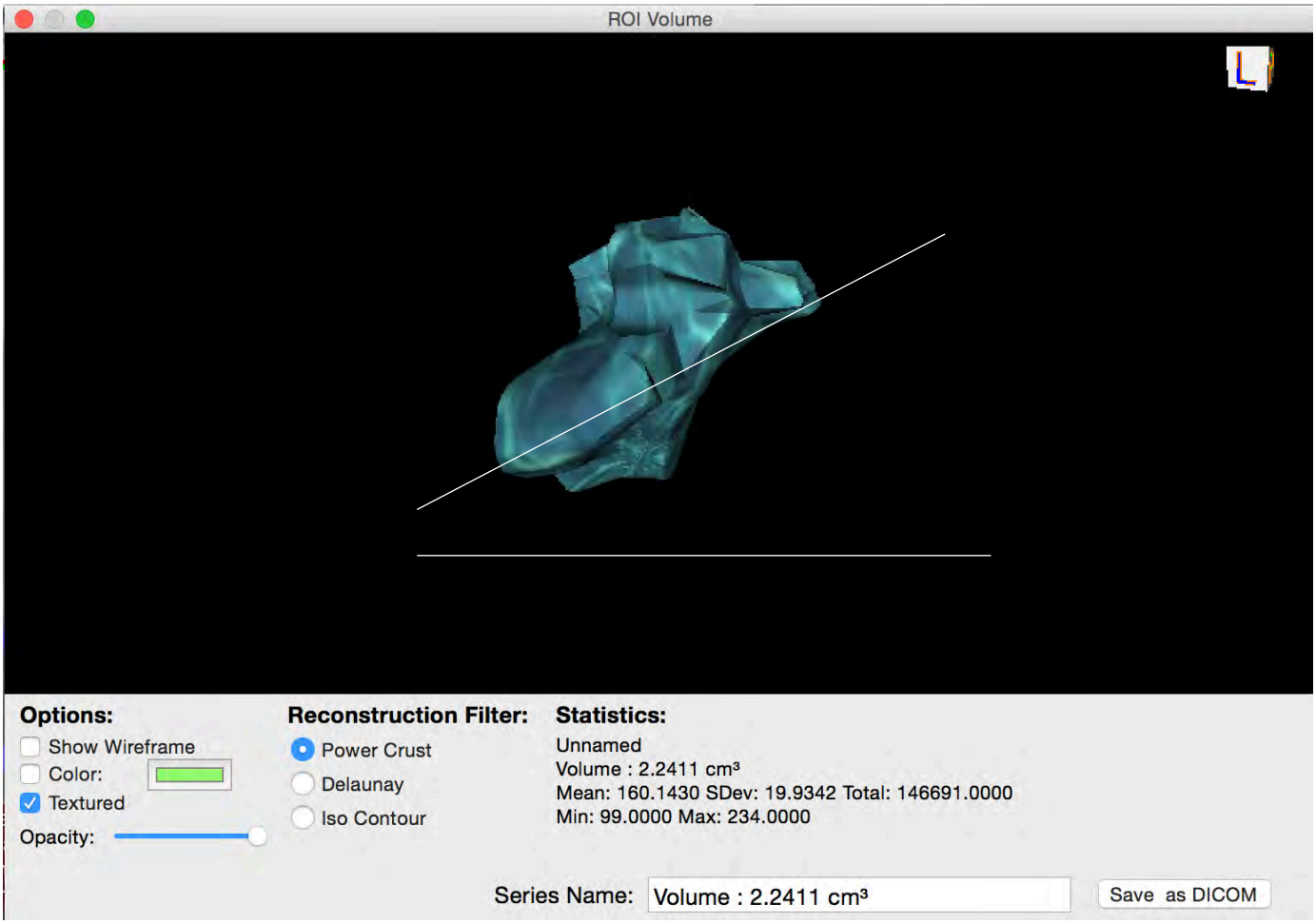

Figure: 26

Volumetric reconstruction of the amygdala. Inferior line denotes the horizontal axis. Superior line denotes the longitudinal axis of the amygdala from anterior to posterior. Volume is shown in the bottom right corner.

Special Considerations:

The sectional anatomy of the amygdala and related structures is highly complicated. To assist in identifying structures and boundaries, the contrast should be adjusted continually. The sagittal plane is constantly referred to so that the longitudinal dimension of the amygdala can be cross-referenced with the coronal section being traced.

The Hippocampus

Regional Anatomy

The hippocampal formation develops from the medial pallium. During the outgrowth of the cerebral hemispheres, first caudalwards and subsequently ventralwards and rostralwards, the retrocommissural part of the hippocampal formation becomes situated in the temporal lobe (Donkelaar et al., (2011). Rudiments of the supracommissural hippocampus can be found on the medial side of the hemisphere above the corpus callosum: the indusium griseum, a thin cell layer, flanked by the stria longitudinalis medialis and the stria longitudinalis lateralis of Lancisi.

The hippocampal formation and its subdivisions are summarized by Donkelaar et al., (2011) who notes that it is composed of three, originally adjacent, cortical areas: the dentate gyrus, the cornu Ammonis and the subiculum (Klingler 1948; Stephan 1975; Braak 1980; Amaral and Insausti 1990; Braak et al., 1996; Duvernoy 1998). The U-shaped cornu Ammonis consists of three fields (CA1–CA3). Within the hilus of the dentate gyrus sometimes a CA4 field is distinguished, following Lorente de Nó's (1934) subdivision. Field CA4 appears to correspond most closely to the polymorph zone of the dentate gyrus, and therefore, is not a field of the hippocampus at all (Blackstad 1956; Amaral 1978, 1987). Since CA3 pyramidal cells extend far into the hilus of the dentate gyrus, Amaral and Insausti (1990) suggested the term CA3h (see also Lim et al., 1997a, b).

The Roses divided the hippocampus proper into five subfields H1–H5 (Rose 1927a, 1938). Their nomenclature is still in use in neuropathology. The H1 or CA1 field and the adjacent subiculum are also known as Sommer's sector (Sommer 1880). In Sommer's sector, the pyramidal cells are especially sensitive to anoxia and other metabolic substances and are often affected in temporal lobe epilepsy. The C-shaped dentate gyrus is adjacent to the CA1 field, and is separated from the subiculum by the sulcus hippocampi. The subicular complex borders on the entorhinal cortex (area 28) of the mesocortical parahippocampal gyrus. It comprises three subdivisions: the subiculum proper, the presubiculum and the parasubiculum.

The border region between the subiculum proper and the CA1 field is also known as the prosubiculum (Lorente de Nó 1933). The hippocampus proper (CA1–CA3) is composed of three layers: a polymorph layer (the stratum oriens), a pyramidal layer (the stratum pyramidale) and a molecular layer, composed of the stratum radiatum, the stratum lacunosum and the stratum moleculare. The dentate gyrus is also composed of three layers (Amaral et al., 2007; Seress 2007): a polymorph hilus, a granular layer (the stratum granulosum) and a molecular layer (the stratum moleculare), which is continuous with the molecular layer of the hippocampus.

The subiculum proper also has 3 layers: an external plexiform or molecular layer, the primary or pyramidal cell layer and a deep polymorph cell layer. With diffusion tensor microscopy, it is possible to identify the different laminae of the human hippocampus (Shepherd et al., 2007).

The entorhinal cortex is a multilayered cortical area that varies regionally in complexity (Amaral et al., 1987). The entorhinal territory consists of entorhinal and transentorhinal (German terminology) or perirhinal (Anglo-Saxon terminology) cortical areas found over the ambient gyrus and the rostral part of the parahippocampal gyrus (Braak and Braak 1992; Insausti et al., 1995; Solodkin and Van Hoesen 1996; Suzuki and Amaral 2003a, b).

The transentorhinal region is located between the proper entorhinal region and the adjoining temporal isocortex, and is largely buried within the rhinal sulcus (Braak and Braak 1992). The surface of the entorhinal cortex exhibits small, macroscopically visible wart-like elevations, the verrucae hippocampi, first described by Gustav Retzius (Retzius 1896), that are produced by clusters of neurons in layer II (or layer Pre- α). In primates and humans, the entorhinal cortex shows morphological modifications along rostrocaudal and mediolateral gradients (Amaral 1987; Insausti et al., 1995; Insausti and Amaral 2008). Its more “primitive” levels are located rostrally, below the amygdaloid complex. This part of the entorhinal cortex receives secondary olfactory projections. In monkeys, only about 10% of the entorhinal cortex receives a direct projection from the olfactory bulb (Turner et al., 1978; Amaral et al., 1987. Progressing caudally, the monkey entorhinal cortex becomes more clearly laminated and the cells are organized into distinct columns.

At least six cell and fibre layers can be distinguished in the entorhinal cortex. The cortex consists of a molecular layer, an external principal layer, a cell-sparse lamina dissecans, an internal principal layer and, within the white matter, a profound cellular layer (Rose 1927a; Braak and Braak 1992). The principal layers can each be divided into three layers Pre- α, β, γ, and Pri-α, β and γ. In experimental studies in monkeys, however, mostly Amaral and Insausti’s (1990) subdivision into six layers is used, of which layer 1 is the molecular layer, layer 2 Pre-α, layer 3 Pre-β and Pre-γ, layer 4 the lamina dissecans, layer 5 Pri-α, and layer 6 Pri-β and Pri-γ. The human entorhinal cortex has been subdivided into eight different subfields (Insausti et al., 1995). The olfactory subfield, the rostralmost field, is little laminated. This parcellation of the human entorhinal cortex parallels that in monkeys (Donkelaar et al., 2011)

Hippocampus Tracing Protocol

Step I

The hippocampus is traced in the coronal plane, and the anterior most aspect of the hippocampus is defined in the axial plane, where the medial projection of the pes hippocampi marks the anterior boundary. Once the anterior boundary is ascertained, the first tracing is made. By exaggerating the contrast in the coronal plane, the internal structure of the hippocampus can be delineated from that of the overlying amygdala, and the underlying parahippocampal gyrus (Fig. 27.).

Step II

Consecutive tracings are performed with the sagittal plane as reference to discern the longitudinal progression of the tracing (Fig. 28). The hippocampus becomes more easily delineated the further posteriorly the tracing progresses. This is because a fair amount of cerebrospinal fluid surrounds the hippocampus as it forms the floor of the temporal horn of the lateral ventricle.

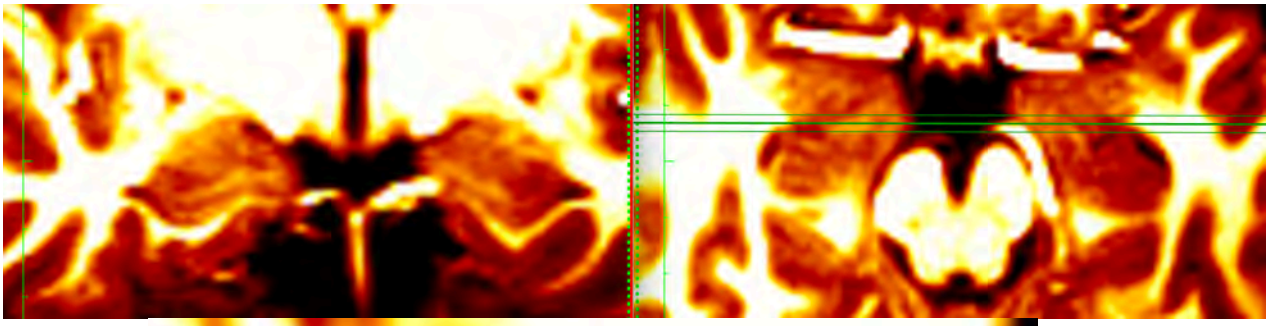

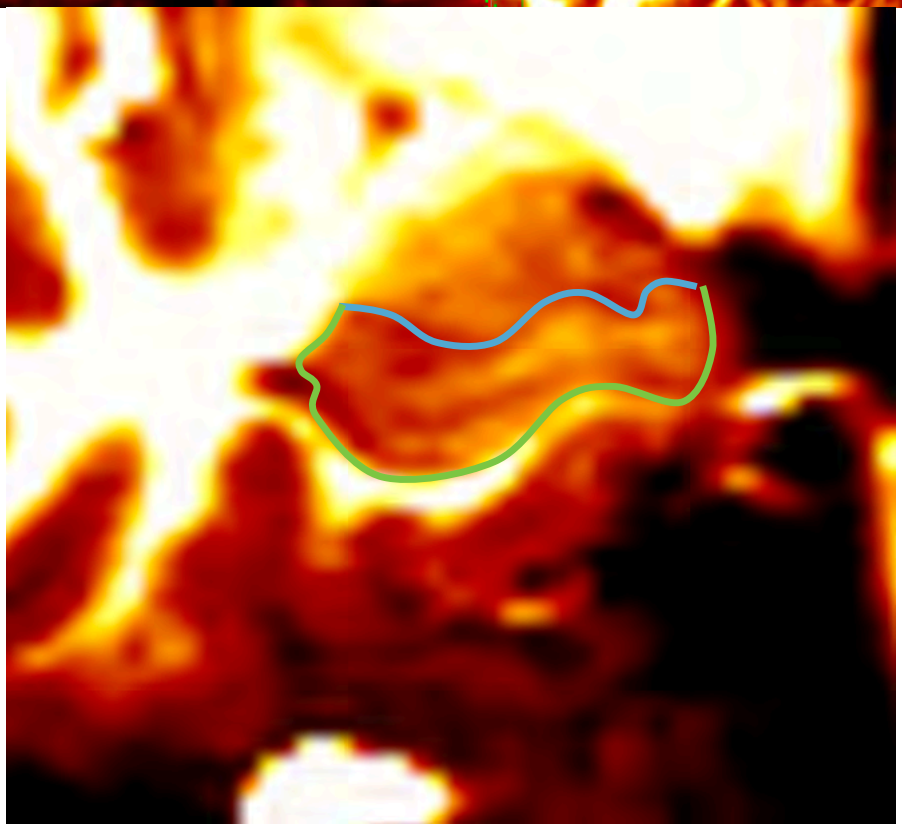

Figure: 27

Side by side display of the coronal (left) and axial (right) planes. The green guidelines in the axial plane is seen intersecting the most anterior aspect of the hippocampus. Magnification of the coronal section demonstrates the superior boundary of the hippocampus (blue line) which also marks the interface between amygdala and hippocampus. The inferior boudnary of the hippocampus is indicated (green line).

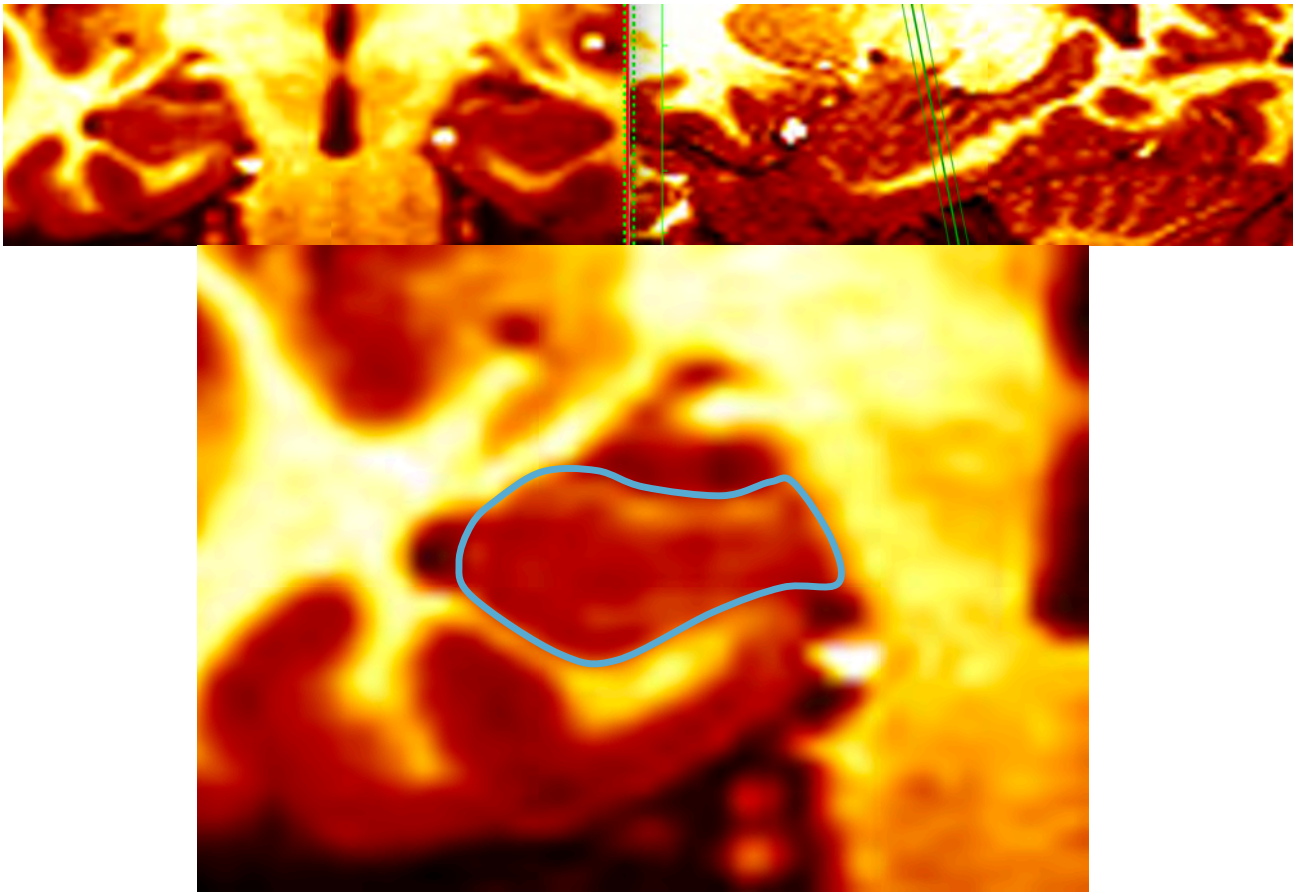

Figure: 28

Consecutive tracing of the hippocampus with the sagittal plane in sumultaneous display to determine the longitudinal progression of the tracing. The posterior dimension of the hippocampus is clearly visible on the sagittal section (right top). The outline of the hippocampus is indicated in the close up coronal view (bottom).

Step III

The final tracing is performed when the most posterior aspect of the hippocampus is reached in the sagittal plane. In the coronal, the most posterior slice can be determined by navigating one slice beyond the most posterior edge seen in the sagittal plane, to confirm that the posterior boundary of the hippocampus is reached (Fig. 29.).

Step IV

Once the tracing is complete, the volume is reconstructed for inspection of anatomical continuity and volume calculation (Fig. 30.).

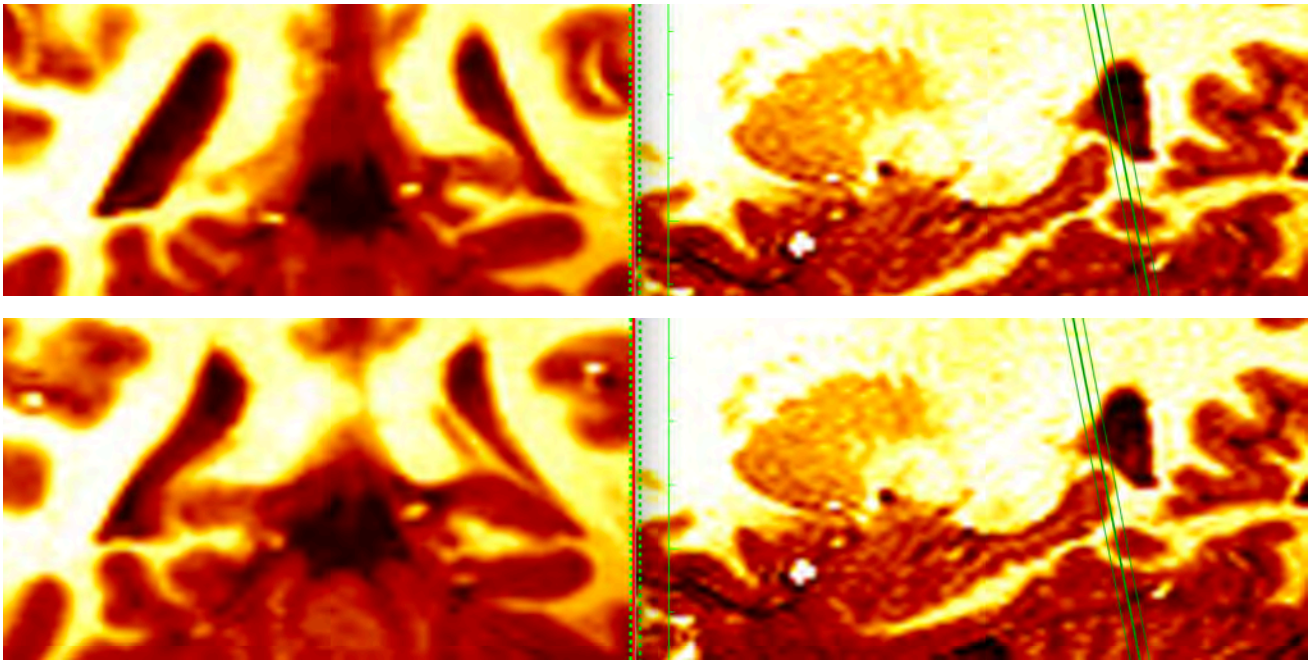

Figure: 29

The most posterior edge of the hippocampus is seen by the green guidelines transecting the posterior hippocampus (top right). Navigating one slice beyond this point confirms that this is the last visible aspect of the hippocampus posteriorly (bottom left and right).

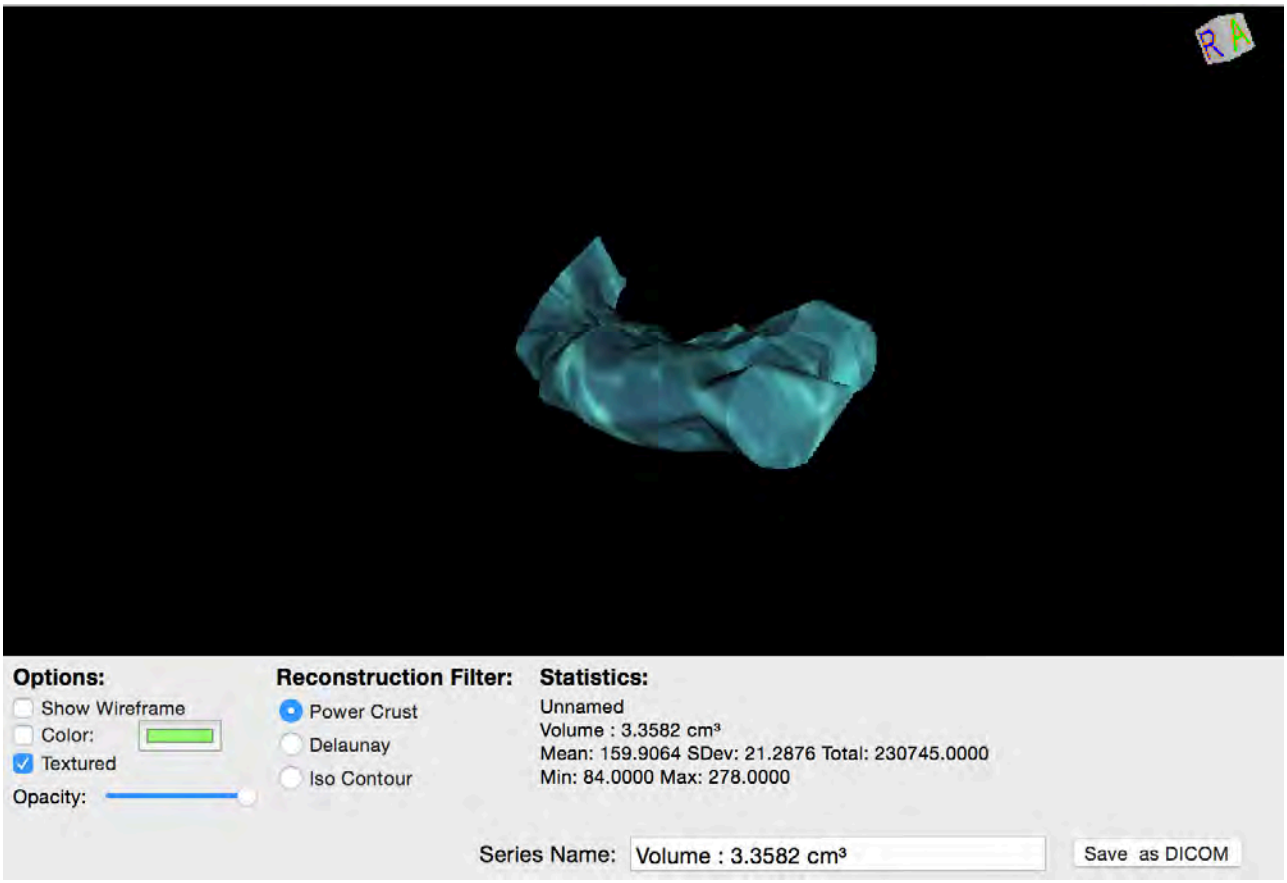

Figure: 30

Volumetric reconstruction of the hippocampus. The medial projection of the hippocampus is maintained. The volume is shown bottom right of the screen.

Special Considerations

The most difficult aspect of tracing the hippocampus is distinguishing the anterior most boundary between the hippocampus and the closely approximated amygdala. Adjusting the contrast and exaggerating it is helpful to make these boundaries more easily discernable.

Summary

Presented here is an in-depth step by step protocol for tracing the most prominent anatomically definable subcortical gray matter structures. Most of these structures have clear anatomical boundaries that are easily observed. However some structures present a challenge to being manually traced because of the anatomical arrangement. These structures include the nucleus accumbens and the amygdala.

Indeed, a human element is clearly relevant here. The neuroanatomist tracing these structures is continually interpreting the anatomy on a case-by-case, hemisphere for hemisphere basis, due to the considerable breadth of normal anatomical variation between hemispheres, and between individuals. How one anatomist defines the boundary of a particular structure could be different from how another defines that same boundary. On the one hand this is a possible source of bias. On the other hand it also arguably a strength of the manual tracing technique, because the anatomy is so incredibly variable, constant interpretation is necessary to accurately discern the boundaries of a particular structure. This visual and intellectual interpretation and judgment is far more complex and adaptable than any of the current automated tracing techniques.

Because of the anatomical heterogeneity of the brain, standardized measures that are built into automated methods may incorrectly determine the boundary of the amygdala due to a smaller cleft of cerebrospinal fluid, which interposes the pes hippocampi from the roof of the anterior tip of the temporal horn of the lateral ventricle. If the hippocampus and the amydaloid floor come into opposition, its extremely difficult to determine the boundaries of these structures. The neuroanatomist must then assess the different views and simultaneous displays along with adjusting and exaggerating the contrast settings, and then make a decision on where to draw the line. This makes for a complicated series of adjustments and consequent interpretations that the neuroanatomist must contend with on each sectional slice of the structure being segmented. Although automated techniques are necessary to extract volumetric data from large data-sets, the role of the neuroanatomist in this work remains indispensible.

References:

1. Aggleton JP, Burton MJ, Passingham RE (1980) Cortical and subcortical afferents to the amygdala of the rhesus monkey (Macacamulatta). Brain Res 190:347–368
2. Aggleton JP, Burton MJ, Passingham RE (1980) Cortical and subcorti- cal afferents to the amygdala of the rhesus monkey (*Macaca mulatta*). Brain Res 190:347–368
3. Alexander GE, Crutcher MD (1990) Functional architecture of basal ganglia circuits. Neural substrates of parallel processing. Trends Neurosci 13:266–271
4. Alheid GF, de Olmos JS, Beltramino CA (1995) Amygdala and extended amygdala. In: Paxinos G (ed) The rat nervous system, 2nd edn. Academic, San Diego, CA, pp 495–578
5. Alheid GF, Heimer L (1988) New perspectives in basal forebrain organization of special relevance for neuropsychiatric disorders: the striatopallidal, amygdaloid, and corticopetal components of substantia innominata. Neuroscience 27:1–39
6. Amaral DG (1987) Memory: anatomical organization of candidate brain regions. In: Plum F (ed) Handbook of physiology, sect 1: the nervous system, vol V, Higher functions of the nervous system. American Physiological Society, Bethesda, MD, pp 211–294
7. Amaral DG, Behniea H, Kelly JL (2003) Topographic organization of projections from the amygdala to the visual cortex in the macaque monkey. Neuroscience 118:1099–1120
8. Amaral DG, Insausti R, Cowan WM (1987) The entorhinal cortex in the monkey. I. Cytoarchitectonic organization. J Comp Neurol 264: 326–355
9. Amaral DG, Price JL, Pitkänen A, Carmichael ST (1992) Anatomical organization of the primate amygdaloid complex. In: Aggleton JP (ed) The amygdala: neurobiological aspects of emotion, memory, and mental dysfunction. Wiley-Liss, New York, pp 1–66
10. Arana, F.S., Parkinson, J.A., Hinton, E., Holland, A.J., Owen, A.M., Roberts, A.C., 2003.
11. Bayer SA (1980) Quantitative 3H-thymidine radiographic analyses of neurogenesis in the rat amygdala. J Comp Neurol 194:845–875
12. Bayer SA, Altman J (1987) Directions in neurogenetic gradients and patterns of anatomical conections in the telencephalon. Prog Neurobiol 29:57–106
13. Beer JS, Knight RT, D'Esposito M (2006) Controlling the integration of emotion and cognition: the role of frontal cortex in distinguishing helpful from hurtful emotional information. Psychol Sci 17:448 – 453.

14. Beer, J.S., Ochsner, K.N. (2006). Social cognition: a multi level analysis. Brain Research, 1079, 98–105.
15. Berg, E.A., 1948. A simple objective technique for measuring flexibility in thinking. J. Gen. Psychol. 39, 15–22.
16. Berns, G.S., McClure, S.M., Pagnoni, G., Montague, P.R., 2001. Predictability modulates human brain response to reward. J. Neurosci. 21, 2793–2798.
17. Breiter, H.C., Aharon, I., Kahneman, D., Dale, A., Shizgal, P., 2001. Functional imaging of neural responses to expectancy and experience of monetary gains and losses. Neuron 30, 619–639.
18. Brockhaus H (1938) Zur normalen und pathologischen Anatomie des Mandelkerngebietes. J Psychol Neurol (Lpz) 49:1–136
19. Brühl, A. B., Delsignore, A., Komossa, K., & Weidt, S. (2014). Neuroimaging in social anxiety disorder—A meta-analytic review resulting in a new neurofunctional model. *Neuroscience & Biobehavioral Reviews*, 1–21. doi:10.1016/j.neubiorev.2014.08.003
20. Buzsaki G. Large-scale recording of neuronal ensembles. Nat. Neurosci 2004;7:446–451.
21. Cardinal RN, et al., Impulsive choice induced in rats by lesions of the nucleus accumbens core. Science 2001;292:2499–2501
22. Cherbuin, N., Anstey, K. J., Réglade-Meslin, C., & Sachdev, P. S. (2009). In Vivo Hippocampal Measurement and Memory: A Comparison of Manual Tracing and Automated Segmentation in a Large Community-Based Sample. PLoS ONE, 4(4), e5265. doi:10.1371/journal.pone.0005265
23. Condon, B., Patterson, J., Wyper, D., Hadley, D., Grant, R., Teasdale, G., & Rowan, J. (1986). Use of magnetic resonance imaging to measure intracranial cerebrospinal fluid volume. Lancet, 1(8494), 1355–1357.
24. Costafreda, S. G., Brammer, M. J., David, A. S., & Fu, C. H. Y. (2008). Predictors of amygdala activation during the processing of emotional stimuli: A meta-analysis of 385 PET and fMRI studies. *Brain Research Reviews*, *58*(1), 57–70. doi:10.1016/j.brainresrev.2007.10.012
25. Crosby EC, Humphrey T (1941) Studies of the vertebrate telencephalon. II. The nuclear pattern of the anterior olfactory nucleus, tuber- culum olfactorium and the amygdaloid complex in adult man. J Comp Neurol 74:309–352

26. de Carvalho, M. R., Rozenthal, M., and Nardi, A. E. (2010). The fear circuitry in panic disorder and its modulation by cognitive-behaviour therapy interventions. *World J. Biol. Psychiatry* 11(2 Pt 2), 188–198.
27. de Olmos J (1972) The amygdaloid projection field in the rat as studied with the cupric-silver method. In: Eleftheriou BE (ed) The neurobi- ology of the amygdala. Plenum, New York, pp 145–204
28. de Olmos J (2004) Amygdala. In: Paxinos G, Mai JK (eds) The human nervous system, 2nd edn. Elsevier, Amsterdam, pp 739–868
29. de Olmos J, Ingram WR (1972) The projection fields of the stria termi- nalis in the rat brain. An experimental study. J Comp Neurol 146: 303–334
30. Delgado MR, Nearing KI, Ledoux JE, Phelps EA (2008) Neural circuitry underlying the regulation of conditioned fear and its relation to extinction. Neuron 59:829 – 838.
31. Delgado MR, Nearing KI, Ledoux JE, Phelps EA (2008) Neural circuitry underlying the regulation of conditioned fear and its relation to extinc- tion. Neuron 59:829 – 838.
32. Delgado, M.R., Nystrom, L.E., Fissell, C., Noll, D.C., Fiez, J.A., 2000. Tracking the hemodynamic responses to reward and punishment in the striatum. J. Neurophysiol. 84, 3072–3077.
33. Delgado, M.R., Stenger, V.A., Fiez, J.A., 2004. Motivation-dependent responses in the human caudate nucleus. Cereb. Cortex 14, 1022–1030.
34. DeLong MR (1990) Primate models of movement disorders of basal ganglia origin. Trends Neurosci 13:281–285
35. Dewey, J., Hana, G., Russell, T., Price, J., McCaffrey, D., Harezlak, J., et al., (2010). Reliability and validity of MRI-based automated volumetry software relative to auto-assisted manual measurement of subcortical structures in HIV-infected patients from a multisite study. NeuroImage, 51(4), 1334–1344. doi:10.1016/j.neuroimage.2010.03.033
Dissociable contributions of the human amygdala and orbitofrontal cortex to incentive motivation and goal selection. J. Neurosci. 23 (29), 9632–9638.
36. Donkelaar (2011) Clinical neuroanatomy; brain circuitry and its disorders. Springer-Verlag Berlin Heidelberg
37. Donkelaar HJ, Lammers GJ, Gribnau AAM (1979) Neurogenesis in the amygdaloid complex of a rodent (the Chinese hamster). Brain Res 165:348–353
38. Elliott, R., Friston, K.J., Dolan, R.J., 2000. Dissociable neural responses in human reward systems. J. Neurosci. 20, 6159–6165.

39. Elliott, R., Newman, J.L., Longe, O.A., Deakin, J.F., 2003. Differential response patterns in the striatum and orbitofrontal cortex to financial reward in humans: a parametric functional magnetic resonance imaging study. J. Neurosci. 23, 303–307.
40. Foland LC, Altshuler LL, Bookheimer SY, Eisenberger N, Townsend J, Thompson PM (2008) Evidence for deficient modulation of amygdala response by prefrontal cortex in bipolar mania. Psychiatry Res 162:27–37.
41. Foland LC, Altshuler LL, Bookheimer SY, Eisenberger N, Townsend J, Thompson PM (2008) Evidence for deficient modulation of amygdala response by prefrontal cortex in bipolar mania. Psychiatry Res 162:27–37.
42. Fox, A. S., & Kalin, N. H. (2014). A Translational Neuroscience Approach to Understanding the Development of Social Anxiety Disorder and Its Pathophysiology. *The American Journal of Psychiatry*. doi:10.1176/appi.ajp.2014.14040449
43. Goto, Y., & Grace, A. A. (2008). Limbic and cortical information processing in the nucleus accumbens. *Trends in Neurosciences, 31*(11), 552–558. doi:10.1016/j.tins.2008.08.002
44. Grace AA. Gating of information flow within the limbic system and the pathophysiology of schizophrenia. Brain Res. Brain Res. Rev 2000;31:330–341.
45. Grahn, J. A., Parkinson, J. A., & Owen, A. M. (2008). The cognitive functions of the caudate nucleus. Progress in Neurobiology, 86(3), 141–155. doi:10.1016/j.pneurobio.2008.09.004
46. Haber SN, Mc Farland NR (1999) The concept of the ventral striatum in nonhuman primates. Ann N Y Acad Sci 877:33–48
47. Hariri AR, Bookheimer SY, Mazziotta JC (2000) Modulating emotional responses: effects of a neocortical network on the limbic system. Neuroreport 11:43– 48.
48. Hariri AR, Mattay VS, Tessitore A, Fera F, Weinberger DR (2003) Neocortical modulation of the amygdala response to fearful stimuli. Biol Psychiatry 53:494 –501.
49. Heimer L, de Olmos J, Alheid GF, Zaborsky L (1991) “Perestroika” in the basal forebrain: opening the border between neurology and psy- chiatry. Prog Brain Res 87:109–165
50. Heimer L, Harlan RE, Alheid GF, Garcia MM, de Olmos J (1997b) Substantia innominata: a notion which impedes clinico-anatomical correlations in neuropsychiatric disorders. Neuroscience 76: 957–1006
51. Ishikawa A, et al., Dorsomedial prefrontal cortex contribution to behavioral and nucleus accumbens neuronal responses to incentive cues. J. Neurosci 2008;28:5088–5098

52. Johnston JB (1923) Further contibutions to the study of the evolution of the forebrain. J Comp Neurol 35:337–481
53. King-Casas, B., Tomlin, D., Anen, C., Camerer, C.F., Quartz, S.R., Montague, P.R., 2005. Getting to know you: reputation and trust in a two-person economic exchange. Science 308, 78–83.
54. Knutson, B., Adams, C.M., Fong, G.W., Hommer, D., 2001a. Anticipation of increasing
55. Knutson, B., Fong, G.W., Adams, C.M., Varner, J.L., Hommer, D., 2001b. Dissociation of reward anticipation and outcome with event-related fMRI. Neuroreport 12, 3683–3687.
56. Knutson, B., Westdorp, A., Kaiser, E., Hommer, D., 2000. FMRI visualization of brain activity during a monetary incentive delay task. Neuroimage 12, 20–27.
57. Kohn, M. I., Tanna, N. K., Herman, G. T., Resnick, S. M., Mozley, P. D., Gur, R. E., et al., (1991). Analysis of brain and cerebrospinal fluid volumes with MR imaging. Part I. Methods, reliability, and validation. Radiology, 178(1), 115–122. doi:10.1148/radiology.178.1.1984289
58. Kordower JH, Piecinski P, Rakic P (1992) Neurogenesis of the amygdaloid nuclear complex in the rhesus monkey. Dev Brain Res 68:9–15
59. Lammers HJ (1972) The neural connections of the amygdaloid com- plex in mammals. In: Eleftheriou BE (ed) The neurobiology of the amygdala. Plenum, New York, pp 123–144
60. Lansink CS, et al., Preferential reactivation of motivationally relevant information in the ventral striatum. J. Neurosci 2008;28:6372–6382.
61. Lauer EW (1945) The nuclear pattern and fiber connections of certain basal telencephalic centers in the macaque. J Comp Neurol 82: 215–255
62. Lauer M, Heinsen H (1996) Cytoarchitectonics of the human nucleus accumbens. J Hirnforsch 37:243–254
63. Lieberman MD, Eisenberger NI, Crockett MJ, Tom SM, Pfeifer JH, Way BM (2007) Putting feelings into words: affect labeling disrupts amygdala activity in response to affective stimuli. Psychol Sci 18:421– 428.
64. Lieberman MD, Eisenberger NI, Crockett MJ, Tom SM, Pfeifer JH, Way BM (2007) Putting feelings into words: affect labeling disrupts amygdala ac- tivity in response to affective stimuli. Psychol Sci 18:421– 428.
65. Looi, J. C. L., Lindberg, O., Liberg, B., Tatham, V., Kumar, R., Maller, J., et al., (2008). Volumetrics of the caudate nucleus: Reliability and validity of a new manual tracing protocol. Psychiatry Research: Neuroimaging, 163(3), 279–288. doi:10.1016/j.pscychresns.2007.07.005

66. Machado-de-Sousa, J. P., Osório, F. de L., Jackowski, A. P., Bressan, R. A., Chagas, M. H. N., Torro-Alves, N., et al., (2014). Increased Amygdalar and Hippocampal Volumes in Young Adults with Social Anxiety. *PLoS ONE*, *9*(2), e88523. doi:10.1371/journal.pone.0088523
67. Mai, J., Paxinos. G., Voss, T., 2008. Atlas of the Human Brain Third Ed. Elsevier Academic Press
68. McCandliss, B.D., Fiez, J.A., Protopapas, A., Conway, M., McClelland, J.L., 2002. Success and failure in teaching the [r]-[l] contrast to Japanese adults: tests of a Hebbian model of plasticity and stabilization in spoken language perception. Cogn. Affect. Behav. Neurosci. 2, 89–108.
69. McClure, S.M., Berns, G.S., Montague, P.R., 2003. Temporal prediction errors in a passive learning task activate human striatum. Neuron 38, 339–346.
70. McConnell J, Angevine JB (1983) Time of neuron origin in the amygdaloid complex of the mouse. Brain Res 272:150–156
71. Milner, B., 1963. Effects of brain lesions on card sorting. Arch. Neurol. 9, 90–100.
72. Monchi, O., Petrides, M., Strafella, A.P., Worsley, K.J., Doyon, J., 2006. Functional role of the basal ganglia in the planning and execution of actions. Ann. Neurol. 59, 257–264. monetary reward selectively recruits nucleus accumbens. J. Neurosci. 21, RC159.
73. Montague, P.R., Berns, G.S., Cohen, J.D., McClure, S.M., Pagnoni, G., Dhamala, M., Wiest, M.C., Karpov, I., King, R.D., Apple, N., Fisher, R.E., 2002. Hyperscanning: simultaneous fMRI during linked social interactions. Neuroimage 16, 1159– 1164.
74. Montague, P.R., King-Casas, B., Cohen, J.D., 2006. Imaging valuation models in human choice. Annu. Rev. Neurosci. 29, 417–448.
75. Morey, R. A., Petty, C. M., Xu, Y., Hayes, J. P., Wagner, H. R., II, Lewis, D. V., et al., (2009). A comparison of automated segmentation and manual tracing for quantifying hippocampal and amygdala volumes. NeuroImage, 45(3), 855–866. doi:10.1016/j.neuroimage.2008.12.033
76. Neto LL, Oliveira E, Correia F, Ferreira AG (2008) The human nucleus accumbens: Where is it? A stereotactic, anatomical and magnetic resonance imaging study. Neuromodulation 11:13–22
77. O'Doherty, J.P., Buchanan, T.W., Seymour, B., Dolan, R.J., 2006. Predictive neural coding of reward preference involves dissociable responses in human ventral midbrain and ventral striatum. Neuron 49, 157–166.

78. O'Doherty, J.P., Dayan, P., Friston, K., Critchley, H., Dolan, R.J., 2003. Temporal difference models and reward-related learning in the human brain. Neuron 38, 329–337.
79. Ochsner KN, Bunge SA, Gross JJ, Gabrieli JD (2002) Rethinking feelings: an FMRI study of the cognitive regulation of emotion. J Cogn Neurosci 14:1215–1229.
80. Ochsner, K.N., Bunge, S.A., Gross, J.J., Gabrieli, J.D.E., 2002. Rethinking feelings: an fMRI study of the cognitive regulation of emotion. J. Cogn. Neurosci. 14, 1215–1229.
81. Packard MG, Knowlton BJ: Learning and memory functions of the basal ganglia, Annu Rev Neurosci 25:563, 2002.
82. Price JL, Russchen FT, Amaral DG (1987) The limbic region. II. The amygdaloid complex. Handb Chem Neuroanat 5:279–388
83. Reading PJ, Dunnett SB. The effects of excitotoxic lesions of the nucleus accumbens on a matching to position task. Behav. Brain Res 1991;46:17–29.
84. Sergerie K, Chochol C, Armony JL (2008) The role of the amygdala in emotional processing: a quantitative meta-analysis of functional neuroimaging studies. Neurosci Biobehav Rev 32:811– 830.
85. Sergerie K, Chochol C, Armony JL (2008) The role of the amygdala in emo- tional processing: a quantitative meta-analysis of functional neuroimag- ing studies. Neurosci Biobehav Rev 32:811– 830.
86. Seymour, B., O'Doherty, J.P., Dayan, P., Koltzenburg, M., Jones, A.K., Dolan, R.J., Friston, K.J., Frackowiak, R.S., 2004. Temporal difference models describe higher-order learning in humans. Nature 429, 664–667.
87. Standring, S. (2008). Gray's Anatomy: The Anatomical Basis of Clinical Practice 40th ed. Churchill Livingstone
88. Stephan H, Andy OJ (1977) Quantitative comparison of the amygdala in insectivores and primates. Acta Anat (Basel) 98:130–153
89. Stewart, L., Meyer, B.-U., Frith, U., Rothwell, J., 2001. Left posterior BA37 is involved in object recognition: a TMS study. Neuropsychologia 39, 1–6.
90. Swanson LW, Petrovich GD (1998) What is the amygdala? Trends Neurosci 21:323–331
91. Tricomi, E., Delgado, M.R., McCandliss, B.D., McClelland, J.L., Fiez, J.A., 2006. Performance feedback drives caudate activation in a phonological learning task. J. Cogn. Neurosci. 18, 1029–1043.
92. Tricomi, E.M., Delgado, M.R., Fiez, J.A., 2004. Modulation of caudate activity by action contingency. Neuron 41, 281–292.

93. Urry HL, van Reekum CM, Johnstone T, Kalin NH, Thurow ME, Schaefer HS, Jackson CA, Frye CJ, Greischar LL, Alexander AL, Davidson RJ (2006) Amygdala and ventromedial prefrontal cortex are inversely coupled during regulation of negative affect and predict the diurnal pattern of cortisol secretion among older adults. J Neurosci 26:4415– 4425.
94. Urry HL, van Reekum CM, Johnstone T, Kalin NH, Thurow ME, Schaefer HS, Jackson CA, Frye CJ, Greischar LL, Alexander AL, Davidson RJ (2006) Amygdala and ventromedial prefrontal cortex are inversely cou- pled during regulation of negative affect and predict the diurnal pattern of cortisol secretion among older adults. J Neurosci 26:4415– 4425.
95. Volsch M (1906) Zur vergleichenden Anatomie des Mandelkerns und seine Nachbargebilde, Teil I. Arch Mikrosk Anat 68:573–683
96. Volsch M (1910) Zur vergleichenden Anatomie des Mandelkerns und seine Nachbargebilde, Teil II. Arch Mikrosk Anat 76:373–523
97. Yamada, H., Matsumoto, N., Kimura, M., 2004. Tonically active neurons in the primate caudate nucleus and putamen differentially encode instructed motivational outcomes of action. J. Neurosci. 7, 3500–3510.

CHAPTER III

Manual Tracing of Subcortical Gray Matter in Patients with Social Anxiety Disorder

Introduction:

As noted previously, social anxiety disorder (SAD) is a prevalent disorder associated with significant morbidity and co-morbidity. A large body of neuroscientific enquiry into the neurobiology associated with SAD exists, however very few structural studies, and only one manual tracing study in SAD has been published to date. Machado-de-Sousa et al., (2014) defined the hippocampus and amygdala as a priori regions of interest and used a manual tracing protocol described by Schummanet al., (2004). They found that bilateral amygdala and left hippocampus were enlarged in individuals with SAD relative to controls. Potential limitations to this study's approach include the fact that the protocol they used to manually segment these structures (Schumman et al. 2004) is quite out dated, considering advances in gradient and receiver coil technology and magnetic field strength, which has significantly increased imaging resolution and anatomical detail. Another potential limitation is that the study population was small (n=11).

The aims of the current study was to acquire high resolution (3T and >1mm slice thickness) structural whole brain MRI's in a treatment naïve population of individuals with SAD, who have no psychiatric, medical or other co-morbidities, and to segment all of the macroscopically visible subcortical gray matter structures with a tracing protocol specifically designed for this study.

Regions of Interest:

The animal literature concerning anxiety overlaps with what is found in the functional human neuroimaging literature, and implicates the amygdala, nucleus accumbens, and other striatal structures (Le Doux et al. 2000; Davis et al. 2006; Panksepp et al. 2011). The functional neuroimaging literature regarding SAD implicates several subcortical structures, such as the amygdala, nucleus accumbens, lentiform nuclear complex, and hippocampus (Freitas-Ferrari et al., 2010).

The Amygdala:

The Amygdala has been extensively implicated in social anxiety in the functional imaging literature in which amygdala hyperactivity has been noted (Evans et al., 2008; Shah, Klumpp, Angstadt, Nathan, & Phan, 2009). Noted previously by

several authors (Etkin and Wager, 2007; Freitas-Ferrari et al., 2010) the amygdala and its connections play a key role in the attribution of emotional salience to stimuli and in the top-down modulation of associative, attentional, and interpretative processes (de Carvalho et al., 2009). The abnormal functioning of this circuitry in SAD, resulting in impaired communication with prefrontal areas responsible for inhibitory responses, could lead to increased amygdala responsivity and a consequent sustained threat-related processing bias in SAD (Freitas-Ferrari et al., 2010)

The Caudate Nucleus:

The caudate nucleus has previously been implicated in the social anxiety functional literature in which increase caudate functional connectivity with the medial prefrontal cortex has been noted (Gimenez et al., 2012; Liao et al., 2011), however no volumetric data relating to social anxiety disorder has been published to date. The caudate plays a significant role in action contingencies and the evaluation of subsequent outcomes, it might be possible that the preconceived negative evaluation by others in social situations seen in SAD has to do with aberrant caudate circuitry. The normal response-dependent feedback mediated by the caudate is somehow negatively biased in SAD, resulting in the phobic preconceived response to social stimuli.

The Lentiform Complex:

The various components of the lentiform nuclear complex have previously been implicated in the social anxiety literature in which increased functional connectivity is seen in the putamen and globus pallidi (Arnold Anteraper et al., 2014) but no volumetric data relating to social anxiety disorder has been published to date. The functions of the putamen can be classified as mainly motoric (De Long et al., 1990; Alexander et al., 1990) as well as having a role in reinforcement and implicit learning (Packard et al., 2002; Yamada et al., 2004). Both reinforcement and implicit learning play a significant role in the integration and processing of aversive stimuli, and may therefore have an important role to play in SAD pathogenesis. The role that the globus pallidi play in essentially forming the prinicple output pathay for the basal ganglia as a whole is important to consider in the context of SAD, as fear circuitry, as well as other limbic circuitry, are intimately interconnected with basal ganglia projections.

The Nucleus Accumbens:

The nucleus accumbens itself has previously been noted to show increased functional connectivity in SAD (Brühl et al. 2014). Considering the nucleus accumbens' role in wanting and liking behavior (Peciña et al., 2008), it is possible that accumbens circuitry is involved in facilitating the avoidance seen in SAD, by "not liking" social situations and facilitating avoidance by not investing pleasure in social situations. Due to its difficult neuroanatomical location, this region may benefit from being segmented manually in social anxiety — here, segmentation has previously been accomplished (Mavridis, Boviatsis, & Anagnostopoulou, 2011).

The Hippocampus:

Hyperactivation of limbic circuitry including the hippocampus likely mediates the symptoms of SAD (Hattingh et al., 2013) by way of behavioural inhibition and causally influencing anxious temperament and dispositional anxiety (Fox et al., 2014) which likely plays a role in the avoidant behaviour seen in SAD, however no manually traced volumetric data relating to social anxiety disorder has been published to date.

Methods:

Participants:

The present study was conducted on outpatients assessed at an anxiety disorders research unit. Patients were referred from specialist psychiatrists, primary care practitioners, and advocacy groups. Eighteen patients (n=18: 7 male; 11 female) with generalized SAD were recruited for participation. All patients met DSM-IV criteria for a primary diagnosis of SAD on the Structured Clinical Interview for the Diagnosis of Axis I Disorders-Patient Version (SCID-I/P) (First et al., 1998) as assessed by an experienced clinician. However, a cut-off value of N18 on the Social Phobia Inventory (SPIN) was used to confirm SAD diagnoses. In other words, only patients with SPIN-scores higher than 18, i.e. with clinically significant social phobic symptoms (Connor et al., 2000) were included. The presence of any other psychiatric disorder was considered criteria for exclusion from the study.

The decision to exclude patients with a primary diagnosis of SAD with comorbidity was based upon the fact that other psychiatric comorbidities might prove to be a potential confounding factor when the neuroimaging measures used are exquisitely sensitive. Our aim was to investigate the neurobiological associations of SAD in isolation without any potential confounding factors as far was in out control

The study protocol was approved by the Institutional Review Board of the University of Cape Town.

Measures:

Demographic data from patients (including age, age of onset of SAD, gender, population group and education level) were collated. The severity of social anxiety symptoms was assessed using the SPIN (Connor et al., 2000) and the Liebowitz Social Anxiety Scale (LSAS) (Liebowitz, 1987). The SPIN is a self-rated scale consisting of questions that evaluate fear, avoidance and physiological discomfort. Each of the 17 items is rated on a scale from 0 to 4: not at all, a little bit, somewhat, very much, and extremely; with higher scores corresponding to greater distress. The full-scale score ranges from 0 to 68.

The SPIN demonstrates solid psychometric properties, is used as a valid measure of severity of social phobia symptoms. The LSAS, a clinician-administered social anxiety rating scale with much support for its validity (Heimberg et al., 1999), is used to assess anxiety or avoidance in a number of typical social and performance situations. Comorbid disorders were assessed using the SCID-I/P and selected parts of the Structured Clinical Interview for the Diagnosis of Axis II Disorders (SCID-II/P) (First et al., 1998).

All healthy control participants were subjected to the same intensive psychodiagnostic interview process. This ensured consistency in the quality of the recruited sample by preventing any control subjects with possible subclinical symptoms included in the study.

Imaging:

Magnetic resonance imaging was conducted on the 3T Siemens system (MAGNETOM Allegra, Erlangen, Germany) at the Cape Universities Brain Imaging Centre. Whole brain T1- weighted 3D magnetization-prepared rapid gradient echo (MPRAGE) images were acquired using the following parameters: spatial resolution

0.5 × 0.5 × 0.5 mm3; slices 0 160; matrix 0 179×256; TR 0 2,300 ms; TE 0 3.93 ms; TI 0 1,100 ms; and flip angle 0 12°.

Tracing:

A region specific tracing protocol was specifically developed for the purposes of this study and is described in greater detail in Chapter X. OsiriX DICOM imaging software was used to conduct the tracing. The image contrast was optimized for each region, and the outline was traced where after the volume of the structure was reconstructed for inspection of anatomical continuity and volume estimation. For a detailed review of the tracing methodology and protocol, please refer to Chapter II.

Statistical Analyses:

Clinical and demographic data were analyzed using Student's t test for continuous variables and chi-square tests for nominal variables to compare the mean brain measurements for the ROIs stipulated, between SAD and HC. We did not correct for age and gender because these were normally distributed and not significantly different between groups. Table 1 and 2 summarize this data.

Results:

We found no statistically significant differences among the SAD, and HC groups in terms of their socio-demographic characteristics, as shown in Table 1. In respect to the volumetric analysis there were specific differences in the right globus pallidus. The volume of the right globus pallidus was significantly increased in the SAD group ($p = 0.022$) compared to healthy controls.

The mean volumes of all brain structures examined in the two groups are presented in Table 2. There were no differences between the SAD group and the HC regarding the caudate, nucleus accumbens, putamen, left globus pallidus, hippocampus and amygdala volumes. Figure 1 provides a graphic representation of these differences.

Discussion:

This study investigated the existence of structural abnormalities in the caudate, nucleus accumbens, putamen, globus pallidus, hippocampus and amygdala of treatment-naïve individuals with a primary Axis I diagnosis of SAD in the absence of any psychiatric or medical comorbidities in comparison to healthy controls. These brain regions were chosen for their functional relevance to the development of SAD, and to highlight the difficulty in manually tracing these structures. The rationale for this study was set a platform for improving manual tracing of these regions, and also to highlight how a clinical diagnosis may alter structural integrity of these regions. The following discussion will attempt to examine how differential function in those with SAD may alter the structural integrity of these regions, for example, by considering potential neuroplasticity versus excito-toxicity effects. As hypothesized, volumetric alterations were found in subjects with SAD compared to healthy controls. Specifically, the SAD participants examined here had significantly increased right globus pallidus volumes.

These data do not support findings reported by Machado-de-Sousa et al., (2014), who found increased volume in the hippocampus and amygdala in patients with SAD compared to controls. Methodological differences in the tracing protocols that were applied to the data may explain why there were differences between the two studies. The tracing protocol used by Machado-de-Sousa et al., (2014) is potentially outdated, being published more than ten years ago. Since 2004, considerable technological improvements in MRI hardware such as increased field strength, gradient coil design and software improvements that allow more accurate data transformation, have allowed for exponential increases in image resolution and anatomical detail. There were also differences in the size of the participant population which was n=12 per group.

Research on stress-induced brain plasticity has shown that chronic immobilization stress increases anxiety-like behavior in rats and that this is accompanied by dendritic hypertrophy (Vyas et al., 2004). In the molecular level, dendritic architecture is mediated by brain derived neurotropic factor (BDNF) (Lakshminarasimhan et al., 2012). Social anxiety implies chronic stress and consequent increased excitatory neurotransmission. Increased chronic excitatory neurotransmission may lead to excitoxicity of involved brain regions. Increased

BDNF expression in the globus pallidus has previously been reported (Kawamoto et al., 1999) during states neurometabolic stress. It is possible that the same mechanisms may be applied to SAD and that upregulated expression of BDNF may occur as a protective mechanism, which results in dendritic hypertrophy and consequent increases in volume of the globus pallidus.

To date, no other imaging studies have been published that specifically report on alterations in globus pallidus in SAD. The globus pallidus plays a central role in functioning as intrinsic connection and the output pathway of the basal ganglia. Output generated from the limbic loop of the basal ganglia, is projected to the frontal lobe via the globus pallidi. These findings make sense in the context of hyperactivity of limbic circuitry in SAD, which utilizes the globus pallidus as gateway towards cortical expression. Even though this interpretation might be correct, our finding of unilateral globus pallidus enlargement as well as the absence of significant differences in other subcortical gray matter structures in subjects with SAD relative to controls remains unexplained. A closer analysis of the samples enrolled here and in the study by Machado-de-Sousa et al. (2014) might help reduce the discrepancy between findings and shed light into limbic plasticity processes underlying social anxiety.

While the mean age of our participants was around 29 years in the two groups, participants in the study by Machado-de-Sousa et al. (2014) were on average 9 years younger. This is of particular importance because prolonged stress has been linked to brain atrophy believed to result from chronic exposure to glucocorticoids (Sapolsky et al. 1990) Taken together, evidence from neuroimaging, cellular, and molecular studies show that our findings and those of Machado-de-Sousa et al. (2014) though different in implicating different neuroanatomical structures, may still be seen in context with one another and can actually be combined in a more comprehensive hypothesis postulating that limbic plasticity in SAD is biphasic, with volume increases in early stages followed by atrophy resulting from excitotoxic processes in the long run.

It is hypothetically possible that by age 30, individuals with SAD are at a transitional phase in the subcortical gray matter volumes, where some structures are larger, such as the globus pallidus reflecting hypertrophy due to excessive stimulation, and other structures appear unaffected. This line of thinking can then be extended to suggest that the absence of enlargement in more structures at the age of our sample, is actually possible evidence that atrophy might be occurring, which only becomes

evident later in life, presenting currently as unchanged volumes when compared to controls. This fits in with the reductions in cortical and subcortical gray matter volumes seen in most structural imaging studies in SAD (see Brühl et al. 2014). This reduction in volume could then be accounted for by prolonged excitotoxic processes seen in SAD in patient samples who are older than our current sample.

There are further strengths and limitations to the present study that must be considered when interpreting the findings. With respect to our methods, ROI-based analyses have been reported to increase the risk of false positive and negative results (Freitas-Ferrari et al. 2010) that cannot be ruled out. Future multicenter studies using the same tracing protocol as discussed in this article, with similar imaging parameters and hardware, as well as larger sample sizes will certainly need to be done to add reproducibility to the findings of this study, and to test the hypotheses discussed above.

There are various differences between this study, and the one previous manual tracing study in SAD that might influence results. Such differences include sample size, imaging hardware, software reconstruction algorithms and tracing methodology. Variation in imaging sequence parameters for instance, and between actual hardware such as the volume coil resolution, can influence tissue contrast, which directly affects the ability to discern one structure from another. Tracing methodology is also a significant factor to consider in variability between study results. The tracing protocol actually defines how one identifies and traces the volume in question. Variation in how one defines the superior aspect of a structure for instance can have significant effects on results.

Another potential factor that could have contributed to the differences in results is the presence of slightly more female participants than male participants in both control and patient groups; although the sample was normally distributed. Various severity measures were used in the assessment procedure such as the LSAS so that the clinical sample could be further characterized. Unfortunately some of this data was missing, for various reasons such as participants not returning self-report measures, therefore we elected not to focus on this scale. However, going forwards, the LSAS will be included in publications and in future research.

Conclusions:

We found structural differences in the right globus pallidus of individuals with SAD compared to controls. The right globus pallidus was larger in subjects with SAD than in controls. These findings may be due to dendritic hypertrophy of the globus pallidus considering its central roll as output nucleus of the limbic loop of the basal ganglia, and co-occurring hyperactivity previously reported in these circuits. The increased volume, and likely dendritic hypertrophy could be mediated by increased expression of BDNF which mediates dendritic proliferation. Further neuroimaging investigations on a multicenter level is required to assess the reproducibility of the tracing protocol, and test the hypotheses of dendritic hypertrophy and BDNF expression in the globus pallidi of individuals with SAD.

Table 1. Demographic characteristics of groups SAD and HC

	Group				
	SAD	HC			
N	18	18	x_2	df	ϕ
Gender (M/F)	7/11	10/8	1.003	1	-.167
			F	df	
Age	29.55	29.66	0.75	34	

SAD = Social Anxiety Disorder; HC = Healthy Controls

Table 2. Mean volumes (cm^3) of manually traced subcortical gray matter structures

		Mean Volume (cm^3) ± SD per group				95% Confidence Interval of the Difference	
Structure	**Hemisphere**	**SAD (n=18)**	**HC (n=18)**	**F**	**Sig. (2-tailed)**	**Lower**	**Upper**
Caudate Nucleus	L	3.747 | 0.543	3.704 | 0.576	.516	0.819	-0.336	0.423
	R	3.959 | 0.503	3.794 | 0.503	.204	0.333	-0.176	0.505
Nucleus Accumbens	L	0.476 | 0.189	0.424 | 0.165	.076	0.390	-0.069	0.172
	R	0.486 | 0.147	0.414 | 0.101	2.939	0.098	-0.014	0.157
Putamen	L	4.873 | 0.957	4.793 | 0.736	.584	0.779	-0.498	0.659
	R	4.635 | 0.715	4.810 | 0.556	.560	0.417	-0.609	0.258
Globus Pallidus	L	1.563 | 0.352	1.624 | 0.289	.754	0.575	-0.279	0.157
	R	1.323 | 0.224	1.153 | 0.197	.182	**0.022****	0.027	0.313
Amygdala	L	1.863 | 0.390	2.016 | 0.467	.496	0.293	-0.444	0.138
	R	1.822 | 0.341	2.038 | 0.337	.255	0.064	-0.446	0.013
Hippocampus	L	3.152 | 0.772	3.360 | 0.525	3.093	0.352	-0.655	0.239
	R	3.226 | 0.632	3.438 | 0.571	.638	0.297	-0.621	0.195

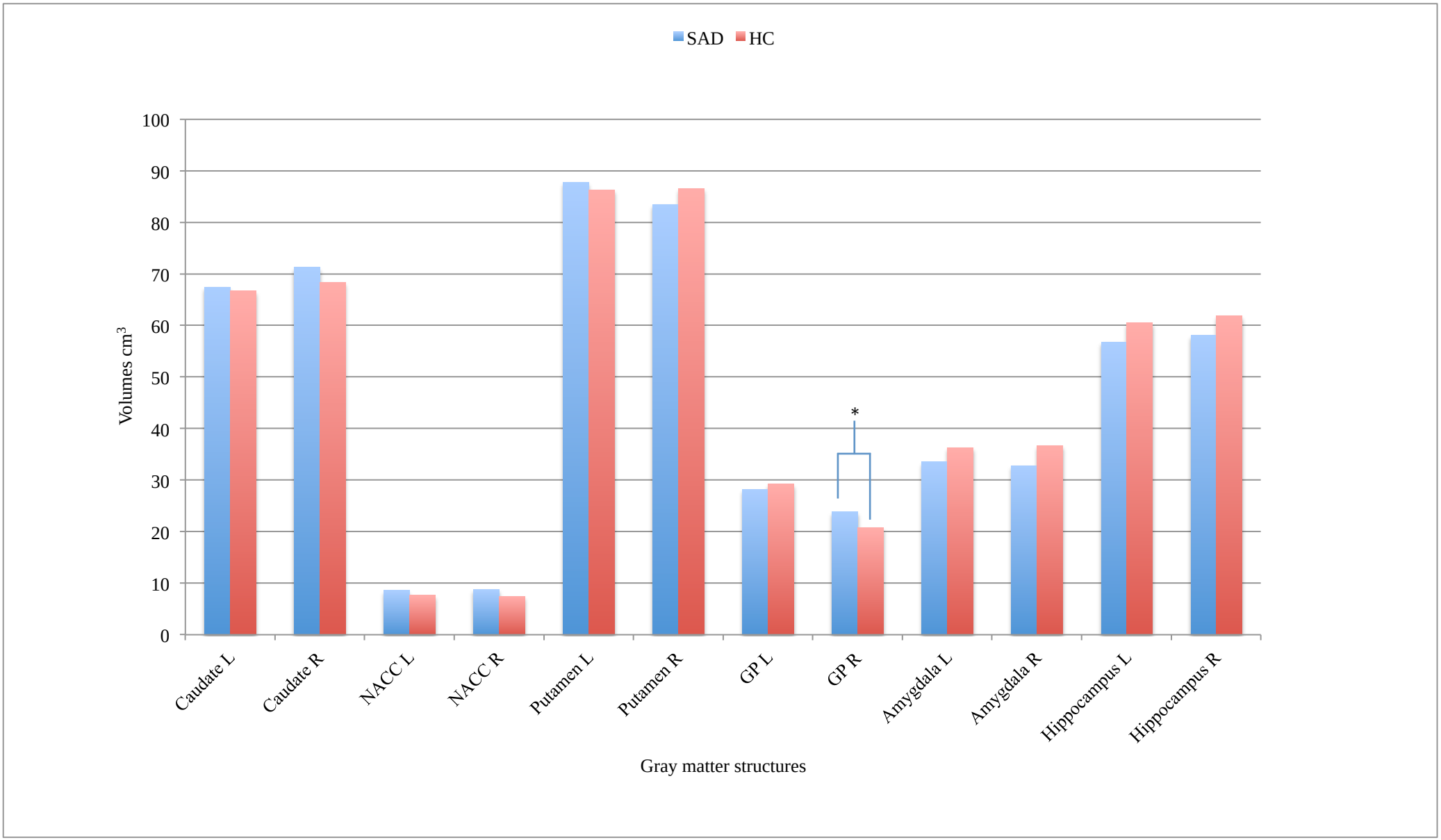

Figure 1. Volumetric differences in the subcortical gray matter volumes of participants with social anxiety disorder (SAD), healthy controls (HC). (*) Indicate statistically significant differences between groups.

References:

1. Amir, N., Klumpp, H., Elias, J., Bedwell, J. S., Yanasak, N., & Miller, L. S. (2005). Increased activation of the anterior cingulate cortex during processing of disgust faces in individuals with social phobia. Biological Psychiatry, 57(9), 975–981. doi:10.1016/j.biopsych.2005.01.044
2. Arnold Anteraper, S., Triantafyllou, C., Sawyer, A.T., Hofmann, S.G., Gabrieli, J.D., Whitfield-Gabrieli, S., 2014. Hyper-connectivity of subcortical resting-state net- works in social anxiety disorder. Brain Connect. 4, 81–90.
3. Brühl, A. B., Delsignore, A., Komossa, K., & Weidt, S. (2014). Neuroimaging in social anxiety disorder—A meta-analytic review resulting in a new neurofunctional model. Neuroscience & Biobehavioral Reviews, 1–21. doi:10.1016/j.neubiorev.2014.08.003
4. Connor, K.M., Davidson, J.R., Churchill, L.E., Sherwood, A., Foa, E., Weisler, R.H., 2000. Psychometric properties of the Social Phobia Inventory (SPIN). New self-rating scale. Br. J. Psychiatry 176, 379 – 386.
5. Davis M. 2006. Neural systems involved in fear and anxiety measured with fear-potentiated startle. Am Psychol 61:741–756.
6. Evans KC, Wright CI, Wedig MM, Gold AL, Pollack MH, Rauch SL. A functional MRI study of amygdala responses to angry schematic faces in social anxiety disorder. Depress Anxiety 2008;25(6):496–505.
7. First MB, Spitzer RL, Gibbon M, Williams JBW (1997) Structured Clinical Interview for DSM-IV Axis I Disorders – Clinical Version (SCID-CV). Washington DC: American Psychiatric Press.
8. First, M.B., Spitzer, R.L., Gobbon, M., Williams, J.B.W., 1998. Structured Clinical Interview for DSM-IV Axis I Disorders- Patient Edition (SCID-I/P, Version 2.0, 8/98 revision). New York State Psychiatric Institute Biometrics Research Department, New York.
9. Freitas-Ferrari MC, Hallak JE, Trzesniak C, Filho AS, Machado-de-Sousa JP, et al. (2010) Neuroimaging in social anxiety disorder: a systematic review of the literature. Prog Neuropsychopharmacol Biol Psychiatry 34: 565–580.
10. Frick, A., Gingnell, M., Marquand, A.F., Howner, K., Fischer, H.k., Kristiansson, M., 1125 Williams, S.C.R., Fredrikson, M., Furmark, T., 2014. Classifying social anxiety dis- 1126 order using multivoxel pattern analyses of brain function and structure. Behav. 1127 Brain Res. 259, 330–335.
11. Gimenez, M., Pujol, J., Ortiz, H., Soriano-Mas, C., Lopez-Sola, M., Farre, M., Deus, J., 1155 Merlo-Pich, E., Martin-Santos, R., 2012. Altered brain functional connectivity in 1156 relation to perception of scrutiny in social anxiety disorder. Psychiatry Res. 202, 1157 214–223.
12. Heimberg, R.G., Horner, K.J., Juster, H.R., Safren, S.A., Brown, E.J., Schneier, F.R., Liebowitz, M.R., 1999. Psychometric prop- erties of the Liebowitz Social Anxiety Scale. Psychol. Med. 29, 199 – 212.
13. Kawamoto, Y., Nakamura, S., Akiguchi, I., & Kimura, J. (1999). Increased brain-derived neurotrophic factor-containing axons in the basal ganglia of patients with multiple system atrophy. Journal of Neuropathology and Experimental Neurology, 58(7), 765–772.
14. LeDoux, J.E., 2000. Emotion circuits in the brain. Annu. Rev. Neurosci. 23, 155–184.

15. Liao, W., Xu, Q., Mantini, D., Ding, J., Machado-de-Sousa, J.O.P., Hallak, J.E.C.,
16. Liebowitz, M.R., 1987. Social phobia. Mod. Probl. Pharmacopsychia- try 22, 141–173.
17. Machado-de-Sousa, J. P., Osório, F. de L., Jackowski, A. P., Bressan, R. A., Chagas, M. H. N., Torro-Alves, N., et al. (2014). Increased Amygdalar and Hippocampal Volumes in Young Adults with Social Anxiety. PLoS ONE, 9(2), e88523. doi:10.1371/journal.pone.0088523
18. Mavridis I, Boriatsis E, Anagnostopoulous S (2011) Anatomy of the human nucleus accumbens: a combined morphometric study. Surg Radiol Anat 33:405–414
19. Sapolsky RM, Uno H, Rebert CS, Finch CE (1990) Hippocampal damage associated with prolonged glucocorticoid exposure in primates. J Neurosci 10: 2897–2902.
20. Schumann CM, Hamstra J, Goodlin-Jones BL, Lotspeich LJ, Kwon H, et al. (2004) The amygdala is enlarged in children but not adolescents with autism; the hippocampus is enlarged at all ages. J Neurosci 24: 6392–6401.
21. Shah SG, Klumpp H, Angstadt M, Nathan PJ, Phan KL. Amygdala and insula response to emotional images in patients with generalized social anxiety disorder. J Psychiatry Neurosci 2009;34(4):296–302.
22. Tiihonen, J., Kuikka, J., Bergström, K., Lepola, U., Koponen, H., & Leinonen, E. (1997). Dopamine reuptake site densities in patients with social phobia. The American Journal of Psychiatry, 154(2), 239–242.
23. Trzesniak, C., Qiu, C., Zeng, L., Zhang, W., Crippa, J.A.S., Gong, Q., Chen, H., 2011. Altered gray matter morphometry and resting-state functional and structural connectivity in social anxiety disorder. Brain Res. 1388, 167–177.
24. Vyas A, Pillai AG, Chattarji S (2004) Recovery after chronic stress fails to reverse amygdaloid neuronal hypertrophy and enhanced anxiety-like behavior. Neurosci 128: 667–673.

CHAPTER IV

Cortical Thickness in Patients with Social Anxiety Disorder

Introduction

The human cerebral cortex is a highly folded sheet of neurons the thickness of which varies between 1 and 4.5 mm, with an overall average of approximately 2.5 mm (Zilles at al. 1990; von Economo et al. 1929; Brodmann 1909). Regional variations in the cortical thickness can be quite large. For example, Brodmann's area 3 on the posterior bank of the central sulcus is among the thinnest of cortical regions, with an average thickness of less than 2 mm, whereas Brodmann's area 4 on the anterior bank is one of the thickest regions, frequently exceeding 4 mm. The distribution of the thickness is not uniform by layer, nor is the variation in the thickness of the cortical layers proportional to the variation in the total thickness.

The thickness of the cortex is of great interest in both normal development as well as in a wide variety of neurodegenerative and psychiatric disorders, and may be indicative of altered function, for example in neuropathology or expertise, in individuals that demonstrate expert skill or knowledge in a particular field (Zahodne et al., 2014; Hanggi et al., 2014). Changes in the gray matter that makes up the cortical sheet are manifested in normal aging (De Leon et al 1997; Jack et al. 1997), Alzheimer's disease (Rusinek et al. 1999) and other dementias (Kaye et al. 1997) as well as schizophrenia (Zipursky et al. 1992). The cortical thinning is frequently regionally specific, and the progress of the atrophy can therefore reveal much about the evolution and causative factors of a disease.

To date, few studies have been completed comparing the thickness of the cortical ribbon in individuals with SAD. Syal et al. (2012) was the first to look at cortical thickness in SAD and found that patients with SAD demonstrated bilateral thinning of the fusiform and the post central cortices as well as significant right hemisphere specific thinning of three frontal regions—the right frontal pole, the right rostral middle frontal gyrus within the dorsolateral prefrontal cortex and right medial orbitofrontal cortex. Additional right hemisphere thinning was noted in primary motor cortex including the right precentral and paracentral regions; the adjacent right superior marginal gyrus within the inferior parietal lobule, the right temporal pole and right inferior temporal cortex within the temporal lobe, and the right insular cortex of patients. These regions are prototypically involved in social and emotional processing suggested that social anxiety disorder extends to a distributed network of cerebral regions involved in social cognition, perceptual

processing and attention. No regions were found to be thicker in SAD patients than in the control individuals.

In 2013, Frick et al. found significantly thicker left hemispheric lingual and fusiform gyri in patients with SAD. In the SAD group a negative association was found between social anxiety symptom severity and thickness of the right rostral anterior cingulate cortex. The the rostral anterior cingulate cortex being involved in direct regulation of limbic structures implicated in emotional responses, and the dorsal part associated with attention, cognitive reappraisal, and emotion expression (Etkin et al., 2011)

Recently Brühl et al. (2014) conducted a large study with 46 patients with SAD and 46 healthy controls in which they found patients with SAD had significantly increased cortical thickness in the right temporal pole, anterior cingulate cortex and left anterior insula as well as in the right dorsolateral prefrontal cortex and the right superior parietal lobule and angular gyrus which extended in part into the right precuneus and inferior parietal lobule. From a general functional perspective, these brain regions fit into models of hyperactive neural circuits involved in the processing of emotional stimuli (temporal pole, anterior insula) and of frontoparietal networks particularly associated with executive, emotion regulating and attentional functions (dorsolateral prefrontal cortex, anterior cingulate, parietal lobe) [e.g. Etkin et al., 2009; Ochsner et al., 2012]. Potential limitations to this study are that the patient population were not treatment naïve and some exhibited comorbid depressive symptomology.

The findings across the three existing studies investigating cortical thickness in SAD appear inconsistent and regionally variable. These findings are summarized in table 3 and 4). Further investigation to understand the significance of altered cortical thickness in its association with SAD neurobiology is therefore necessary, since cortical thickness is a measure of structural integrity. In the current study, 18 individuals with a primary Axis I diagnosis of SAD who were completely psychotherapeutically and psychopharmacologically treatment naïve and free of any other psychiatric or medical comorbidities, and 18 healthy controls underwent high resolution MRI. Whole brain group-wise changes in thickness over the entire span of cortical grey matter were calculated using FreeSurfer (version 4.5.0). Our hypotheses were, considering chronic states of anxiety, that regions of the cererebral cortex would demonstrate thinning which might be explained for by excitotoxic changes which accompany chronic states of anxiety.

Methods:

Participant recruitment and diagnostic measures are discussed in detail in chapter III

Imaging:

Magnetic resonance imaging was conducted on the 3T Siemens system (MAGNETOM Allegra, Erlangen, Germany) at the Cape Universities Brain Imaging Centre. Whole brain T1- weighted 3D magnetization-prepared rapid gradient echo (MPRAGE) images were acquired using the following parameters: spatial resolution 0.5 × 0.5 × 0.5 mm3; slices 0 160; matrix 0 179×256; TR 0 2,300 ms; TE 0 3.93 ms; TI 0 1,100 ms; and flip angle 0 12°.

Cortical thickness analysis:

Cortical thickness and subcortical volumes were estimated from the T1-weighted images using Freesurfer Version 4.5 (http://surfer.nmr.mgh.harvard.edu) Brain surfaces were reconstructed and inflated and local cortical thickness measurements were obtained by calculating the distance (in mm) between the pial and grey-white matter surfaces at each surface location (Dale et al. 1999; Fischl and Sereno 1999) These well-validated and fully automated procedures have been extensively described elsewhere (Fischl and Dale 2000). The whole cortex and subcortical volumes of each individual subject were then visually inspected for inaccuracies in segmentation and manual corrections were per- formed where necessary. Using gyral and sulcul anatomy, the cortex was auto-parcellated into 34 different gyral regions per hemisphere, for each of which a mean cortical thickness value was calculated (Desikan et al. 2006; Fischl et al. 2004b) Automated Freesurfer subcortical parcellation was employed to extract volumes for the amygdala, hippocampus, whole brain grey and white matter (Fischl et al. 2002, 2004a) These values were exported to SPSS 19.0 for statistical analysis.

Statistical analyses:

Clinical and demographic data were analyzed using Student's t test for continuous variables and chi-square tests for nominal variables to compare the mean brain measurements for regions of the cerebral cortex defined by the FreeSurfer neuroanatomical atlas, between SAD and HC. We did not correct for age and gender

because these were normally distributed and not significantly different between groups.

Results:

We found no statistically significant differences between the SAD, and HC groups in terms of their socio-demographic characteristics. These are summarized Table 1 in Chapter 3. In respect to the cortical thickness analysis there were specific differences in the left isthmus of the cingulate gyrus ($p = 0.020$), the left superior temporal gyrus ($p = 0.043$) and the left temporal pole ($p = 0.007$). The thickness in these specific regions was significantly decreased in the SAD group compared to healthy controls. The mean cortical thickness of all cortical areas examined in the two groups are presented in Table 2. Figure 1a-c provides a graphic representation of the differences found in this current investigation, as well as the differences found in previous studies.

Discussion:

This study investigated the existence of differences in cortical thickness across the entire cerebral cortex of treatment-naïve individuals with a primary Axis I diagnosis of social anxiety disorder (SAD) in the absence of any psychiatric or organic medical comorbidities in relation to healthy controls using MRI and FreeSurfer. Alterations in cortical thickness were found in subjects with SAD compared to healthy controls with no current or previous history of SAD. Specifically, socially anxious participants had left sided significant decreases in cortical thickness in the isthmus of the cingulate gyrus, the superior temporal gyrus and the temporal pole.

The findings of the current analyses are in part consistent with what has previously been reported in cortical thickness in SAD. Here we found decreased cortical thickness in the left temporal pole. Syal et al., (2012) previously reported decreased cortical thickness in the right temporal pole. The temporal pole has also previously been implicated by Brühl et al (2014), in which they found increased cortical thickness. No other studies investigating cortical thickness have found involvement of the isthmus of the cingulate gurus or the superior temporal gyrus. however despite these similarities, there remains considerable heterogeneity in findings between the three previous studies and the findings of the current study.

The main advantage of the current study in relation to previous cortical thickness studies of SAD is the quality of the participant population, which enabled us

to obtain imaging data as free from potential confounding factors as possible. In the current study rigorous procedures were adopted to ensure that all participants met the DSM-V criteria for an Axis I diagnosis of SAD and that none had comorbidities. All participants were psychotherapeutically, and psychopharmacologically treatment naïve and had no Axis I, Axis II or other medical co-morbidities. None of the previous three studies confirmed treatment naivety, or lack of comorbidity. Syal et al (2012) noted that patients were not on any treatment at the time of imaging, however did not note whether patients were completely treatment naïve. Frick et al. (2013) disclosed that some of the patients included in their analyses had co-morbid Axis I pathology and were on psychotropic treatment at the time of imaging. Brühl et al (2014) also disclosed that patients in their study population were on psychotherapeutic and psychotropic treatment at the time of imaging.

Measuring cortical thickness is a sensitive structural investigation, given that the cortex is already only a few millimeters thick. It is therefore imperative to obtain a sample that is as free from possible confounding factors as possible. Concurrent psychotherapeutic and psychopharmacological treatment, and comorbid pathology may introduce considerable variability in what is already a very sensitive measure. These factors could account for the current heterogeneity seen between existing studies.

The current findings of decreased cortical thickness in multiple cortical regions including the isthmus of the cingulate gyrus, the temporal pole and the superior temporal gyrus, is consistent with the theory that in anxiety states, there is exposure to chronic stress which increases excitotoxic glutamatergic neurotransmission in multiple brain areas which then leads to consequent apoptosis (Gorman et al. 2010) and therefore the decreased cortical thickness. Excitotoxicity refers to an excessive activation of neuronal amino acid receptors. The specific type of excitotoxicity triggered by the amino acid glutamate is the key mechanism implicated in the mediation of neuronal death in many disorders. Glutamate being one of a group of amino acid neurotransmitters in the brain, it is the principal excitatory neurotransmitter. Glutamate receptor overstimulation increases intracellular calcium by directly opening ion channels and secondarily affecting calcium homeostatic mechanisms. The accumulation of high intracellular calcium levels triggers a cascade of membrane, cytoplasmic, and nuclear events leading to neurotoxicity. The key process that triggers the entire excitotoxic cascade is the excessive accumulation of glutamate in the synaptic space (Leighton, M., et al., 2001).

Within the temporal lobe, we found thinning in the left superior temporal gyrus and the left temporal pole. A significant amount of data has highlighted the increasingly important role that the temporal lobes appear to play in social, emotional and empathic processing. Early lesion experiments in monkeys in the 1970s showed that that damage to anterior temporal lobes caused a loss of ability to make social signals and exclusion from groups (Franzen and Myers 1973). Consistent with our current findings left specific temporal pole atrophy as seen in frontotemporal dementia is associated with social ineptitude (Thompson et al. 2003) and face processing difficulties (Snowden et al. 2003, 2004), and left lateralized temporal lobe epilepsy is associated with a high prevalence of Axis-I psychiatric disorders such as major depression and anxiety disorders (Glosser et al. 2000).

Additionally, cortical thinning of the superior temporal cortices has also been noted in individuals with other disorders of social information processing such as autism spectrum disorders (ASD) (Wallace et al. 2010). This suggests decreased effective connectivity with the amygdala in SAD, leading to the possibility that this may underlie the bias towards negative social information processing in this disorder (Liao et al. 2010). Similarly the temporal pole also maintains dense inter- connections with both the amygdala and the OFC, and has been implicated in empathic processes involved in inferring the emotional state of others (Carr et al. 2003; Vollm et al. 2006) with the left temporal pole in particular remaining associated with emotion and socially relevant memory (Olson et al. 2007).

Functional neuroimaging studies of SAD have demonstrated hyperactivity in various regions of the cingulate cortex (Freitas-Ferrari et al. 2010), and cortical thickness differences may provide a link to the neuroplasticity and excitotoxic effects associated with this disorder. For example, the isthmus of the cingulate gyrus is involved in emotional processing and is contiguous with entorhinal and parahippocampal cortices which participate in retrieval and storage various aspects of long term memory (Anderson et al. 2014). Individuals with SAD are typically hypervigilant so that they may recognize situations in which they may feel embarrassed or negatively evaluated, encouraging them to preemptively avoid situations they deem to be socially negative. In order to recognize these kinds of situations in which aversive stimuli might be avoided, these individuals may form vivid memories of such situations. The isthmus of the cingulate is specifically involved in long-term memory formation and retrieval of spatial, verbal and visual information (Katche et al. 2013). It is therefore hypothetically possible that this region

is decreased in thickness due to chronic hyperactivity, and consequent excitotoxic induced apoptosis (Savic, I. et al., 2013). A potential consideration regarding the robustness of cortical thickness analysis is the fact that the brain has a highly variable surface anatomy. Though every normal individual has a superior frontal sulcus, the exact arrangement and appearance of the superior frontal sulcus varies between individuals.

Conclusions:

This study decreased cortical thickness in the left isthmus of the cingulate gyrus, the left temporal pole and the left superior temporal gyrus in individuals with social anxiety disorder when compared to healthy controls. There appears to be considerable heterogenieity amongst previous studies that have examined cortical thickness in SAD, however we propose that a possible confounding factor is the absence of treatment naivety and psychiatric co-morbidity in previous studies.

Furthermore, our findings suggest that the decrease in cortical thickness might be due to excessive recruitment of these regions and consequent excitotoxic apoptosis. The regions affected are involved in various aspects of evaluating, storing and retrieving information about social situations, which appear to be affected in SAD. Further longitudinal structural neuroimaging research is warranted to test these hypotheses in much larger sample sizes with higher statistical power that are clinically “clean” so that the establishment of the direction of morphological alterations in SAD and their time course can be determined.

Figure 1a: Graphic representation of alterations in cortical thickness
Midline sagittal sections demonstrating the medial aspects of the left (left) and right (right) hemispheres respectively.

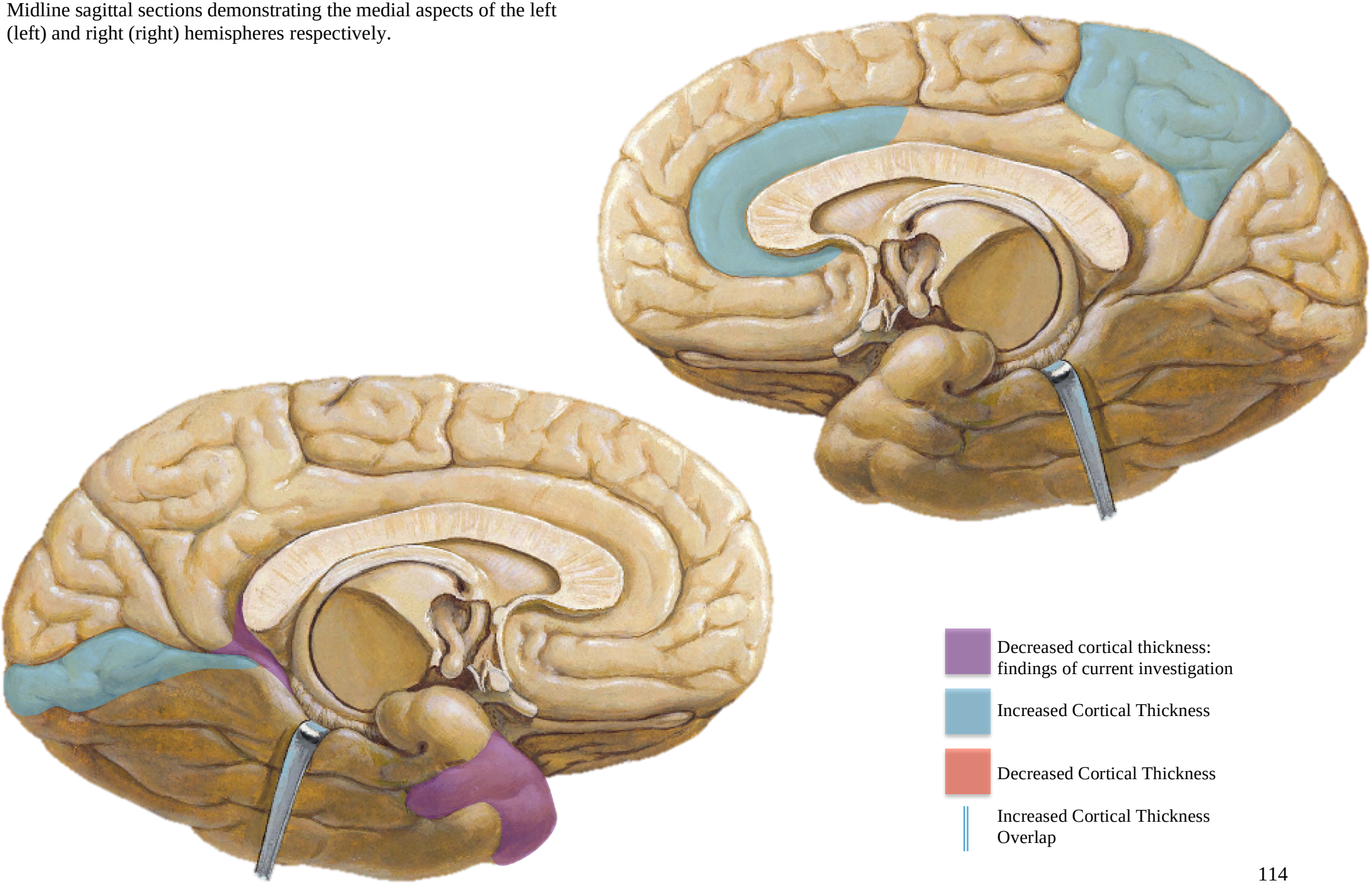

Figure 1b: Graphic representation of alterations in cortical thickness
Inferior view of the whole brain (left); lateral view of the right hemisphere (right) of which the operculum and superior temporal gyrus is retracted to demonstrate the insula.

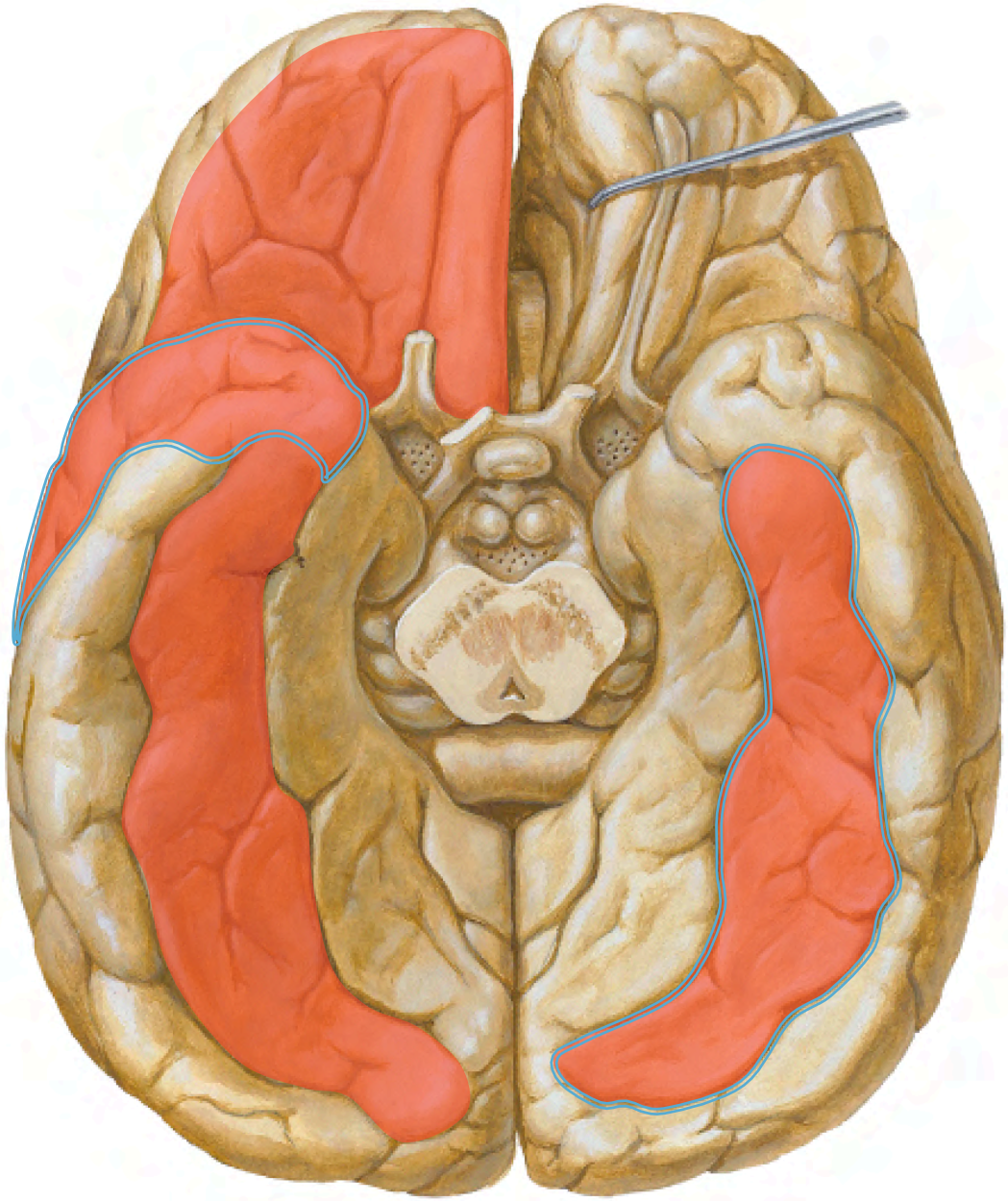

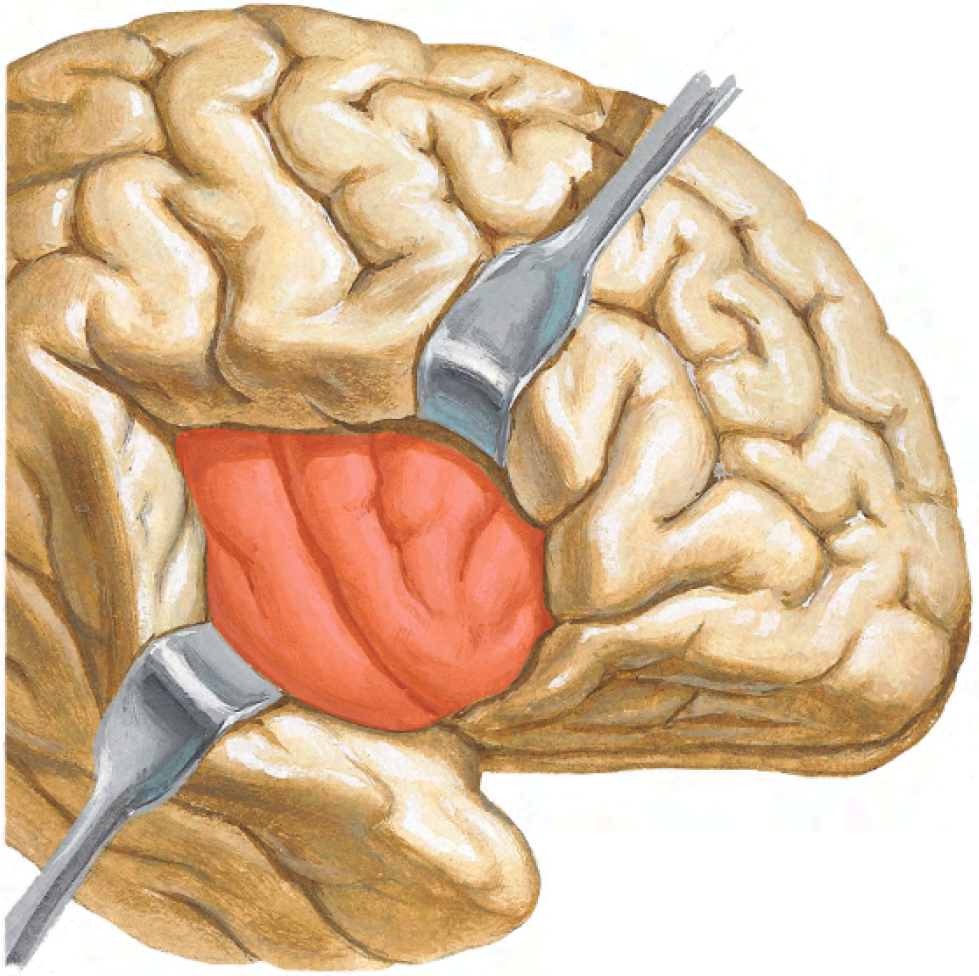

Increased Cortical Thickness

Decreased Cortical Thickness

Increased Cortical Thickness Overlap

Figure 1c: Graphic representation of alterations in cortical thickness
Lateral views of bilateral cerebral convexities. Right hemisphere (left) and left hemisphere (right)

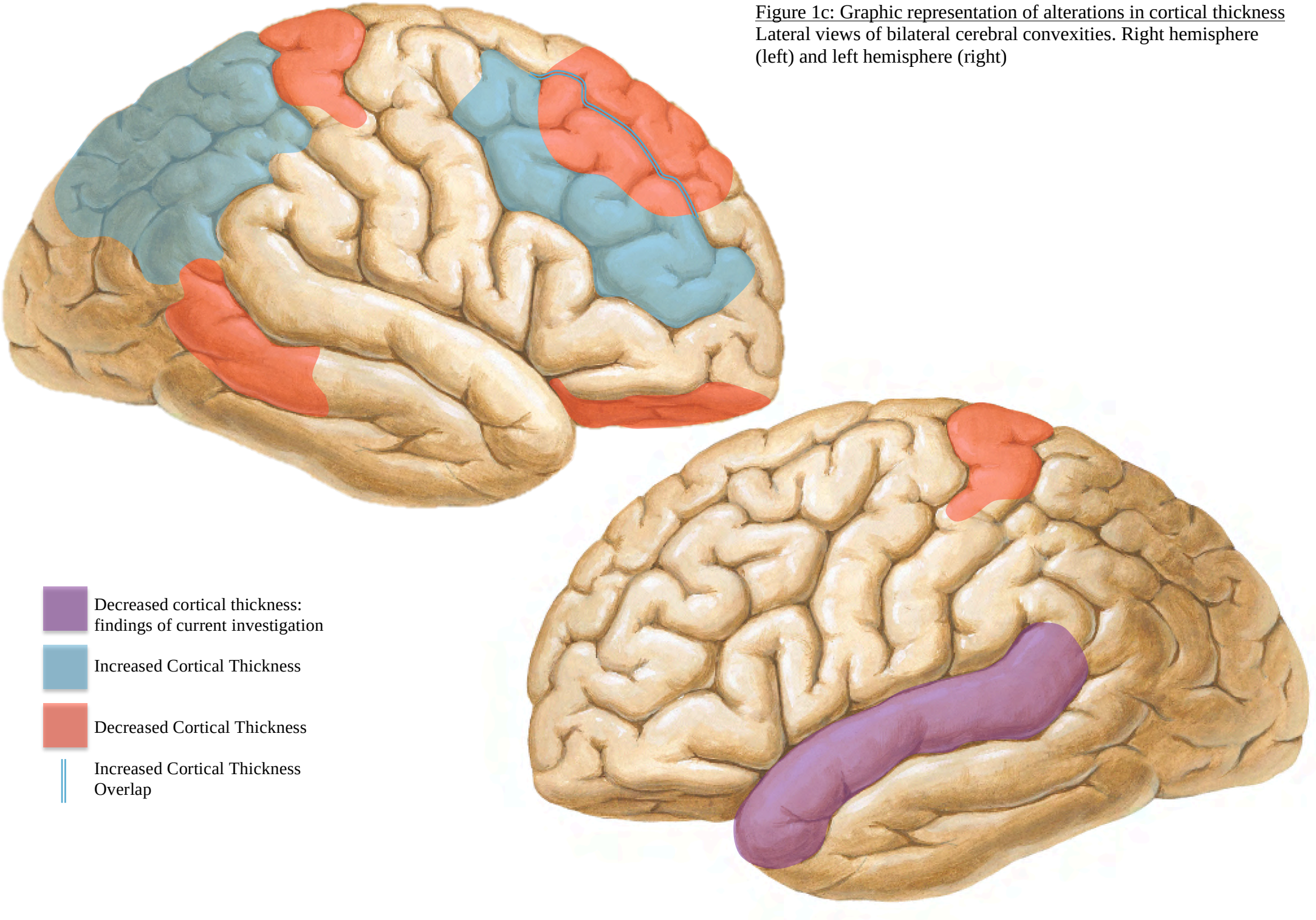

Table 2. Mean volumes (cm^3) of manually traced subcortical gray matter structures

		Mean Thickness in mm ± SD per group				95% Confidence Interval of the Difference	
Region	**Hemisphere**	**SAD (n=18)**	**HC (n=18)**	**F**	**Sig. (2-tailed)**	**Lower**	**Upper**
Isthmus of the Cingulate gyrus	L	2.388 | 0.231	2.565 | 0.181	0.414	**0.020****	-0.323	-0.030
	R	2.378 | 0.240	2.489 | 0.156	3.592	0.124	-0.255	0.032
Temporal Pole	L	3.358 | 0.320	3.675 | 0.317	0.098	**0.007****	-0.540	-0.094
	R	3.768 | 0.401	3.854 | 0.334	0.157	0.508	-0.345	0.174
Superior temporal gyrus	L	2.683 | 0.193	2.802 | 0.124	1.653	**0.043****	-0.234	-0.003
	R	2.773 | 0.176	2.835 | 0.167	0.370	0.299	-0.182	0.058

** Denotes statistical significance

Table: 3
Structural studies in SAD utilizing cortical thickness analyses.

Study	SAD N (M/F)	Mean Age (SD)	HC N (M/F)	Mean Age (SD)	Approach
Syal et al., 2012	13 (8/5)	35.3 (11.8)	13 (8/5)	33.6 (11.2)	Cortical thickness
Frick et al., 2013	14 (14/0)	32.6 (8.7)	12(12/0)	27.9 (7.9)	Cortical thickness
Brühl et al., 2014	46 (29/17)	33.13 (10.61)	46 (29/17)	32.96 (8.87)	Cortical thickness

Table: 4
Main findings of the studies listed in Table 1, and the structures implicated.

Study	Main findings and structures implicated
Syal et al., 2012	↓ **thickness**: **BT** fusiform & post central crtx; **R** rostral PFC, DLPFC, OFC, 1° motor crtx, pre & paracentral regions, temporal pole, inferior temporal crtx, insular crtx
Frick et al., 2013	↑ **thickness: L** fusiform & lingual gyri
Brühl et al., 2014	↑ **thickness: R** temporal pole, ACC, DLPFC, parietal crtx; **L** anterior insula

↓ denotes decreased; ↑ denotes increased
crtx: cortex; L: left; R: right; BT: bilateral; 1°: primary; PFC: prefrontal cortex; DLPFC: dorsolateral prefrontal cortex; OFC: orbitofrontal cortex; ACC: anterior cingulate cortex

References:

1. Amodio, D. M., & Hamilton, H. K. (2012). Intergroup anxiety effects on implicit racial evaluation and stereotyping. Emotion, 12(6), 1273–1280. doi:10.1037/a0029016
2. Anderson, J. S, Shah, L. M. (2014). Speciality imaging: functional MRI. Amyrsys publishing inc
3. Brodmann, K. (1909) Vergleichende Lokalisationslehre der Großhirnrinde in ihren Prinzipien dargestellt auf Grund des Zellenbaues (Barth, Leipzig, Germany).
4. Brühl, A. B., Delsignore, A., Komossa, K., & Weidt, S. (2014). Neuroimaging in social anxiety disorder—A meta-analytic review resulting in a new neurofunctional model. Neuroscience & Biobehavioral Reviews, 1–21. doi:10.1016/j.neubiorev.2014.08.003First, 1997
5. Brühl, A. Hänggi, J. Baur, V. Rufer, M. Delsignore, A. Weidt, S. Jäncke, L. and Herwig, U. (2014). Increased Cortical Thickness in a Frontoparietal Network in Social Anxiety Disorder, 1–12.
6. Carr L, Iacoboni M, Dubeau M-C, Mazziotta JC, Lenzi GL (2003) Neural mechanisms of empathy in humans: a relay from neural systems for imitation to limbic areas. Proc Natl Acad Sci U S A 100(9):5497–5502. doi:10.1073/pnas.0935845100
7. De Leon MJ, George AE, Golomb J, Tarshish C, Convit A, Kluger A, De Santi S, McRae T, Ferris SH, Reisberg B, Ince C, Rusinek H, Bobinski M, Quinn B, Miller DC, Wisniewski HM. Frequency of hippocampal formation atrophy in normal aging and Alzheimer's disease. Neurobiol Aging. 1997 Jan-Feb;18(1):1-11. PubMed PMID: 8983027.
8. Desikan R, Ségonne F, Fischl B, Quinn B (2006) An automated labeling system for subdividing the human cerebral cortex on MRI scans into gyral based regions of interest. NeuroImage
9. Etkin A, Prater KE, Schatzberg AF, Menon V, Greicius MD (2009): Disrupted amygdalar subregion functional connectivity and evidence of a compensatory network in generalized anxiety disorder. Arch Gen Psychiatry 66:1361–1372.
10. Etkin, A. Egner, T. Kalisch, R. Emotional processing in anterior cingulate and medial prefrontal cortex, Trends in Cognitive Sciences 15 (2011) 85–93.
11. Fischl B, Salat DH, Busa E, Albert M, Dieterich M, Haselgrove C, van der Kouwe A et al (2002) Whole brain segmentation: automated labeling of neuroanatomical structures in the human brain. Neu- ron 33(3):341–355
12. Fischl B, Salat DH, van der Kouwe AJW, Makris N, Ségonne F, Quinn BT, Dale AM (2004a) Sequence-independent segmentation of magnetic resonance images. NeuroImage 23(Suppl 1):S69–S84. doi:10.1016/j.neuroimage.2004.07.016
13. Fischl, B., & Dale, A. M. (2000). Measuring the thickness of the human cerebral cortex from magnetic resonance images. Proceedings of the National Academy of Sciences of the United States of America, 97(20), 11050–11055. doi:10.1073/pnas.200033797
14. Fischl, B., Sereno, M. I., & Dale, A. M. (1999). Cortical surface-based analysis. II: Inflation, flattening, and a surface-based coordinate system. NeuroImage, 9(2), 195–207. doi:10.1006/nimg.1998.0396Fischl and Sereno 1999)
15. Franzen EA, Myers RE (1973) Neural control of social behavior: prefron- tal and anterior temporal cortex. Neuropsychologia 11(2):141–157
16. Freitas-Ferrari, M. C., Hallak, J. E. C., Trzesniak, C., Filho, A. S., Machado-de-Sousa, J. P., Chagas, M. H. N., et al. (2010). Neuroimaging in social anxiety disorder: A systematic review of the literature. Progress in Neuropsychopharmacology & Biological Psychiatry, 1–16. doi:10.1016/j.pnpbp.2010.02.028
17. Frick, A., Howner, K., Fischer, H., Eskildsen, S. F., Kristiansson, M., & Furmark, T.

(2013). Cortical thickness alterations in social anxiety disorder. Neuroscience Letters, 536, 52–55. doi:10.1016/j.neulet.2012.12.060
18. Glosser G, Zwil AS, Glosser DS, O'Connor MJ, Sperling MR (2000) Psychiatric aspects of temporal lobe epilepsy before and after anterior temporal lobectomy. J Neurol Neurosurg Psychiatry 68 (1):53–58
19. Gorman, J. M., Docherty, J. P., (2010). A Hypothesized Role for Dendritic Remodeling in the Etiology of Mood and Anxiety Disorders, 1–9.
20. Hänggi, J., Brütsch, K., Siegel, A. M., & Jäncke, L. (2014). The architecture of the chess player's brain. Neuropsychologia, 62, 152–162. doi:10.1016/j.neuropsychologia.2014.07.019
21. Hickok G et al: The cortical organization of speech processing. Nat Rev Neurosci. 8(5):393-402, 2007
22. Jack CR Jr, Petersen RC, Xu YC, Waring SC, O'Brien PC, Tangalos EG, Smith GE, Ivnik RJ, Kokmen E. Medial temporal atrophy on MRI in normal aging and very mild Alzheimer's disease. Neurology. 1997 Sep;49(3):786-94. PubMed PMID: 9305341; PubMed Central PMCID: PMC2730601.
23. Katche C et al: Functional integrity of the retrosplenial cortex is essential for rapid consolidation and recall of fear memory. Learn Mem. 20(4):170-3, 2013
24. Kaye JA, Swihart T, Howieson D, Dame A, Moore MM, Karnos T, Camicioli R, Ball M, Oken B, Sexton G. Volume loss of the hippocampus and temporal lobe in healthy elderly persons destined to develop dementia. Neurology. 1997 May;48(5):1297-304. PubMed PMID: 9153461.
25. Kohn, N., Eickhoff, S.B., Scheller, M., Laird, A.R., Fox, P.T., Habel, U., 2014a. Neural network of cognitive emotion regulation—an ALE meta-analysis and MACM analysis. NeuroImage 87, 345–355.
26. Kohn, N., Falkenberg, I., Kellermann, T., Eickhoff, S.B., Gur, R.C., Habel, U., 2014. Neural correlates of effective and ineffective mood induction. Soc. Cogn. Affect. Neurosci., in press.
27. Leibowitz M (1987) Liebowitz social anxiety scale. Mod Probl Pharmacopsychiatr 22:141–173
28. Leighton, M. P., Prost, R. W., Ulmer, J. L., Smith, M. M., Daniels, D. L., Strottmann, J. M., et al. (2001). Pictorial Review of Glutamate Excitotoxicity: Fundamental Concepts for Neuroimaging. *AJNR. American Journal of Neuroradiology*, 1–12.
29. Liao W, Qiu C, Gentili C, Walter M, Pan Z, Ding J, Zhang W et al (2010) Altered effective connectivity network of the amygdala in social anxiety disorder: a resting-state FMRI study. PLoS One 5 (12):e15238. doi:10.1371/journal.pone.0015238
30. Ochsner KN, Silvers JA, Buhle JT (2012): Functional imaging stud- ies of emotion regulation: A synthetic review and evolving model of the cognitive control of emotion. Ann NY Acad Sci 1251:E1–E24.
31. Olney J. Neurotoxicity of excitatory amino acids. In: McGeer E, Olney J, McGeer P, eds. Kainic Acid as a Tool in Neurobi- ology. New York: Raven Press; 1978:95–121
32. Olney JW. Role of excitotoxins in developmental neuropa- thology. APMIS Suppl 1993;40:103–112
33. Olson IR, Plotzker A, Ezzyat Y (2007) The enigmatic temporal pole: a review of findings on social and emotional processing. Brain 130 (7):1718–1731. doi:10.1093/brain/awm052
34. Olson, I. R., Plotzker, A., & Ezzyat, Y. (2007). The Enigmatic temporal pole: a review of findings on social and emotional processing. Brain, 130(7), 1718–1731. doi:10.1093/brain/awm052
35. Rusinek H, de Leon MJ, George AE, Stylopoulos LA, Chandra R, Smith G, Rand T, Mourino M, Kowalski H. Alzheimer disease: measuring loss of cerebral gray matter with MR imaging. Radiology. 1991 Jan;178(1):109-14. PubMed PMID: 1984287.

36. Savic, I. (2013). Structural Changes of the Brain in Relation to Occupational Stress. *Cerebral Cortex*. doi:10.1093/cercor/bht348
37. Schneier, F.R., Rodebaugh, T.L., Blanco, C., Lewin, H., Liebowitz, M.R., 2011. Fear and avoidance of eye contact in social anxiety disorder. Compr. Psychiatry 52, 81-87.
38. Snowden JS, Gibbons ZC, Blackshaw A, Doubleday E, Thompson J, Craufurd D, Foster J et al (2003) Social cognition in frontotemporal dementia and Huntington's disease. Neuropsychologia 41(6):688–701
39. Snowden JS, Thompson JC, Neary D (2004) Knowledge of famous faces and names in semantic dementia. Brain 127(Pt 4):860–872. doi:10.1093/brain/awh099
40. Syal, S., Hattingh, C. J., Fouché, J.-P., Spottiswoode, B., Carey, P. D., Lochner, C., & Stein, D. J. (2012). Grey matter abnormalities in social anxiety disorder: a pilot study. Metabolic Brain Disease, 27(3), 299–309. doi:10.1007/s11011-012-9299-52013,
41. Thompson SA, Patterson K, Hodges JR (2003) Left/right asymmetry of atrophy in semantic dementia: behavioral-cognitive implica- tions. Neurology 61(9):1196–1203
42. Vollm B, Taylor A, Richardson P, Corcoran R (2006) Neuronal corre- lates of theory of mind and empathy: a functional magnetic resonance imaging study in a nonverbal task. NeuroImage
43. von Economo, C. (1929) The Cytoarchitectonics of the Human Cerebral Cortex (Oxford Univ. Press, London).
44. Wallace GL, Dankner N, Kenworthy L, Giedd JN, Martin A (2010) Age-related temporal and parietal cortical thinning in autism spectrum disorders. Brain 133(12):3745–3754. doi:10.1093/ brain/awq279
45. Zahodne, L. B., Gongvatana, A., Cohen, R. A., Ott, B. R., Tremont, G., Alzheimer's Disease Neuroimaging Initiative. (2013). Are apathy and depression independently associated with longitudinal trajectories of cortical atrophy in mild cognitive impairment? The American Journal of Geriatric Psychiatry : Official Journal of the American Association for Geriatric Psychiatry, 21(11), 1098–1106. doi:10.1016/j.jagp.2013.01.043
46. Zilles, K. (1990) in The Human Nervous System, ed. Paxinos, G. (Academic, San Diego), pp. 757– 802.
47. Zipursky RB, Lim KO, Sullivan EV, Brown BW, Pfefferbaum A. Widespread cerebral gray matter volume deficits in schizophrenia. Arch Gen Psychiatry. 1992 Mar;49(3):195-205. PubMed PMID: 1567274.

CHAPTER V

White Matter Integrity in Patients with Social Anxiety Disorder

Introduction:

The advent of diffusion tensor imaging (DTI) and fiber tractography has opened a new noninvasive window on the white matter connectivity of the human brain. This technique helps illustrate microscopic details about neural architecture, and because of this ability, DTI has become a popular tool to investigate white matter alterations in psychiatric disorders (Hagman et al., 2006). Several studies have investigated white matter alterations associated with social anxiety disorder (tables 3 and 4). Overall, the global white matter volume was not significantly different between SAD and HC in four studies, one study reported reduced global white matter (Baur et al., 2013a) and one study reported globally reduced fractional anisotropy (FA), (Baur et al., 2013a). Significant FA changes were detected in the left uncinate fasciculus in SAD when compared to HC in three studies (Baur et al., 2013a, 2011; Qiu et al., 2014), with one study finding no difference in the left, but reduced FA in the right uncinate fasciculus in SAD compared to HC (Phan et al., 2009).

In the superior longitudinal fasciculus, apparent diffusion coefficient (ADC) was reduced bilaterally in one study, which also reported reduced FA on the left side (Qiu et al., 2014), which is paralleled by another study (Baur et al., 2011). However, two studies found no difference in at least one side of the superior longitudinal fasciculus (Baur et al., 2011; Phan et al., 2009) No changes in FA were reported for the inferior fronto-occipital fasciculus in two studies (Baur et al., 2013a; Phan et al., 2009), while one study showed reduced ADC (Qiu et al., 2014). There is no evidence for increased FA in white matter in most of the existing studies (Phan et al., 2009; Baur et al., 2013a; Qiu et al., 2014) except for increased FA and fiber density in one study (Liao et al., 2011).

The overall finding of reduced FA shown in all DTI studies in SAD suggests that there is a pervasive loss of white matter integrity in individuals with SAD compared to controls. So far, we can only attempt to further characterize these changes in white matter anisotropy by their region specificity using DTI. It is possible that, a more reliable way to do this, is to perform analyses on patients who present with the least potential confounding factors. Previous psychotropic treatment has been show to have significant effects on structural neuroimaging measures (Hafeman et al., 2012). Therefore, this study aims to investigate the white matter structure in SAD by

way of DTI in a treatment naïve, comorbidity free sample population, which has not been attempted by other investigators to date.

Diffusion Tensor Imaging:

Diffusion, also known as “Brownian motion,” refers to constant random microscopic molecular motion due to heat. In clinical diffusion imaging, the type of diffusion being investigated is water self-diffusion, meaning the thermal motion of water molecules in a medium that itself consists mostly of water (Le Bihan et al., 1986; 1988; Thomsen et al., 1987; Turner et al., 1990) In a review of the theoretical underpinnings of diffusion tensor imaging, Mukherjee et al., (2008) note that the diffusion constant, typically expressed in units of square millimeters per second, relates the average displacement of a molecule over an area to the observation time, with higher values of this constant indicating more mobile water molecules.

The apparent diffusion coefficient (ADC) is the diffusion constant measured in the clinical setting, reflecting the limitation that in vivo diffusion cannot be separated from other sources of water mobility, such as active transport, flow along pressure gradients, and changes in membrane permeability. Imaging molecular water diffusion confers the ability to probe the microstructural properties of biologic tissues. This sensitivity to cellular processes has been exploited clinically for the noninvasive mapping of white matter connectivity by using the diffusion tensor model (Basser et al., 1994; 2000; Pierpaoli et al., 1996; Conturo et al., 1999; Mori et al., 1999).

In isotropic diffusion, molecular motion is equal in all directions. Pure water at body temperature demonstrates isotropic diffusion, with an ADC of approximately 3.0^103 mm2/s. In the human brain, isotropic diffusion may be found in the CSF spaces, except in areas of bulk flow such as the jets emanating from the foramina of Monro or through the cerebral aqueduct. Due to its complex microarchitecture, the gray matter of the cerebral cortex in adults is also thought to exhibit isotropic diffusion at the clinical range of b-values (Pierpaoli et al., 1996; Shimony et al., 1999) though some studies differ (Sorensen et al., 1999).

In anisotropic diffusion, molecular mobility is not equal for all directions. White matter tracts with tightly packed coherently oriented fiber bundles hinder water displacement perpendicular to the direction of the fibers, resulting in larger ADC values parallel to the tracts rather than orthogonal to them (Chenevert et al., 1990).

Hence, more than 1 diffusion-encoding direction is required to characterise regions of anisotropic diffusion. If only a single diffusion direction was probed, interpretation of the DWIs would be complicated by variable signal intensity in white matter tracts, depending on their orientation relative to the direction of the diffusion gradient, which could also be affected by changes in the orientation of the patient's head.

The objective of DTI fiber tracking is to determine intervoxel connectivity on the basis of the anisotropic diffusion of water (Conturo et al., 1999; Mori et al., 1999; Basser et al., 2000; Gossl et al., 2002; Parker et al., 2003). DTI white matter tractography has been useful in investigating the white matter ultrastructure in basic neuroscience (Mori et al., 2006), cognitive neuroscience (Catani et al., 2006), and diagnostic neuroradiology (Holodny et al., 2001; Berman et al., 2004; Nimsky et al., 2005). In each brain voxel, the dominant direction of axonal tracts can be assumed to be parallel to the primary eigenvector of the diffusion tensor. Fiber tracking uses the diffusion tensor of each voxel to follow an axonal tract in 3D from voxel to voxel through the human brain. In this way, 3D DTI tractography has opened up a whole new dimension to the ability to depict human neuroanatomy noninvasively.

Methods:

Participant recruitment and diagnostic measures are discussed in detail in Chapter III of this thesis.

Imaging:

Magnetic resonance imaging will be conducted on the 3T Siemens system (MAGNETOM Allegra, Erlangen, Germany) at the Cape Universities Brain Imaging Centre. Whole brain T1- weighted 3D magnetization-prepared rapid gradient echo (MPRAGE) images will acquired using the following parameters: spatial resolution 0 1.0 × 1.0 × 1.0 mm3; slices 0 160; matrix 0 179×256; TR 0 2,300 ms; TE 0 3.93 ms; TI 0 1,100 ms; and flip angle 0 12°. DTI sequences will be acquired in all three orthogonal planes in three acquisitions with the following parameters: 1.8 x 1.8 x 2.0 mm^3 spatial resolution, 220 mm FOV, TR = 8800 ms, TE = 88 ms, 65 slices, 0% distances factor and twofold GRAPPA acceleration. Gradients will be applied in 30 directions with b = 1000 mm/s^2 and three volumes will be acquired without any diffusion-weighting.

Data processing and analyses:

Using SPSS 22, independent-sample t-tests and chi-square tests investigated between-group differences in sociodemographic and anthropometric variables. To prepare DTI data, scan volumes that were re-acquired due to movement as registered by the motion navigator during imaging were removed and the raw data visually inspected to remove further volumes with significant movement or other arte- facts. A minimum of 12 volumes were retained. DTI pre-processing and analyses used the FMRIB Software Library (FSL) v 5.0 and previously validated tract-based spatial statistics (TBSS) (Smith et al. 2006).

In brief, data first underwent eddy current correction and then AP and PA images were corrected for susceptibility artifacts and merged using FSL top-up. Subsequently, FA images were created by fitting a linear tensor model to the raw diffusion data. Brain extraction was per- formed using the FMRIB Software Library brain extraction tool (FSL BET) (Smith et al., 2002) and FA data aligned into MNI space using the non-linear registration tool FNIRT (Andersson and Andersson). A mean FA skeleton was created, representing the centre of the white matter tracts for each subject. Individually aligned FA data were mapped on the skeleton and projection transformations were applied to MD, AD and RD data. Whole-brain group differences in DTI parameters were investigated using FSL randomise that employs a general linear model (Winkler et al., 2014), at 5000 permutations per test at a threshold of 0.2, controlled for gender.

Analyses were corrected for multiple comparisons using threshold-free cluster enhancement (TFCE) (Smith et al., 2009). White matter regions were identified using the International Consortium of Brain Mapping (ICBM) DTI-81 white-matter atlas (Mori et al., 2008). Anatomical regions surrounding white matter tracts were identified using the Harvard cortical and subcortical structural atlases (Makris et al., 2006). Regions of interest (ROIs) were extracted by utilising the ICBM-DTI-81 white matter atlas for mask creation and subsequent estimation of mean values for DTI parameters. These values were exported to SPSS 22 to investigate associations of diffusion parameters with diagnosis of SAD vs HC's. Tests were two-tailed and excluded scores outside the 95% confidence interval.

Results:

With respect to socio-demographic characteristics, there were o statistically significant differences between the SAD, and HC groups (Table 1 in Chapter 3). DTI analyses found that SAD subjects compared with HC demonstrated significantly decreased FA in the genu of the corpus callosum (p=0.031), the splenium of the corpus callosum (p=0.000), the fornix (p=0.000), bilateral corticospinal tracts [R(p=0.029), L(p=0.001)], the right superior aspect of the corona radiata (p=0.011), bilateral aspects of the sagittal striatum [R(p=0.010), L(p=0.011)], the right cingulum (p=0.048) and the tapetum bilaterally [R(p=0.029), L(p=0.009)]. No increased FA was noted. Increased mean diffusivity (MD) was found in bilateral aspects of the corona radiata [R(p=0.009), L(p=0.043)], and the right aspect of the sagittal striatum (p=0.043). SAD subjects demonstrated decreased MD in the left cingulum (p=0.010), and the left superior fronto-occipital fasciculus (p=0.032) when compared to HC. The results are summarized in table 1 and 2.

Table 1: Summary of fractional anisotropic findings in SAD vs HC's

		Mean Fractional Anisotropy ± SD per group				95% Confidence Interval of the Difference	
Structure	**Hemisphere**	**SAD (n=18)**	**HC (n=18)**	**F**	**Sig. (2-tailed)**	**Lower**	**Upper**
Genu of the corpus callosum	M	0.328 | 0.089	0.457 | 0.190	2.996	**0.031****	-0.243	-0.012
Splenium of the corpus callosum	M	0.312 | 0.070	0.512 | 0.136	5.671	**0.000****	-0.284	-0.116
Fornix	M	0.313 | 0.056	0.502 | 0.137	10.742	**0.000****	-0.270	-0.107
Corticospinal tract	R	0.306 | 0.047	0.387 | 0.122	7.616	**0.029****	-0.153	-0.008
	L	0.277 | 0.050	0.295 | 0.109	3.633	**0.001****	-0.184	-0.052
Corona radiata	R	0.245 | 0.048	0.342 | 0.121	6.384	**0.011****	-0.167	-0.024
	L	0.266 | 0.057	0.339 | 0.129	5.791	0.066	-0.150	0.005
Sagittal striatum	R	0.145 | 0.043	0.282 | 0.180	15.765	**0.010****	-0.238	-0.034
	L	0.129 | 0.019	0.262 | 0.180	23.400	**0.011****	-0.232	-0.032
Cingulum	R	0.156 | 0.037	0.227 | 0.122	4.487	**0.048****	-0.141	-0.000
	L	0.311 | 0.040	0.293 | 0.043	0.230	0.264	-0.014	0.050
Tapetum	R	0.337 | 0.081	0.454 | 0.171	2.031	**0.029****	-0.221	-0.013
	L	0.349 | 0.105	0.531 | 0.219	1.424	**0.009****	-0.316	-0.049

Table 2: Summary of mean diffusivity findings in SAD vs HC's

		Mean Diffusivity ± SD per group				95% Confidence Interval of the Difference	
Structure	**Hemisphere**	**SAD (n=18)**	**HC (n=18)**	**F**	**Sig. (2-tailed)**	**Lower**	**Upper**
Corona radiata	R	0.00075 | 0.00003	0.00070 | 0.00006	5.678	**0.009****	0.000	0.000
	L	0.00071 | 0.00003	0.00006 | 0.0006	4.786	**0.043****	0.000	0.000
Sagittal striatum	R	0.00097 | 0.00014	0.00085 | 0.00015	0.519	**0.043****	0.000	0.000
	L	0.00093 | 0.00097	0.00083 | 0.00015	3.029	0.055	-0.000	0.000
Cingulum	R	0.00095 | 0.00013	0.00089 | 0.00014	0.188	0.265	-0.000	0.000
	L	0.00074 | 0.00002	0.00077 | 0.00041	1.857	**0.010****	-0.000	-0.000
Superior fronto-occipital fasciculus	R	0.00087 | 0.00010	0.00096 | 0.00021	3.795	0.173	-0.000	-0.000
	L	0.00084 | 0.00007	0.00097 | 0.00019	2.920	**0.032****	-0.000	-0.000

Values in bold with ** denotes statistical significance

Table: 3

Summary of demographic characteristics of DTI studies in SAD

Study	SAD N (M/F)	Mean Age (SD)	HC N (M/F)	Mean Age (SD)	Approach
Phan et al., 2009	30(15/15)	27.20 (7.80)	30(10/20)	29.90 (8.13)	Diffusion tensor imaging
Bauer et al., 2011	25 (18/7)	32 (10.4)	25 (18/7)	23 (10.1)	Diffusion tensor imaging
Liao et al., 2011	18 (12/6)	22.67 (3.77)	18 (13/5)	21.89 (3.69)	Diffusion tensor imaging
Bauer et al., 2013	25 (18/7)	31.6 (10.4)	25 (18/7)	32.3 (10.1)	Diffusion tensor imaging
Qiu et al., 2014	18 (12/6)	22.72 (3.85)	18 (12/6)	21.78 (3.90)	Diffusion tensor imaging

Table: 4

Summary of the main findings in DTI studies in SAD.

Study	Main findings and structures implicated
Phan et al., 2009	↓ **FA: R** uncinate fasciculus near the OFC
Bauer et al., 2011	↓ **FA: L** uncinate fasciculus, superior longitudinal fasciculus
Liao et al., 2011	↓ **FA: R** arcuate fasciculus; ↑ **FA: L** fronto-occipital fasciculus; ↑ **FA:** Genu of the CC
Bauer et al., 2013	↓ **Vol: L** uncinate fasciculus; ↓ **Mean fibre length: L** uncinate fasciculus
Qiu et al., 2014	↓ **FA: L**: insula, inferior frontal gyrus, middle temporal gyrus, & inferior parietal gyrus ↑ **ADC: BT** inferior frontal gyrus, middle temporal gyrus; **L** inferior parietal gyrus, & insula

↓ denotes decreased; ↑ denotes increased

crtx: cortex; L: left; R: right; BT: bilateral; 1°: primary; FA: fractional anisotropy; Vol: volume; ADC: apparent diffusion coefficient; PFC: prefrontal cortex; DLPFC: dorsolateral prefrontal cortex; OFC: orbitofrontal cortex; ACC: anterior cingulate cortex

Discussion:

The preliminary findings here provide evidence of abnormal white-matter microstructure in SAD patients. Specifically, the findings of this study were as follows: (1) SAD patients showed decreased FA in the genu and splenium of the corpus callosum, the fornix, bilateral corticospinal tracts, the right superior aspect of the corona radiata, bilateral aspects of the sagittal striatum, the right cingulum and the tapetum bilaterally; (2) SAD patients howed increased mean diffusivity in bilateral superior aspects of the corona radiata, and the right sagittal striatum; (3) SAD patients showed decreased MD in the left cingulum and the left superior fronto-occipital fasciculus.

Although all previous studies found decreased FA (Phan et al., 2009; Bauer et al., 2011; Liao et al., 2011; Bauer et al., 2013; Qiu et al., 2014) in SAD, there has been variation in regional specificity of these alterations . The findings regarding uncinate and arcuate fasciculi as well as the superior longitudinal and fronto-occipital fasciculi are consistent with previous studies (Phan et al., 2009; Bauer et al., 2011; Liao et al., 2011; Bauer et al., 2013). The following is a more detailed description of the results and their potential significance.

The Cingulum and Fornix:

Our findings of decreased FA in the fornix and cingulum implicates limbic circuitry, specifically the circuit of Papez, in SAD. Sensory information from the various parietal, temporal, and occipital association cortices converge on the cingulate gyrus, which is then projected by way of the cingulum, down into the parahippocampal gyrus and entorhinal cortex. The entorhinal cortex is the principle input pathway to the hippocampus. The output of the hippocampus starts as the alveus, a thin layer of white matter that overlies the hippocampus (Lovblad et al., 2014). The alveus medially converges to form the fimbriae, which then further converge into the left and right crurae of the fornix. The crurae unite in the midline just anterior to the splenium of the corpus callosum and pass anteriorly in the inferior free edge of the septum pellucidum. At the level of the foramen of Monro, the fibres turn inferiorly and slightly posteriorly to diverge into the columns of the fornix, which divide around the anterior commissure, ending in the septal nuclei (precommissural fibers) and predominantly the mammillary bodies (postcommissural fibers). The

mammillothalamic tract projects posterosuperiorly from the mammillary bodies to the anterior nucleus of the thalamus. From here, the loop is completed via projections back to the cingulum or cingulate cortex (Papez et al., 1937). The circuit of Papez is primarily involved in the cortical control of emotion (Bear et al., 2006). Previous studies in SAD have reported that a disrupted Papez circuit may result in deficits in processing emotions, especially in processing of the external social environment and an increase in self-focused attention in phobias (Feinstein et al., 2010). Increased activity of the cingulate cortex in individuals with SAD when compared to HC has previously been reported in SAD (Freitas-Ferrari et al., 2010). In view of the current findings of decreased FA in the cingulum, possible excitotoxic effects of increased activity in the cingulate cortex previously noted in the imaging literature could account for the reductions in FA and consequent deficits in emotional processing and the processing of external social environmental cues seen in SAD patients.

The Corpus Callosum:

Our findings of decreased FA in three regions of the corpus callosum further suggests an overall excitotoxic picture, as these fibres are far reaching in their projections. The genu of the corpus callosum recurves posteroinferiorly in front of the septum pellucidum. Its fibers curve forwards, as the forceps minor, to connect the lateral and medial surfaces of the frontal lobes. The splenium of the corpus callosum overhangs the posterior ends of the thalami, the pineal gland and tectum. Fibres of the splenium, which form the lateral wall of the posterior horn and the lateral wall of the inferior horn of the lateral ventricle, constitute the tapetum. The remaining fibres of the splenium curve back into the occipital lobes as the forceps major. Alterations in frontoparietal networks have previously been reported in SAD (Brühl et al., 2014). Decreased fiber integrity of the genu, splenium and tapetum may contribute towards these alterations and deficits seen in SAD due to impaired connectivity of frontoparietal regions.

The Projection Pathways:

We are the first to report significant involvement in the form of decreased FA in the major motor projection pathways the corticospinal tracts and their distal projections to the cortex, the corona radiata. These findings may be indicative of the effects of chronic anxiety and panic on the motor system and the peripheral nervous

system as freezing or escape responses may occur during panic associated with social anxiety. Chronic or protracted excitatory stimuli may therefore contribute to excitotoxic changes and consequent reductions in fiber integrity seen here.

Striatal hyperactivity has previously been reported in SAD (Freitas-Ferrari et al., 2010). The reductions in FA seen in the white matter associated with the striatum lends further support to possible excitotoxic effects on white matter microstructure. The overall increases in MD in the corona radiata, sagittal striatum and the cingulum corroborate the findings of decreased FA in the same regions. MD was found to be decreased in the left superior fronto-occipital fasciculus. The fronto-occipital fasciculus is a long association fibre, which originates at the frontal pole and passes back deep to the superior longitudinal fasciculus, separated from it by the projection fibres in the corona radiata. It lies lateral to the caudate nucleus near the central part of the lateral ventricle. Posteriorly, it fans out into the occipital and temporal lobes, lateral to the posterior and inferior horns of the lateral ventricle. Decreased MD in the fronto-occipital fasciculus suggests possible hypo-connectivity between frontal and occipital regions. Increased FA in the fronto-occipital fasciculus has previously been reported by Liao et al., (2011). Decreased FA in the fronto-occipital fasciculus has previously been reported by Bauer et al., (2011). Both studies appear to include the uncinate fasciculus as forming part of the horizontal projection fibers of the fronto-occipital fasciculus. Because the uncinate fasciculus was not found to be significantly altered in the current analyses, the significance of this finding is not yet clear.

With regards to the robustness of the technique, one needs to consider that even as sophisticated a mathematic construct as the diffusion tensor is an oversimplification of the properties of water diffusion in the brain. The limitations of the diffusion tensor in areas of complex white matter architecture, where fiber tracts intersect, branch, or are otherwise partial volume averaged within a voxel, affect the ability of DTI fiber tractography to fully delineate an axonal pathway and may also lead to the generation of spurious tracks. Therefore any results from utlising the DTI approach should be interpreted with caution.

Conclusions:

Overall decreased FA was found in several large white matter tracts in SAD. These findings were corroborated with increased MD found in three of these tracts. These findings seem to suggest that white matter microstructure is impaired in SAD. Although causality is difficult to infer here, it is possible that an underlying excitotoxic mechanism has contributed to alterations in white matter in SAD as well as decreased cortical thickness previously reported (Syal et al., 2012), and currently found (see chapter IV) support this view.

References:

1. Andersson JLR, Jenkinson M, Smith S. Non-linear registration, aka spa- tial normalization. FMRIB technical report TR07JA2. www.fmrib.ox.ac.uk/ analysis/techrep
2. Andersson, JLR., Jenkinson, M., Smith, S. Non-linear optimization. FMRIB tech- nical report TR07JA1. www.fmrib.ox.ac.uk/analysis/techrep
3. Basser PJ, Mattiello J, Le Bihan D. Estimation of the effective self-diffusion-tensor from the NMR spin echo. J Magn Reson B 1994;103:247–54
4. Basser PJ, Pajevic S, Pierpaoli C, et al. In vivo fiber tractography using DT-MRI data. Magn Reson Med 2000;44:625–32
5. Baur, V., Brühl, A. B., Herwig, U., Eberle, T., Rufer, M., Delsignore, A., et al. (2013). Evidence of frontotemporal structural hypoconnectivity in social anxiety disorder: A quantitative fiber tractography study. Human Brain Mapping, 34(2), 437–446. doi:10.1002/hbm.21447Qiu et al., 2014
6. Berman JI, Berger MS, Mukherjee P, et al. Diffusion-tensor imaging-guided tracking of fibers of the pyramidal tract combined with intraoperative cortical stimulation mapping in patients with gliomas. J Neurosurg 2004;101:66 –72
7. Bruhl, A.B., Hanggi, J., Baur, V., Rufer, M., Delsignore, A., Weidt, S., Jancke, L., Her- wig, U., 2014. Increased cortical thickness in a frontoparietal network in social anxiety disorder. Hum. Brain Mapp. 35, 2966–2977.
8. Catani M. Diffusion tensor magnetic resonance imaging tractography in cogni- tive disorders. Curr Opin Neurol 2006;19:599 – 606
9. Chenevert TL, Brunberg JA, Pipe JG. Anisotropic diffusion in human white matter: demonstration with MR techniques in vivo. Radiology 1990;177:401-05
10. Conturo TE, Lori NF, Cull TS, et al. Tracking neuronal fiber pathways in the living human brain. Proc Natl Acad Sci U S A 1999;96:10422–27
11. Feinstein, J.S., Adolphs, R., Damasio, A., Tranel, D., 2010. The human amygdala and the induction and experience of fear. Current Biology 21, 34–38.
12. Freitas-Ferrari, M. C., Hallak, J. E. C., Trzesniak, C., Filho, A. S., Machado-de-Sousa, J. P., Chagas, M. H. N., et al.(2010). Neuroimaging in social anxiety

disorder: A systematic review of the literature. Progress in Neuropsychopharmacology & Biological Psychiatry, 1–16. doi:10.1016/j.pnpbp.2010.02.028

13. Gossl C, Fahrmeir L, Putz B, et al. Fiber tracking from DTI using linear state space models: detectability of the pyramidal tract. Neuroimage 2002;16:378 – 88
14. Guye M, Parker GJ, Symms M, et al. Combined functional MRI and tractography to demonstrate the connectivity of the human primary motor cortex in vivo. Neuroimage 2003;19:1349 – 60
15. Hafeman, D. M., Chang, K. D., Garrett, A. S., Sanders, E. M., & Phillips, M. L. (2012). Effects of medication on neuroimaging findings in bipolar disorder: an updated review. Bipolar Disorders, 14(4), 375–410. doi:10.1111/j.1399-5618.2012.01023.x
16. Holodny AI, Schwartz TH, Ollenschleger M, et al. Tumor involvement of the corticospinal tract: diffusion magnetic resonance tractography with intraoperative correlation. J Neurosurg 2001;95:1082
17. Le Bihan D, Breton E, Lallemand D, et al. MR imaging of intravoxel incoherent motions: application to diffusion and perfusion in neurologic disorders. Radiology 1986;161:401– 07
18. LeBihan D, Breton E, Lallemand D, et al. Separation of diffusion and perfusion in intravoxel incoherent motion MR imaging. Radiology 1988;168:497–505
19. Liao, W., Xu, Q., Mantini, D., Ding, J., Machado-de-Sousa, J. P., Hallak, J. E. C., et al. (2011). Altered gray matter morphometry and resting-state functional and structural connectivity in social anxiety disorder. Brain Research, 1388(C), 167–177. doi:10.1016/j.brainres.2011.03.018
20. Lovblad, K.-O., Schaller, K., & Vargas, M. I. (2014). The Fornix and Limbic System. Seminars in Ultrasound, CT, and MRI, 35(5), 459–473. doi:10.1053/j.sult.2014.06.005
21. Makris N, Goldstein JM, Kennedy D, Hodge SM, Caviness VS, Faraone SV, et al. Decreased volume of left and total anterior insular lobule in schizophrenia. Schizophr Res 2006;83(2-3):155–71.

22. Mori S, Kaufmann WE, Pearlson GD, et al. Three-dimensional tracking of axonal projections in the brain by magnetic resonance imaging. Ann Neurol 1999;45:265– 69
23. Mori S, Oishi K, Jiang H, Jiang L, Li X, Akhter K, et al. Stereotaxic white mat- ter atlas based on diffusion tensor imaging in an ICBM template. Neuroimage 2008;40(2):570–82.
24. Mukherjee, P., Berman, J. I., Chung, S. W., Hess, C. P., & Henry, R. G. (2008). Diffusion tensor MR imaging and fiber tractography: theoretic underpinnings. *American Journal of Neuroradiology*, *29*(4), 632–641. doi:10.3174/ajnr.A1051
25. Nimsky C, Ganslandt O, Hastreiter P, et al. Preoperative and intraoperative dif- fusion tensor imaging-based fiber tracking in glioma surgery. Neurosurgery 2005;56:130 –37
26. Papez JW: A proposed mechanism of emotion. 1937. J Neuropsychiatry Clin Neurosci 7:103-112, 1995
27. Parker GJ, Haroon HA, Wheeler-Kingshott CA. A framework for a streamline- based probabilistic index of connectivity (PICo) using a structural interpretation of MRI diffusion measurements. J Magn Reson Imaging 2003;18:242–54
28. Phan, K. L., Orlichenko, A., Boyd, E., Angstadt, M., Coccaro, E. F., Liberzon, I., & Arfanakis, K. (2009). Preliminary Evidence of White Matter Abnormality in the Uncinate Fasciculus in Generalized Social Anxiety Disorder. Bps, 66(7), 691–694. doi:10.1016/j.biopsych.2009.02.028Baur et al., 2011
29. Pierpaoli C, Jezzard P, Basser PJ, et al. Diffusion tensor MR imaging of the human brain. Radiology 1996;201:637– 48
30. Shimony JS, McKinstry RC, Akbudak E, et al. Quantitative diffusion-tensor anisotropy brain MR imaging: normative human data and anatomic analysis. Radiology 1999;212:770 – 84
31. Smith SM, Jenkinson M, Johansen-Berg H, Rueckert D, Nichols TE, Mackay CE, et al. Tract-based spatial statistics: voxelwise analysis of multi-subject diffusion data. Neuroimage 2006;31(4):1487–505.

32. Smith SM, Nichols TE. Threshold-free cluster enhancement: Addressing problems of smoothing, threshold dependence and localisation in cluster inference. Neuroimage 2009;44(1):83–98.
33. Smith SM. Fast robust automated brain extraction. Hum Brain Mapp 2002;17(3):143–55.
34. Sorensen AG, Wu O, Copen WA, et al. Human acute cerebral ischemia: detection of changes in water diffusion anisotropy by using MR imaging. Radiology 1999;212:785–92
35. Syal, S., Hattingh, C. J., Fouché, J.-P., Spottiswoode, B., Carey, P. D., Lochner, C., & Stein, D. J. (2012). Grey matter abnormalities in social anxiety disorder: a pilot study. Metabolic Brain Disease, 27(3), 299–309. doi:10.1007/s11011-012-9299-5
36. Thomsen C, Henriksen O, Ring P. In vivo measurement of water self diffusion in the human brain by magnetic resonance imaging. Acta Radiol 1987;28:353 61
37. Turner R, Le Bihan D, Maier J, et al. Echo-planar imaging of intravoxel incoherent motion. Radiology 1990;177:407–14
38. Winkler AM, Ridgway GR, Webster MA, Smith SM, Nichols TE. Permutation inference for the general linear model. Neuroimage 2014;92:381–97.

CHAPTER VI

Discussion

Amongst a broad existing literature of functional neuroimaging studies in social anxiety disorder (SAD), comparatively few studies have investigated how brain structure may contribute to the neurobiological basis of SAD. Measuring different aspects of the neuroanatomy in people with SAD may give insight as to how these observed structural differences may contribute to a better understanding of SAD pathogenesis.

Thus, this thesis sought to investigate alterations in brain structure related to SAD. The discussion is organized as follows: 1) summary of the methodological approach used in the current study; 2) potential limitations; 3) relating current findings to previous research; 4) interpretation of current findings; 5) future directions; 6) concluding remarks.

1) Summary of the methodological approach:

In this thesis, I have conducted a comprehensive investigation into the three major structural components comprising the brain parenchyma including the cerebral cortex, the subcortical gray matter, and the white matter, in individuals with SAD. This approach included (a) the development of a detailed manual tracing protocol that is systematic, and which covers all of the major macroscopically visible subcortical gray matter structures; (b) this novel manual tracing protocol was then applied to investigate the subcortical gray matter volumes in individuals with SAD compared to HC's; (c) a cortical thickness analysis was conducted to investigate regional differences in cortical thickness in SAD compared to HC's, and finally, (d) the white matter ultrastructure was investigated utilizing diffusion tensor imaging (DTI) in SAD compared to HC's.

a) Manual tracing protocol:

The first aim of this thesis was to develop a reliable, detailed, step-wise manual tracing protocol, based on regions of interest obtained from an extensive review of the neuroimaging literature. The manual tracing protocol was designed in order to manually segment all of the macroscopically visible gray matter structures on T1 weighted images (T1WI). This protocol can be applied to any imaging study as it describes how to delineate the precise neuroanatomical boundaries of each structure,

including the caudate nucleus, the nucleus accumbens, the putamen, the globus pallidus, the hippocampus, and the amygdala. Once the region of interest is traced by hand, the volume can be calculated and recorded.

b) Manual tracing in SAD:

The second aim of this thesis was to apply the tracing protocol, developed in Chapter 2, to segment the major macroscopically visible subcortical gray matter in individuals with SAD, and healthy controls.

b.i) Hypotheses and results:

The principle hypothesis for manual segmentation in SAD postulated that gray matter volumes in subjects with SAD will be reduced when compared to healthy controls. The rationale is that in anxiety states, there is exposure to chronic stress, which increases excitotoxic neurotransmission, which may lead to consequent apoptosis (Gorman et al. 2010) and reductions in volume. This hypothesis was not supported by the findings of the manual segmentation. The right-sided globus pallidus was shown to be significantly enlarged in individuals with SAD compared to HC's.

c) Cortical thickness in SAD:

The third aim of this thesis was to investigate regional differences in cortical thickness in individuals with SAD compared to HC's. Cortical thickness analysis is a sensitive measure, calculating sub-millimeter regional differences in the cortical ribbon, and the current study is the first to apply this technique in individuals with SAD who had no psychiatric or medical comorbidities, and who were psychotherapeutically and psychopharmacologically treatment naïve.

c.i) Hypotheses and results:

The hypothesis underlying the cortical thickness analysis postulates that subjects with SAD will demonstrate reduced cortical thickness in regions that are functionally involved in fear circuitry. This hypothesis was supported by the findings of reduced cortical thickness in the left isthmus of the cingulate gyrus, the left superior temporal gyrus and the left temporal pole in individuals with SAD compared to HC's.

d) White matter tractography:

The fourth aim of this thesis was to investigate, using Diffusion Tensor Imaging (DTI) how fractional anisotropy (FA), a structural measure of isotropic diffusion indicating the direction, shape and integrity of white matter tracts is different in individuals with SAD compared to HC's.

d.i) Hypotheses and results:

In subjects with SAD, FA will be reduced in white matter tracts mediating limbic circuitry. This hypothesis was supported by the findings of decreased FA in distinct elements of the circuit of Papez – the cingulum and fornix. Other findings include reduced FA in the corpus callosum and its projections, specifically the genu, splenium and tapetum, as well as significantly reduced FA in bilateral corticospinal tracts and the right superior aspect of the corona radiata.

2) Limitations:

During the course of these investigations, general limitations (a) and specific limitations to the manual tracing technique (b), cortical thickness analyses (c) and white matter tractography (d) were identified. These limitations are discussed in the following section.

a) General limitations:

The sample size in the current study (n=18) was relatively small. A larger sample size will improve the statistical power of the study and provide stronger evidence to support the findings and deductions of the various analyses. The current sample size was informed by a power analysis that determined an n=18 would provide 99% statistical power, and would thus be sufficiently sensitive for the various analyses to be conducted. Although a larger sample would provide considerable advantage to statistical power and lend support to the findings, the effect of the small sample size was partially negated by the quality of the sample.

All participants with SAD included in this study had no psychiatric or medical comorbidities and were treatment naïve. These factors are potentially important,

considering that the measures used are exquisitely sensitive, measuring variations in sub-millimeter differences between groups, and any potential confounding factors should be limited as far as possible. Psychotropic use has previously been found to significantly alter brain structure in SAD (Talati et al., 2015), and psychotherapy has been shown to alter resting state functional connectivity in SAD (Klumpp et al., 2014).

b) Limitations in manual tracing:

Although the manual tracing protocol developed and utilized in the current study is systematic and highly detailed in terms of identifying anatomical boundaries, an inherent limitation in this technique involves the fact that the accuracy of such anatomical identification relies to a large extent upon the expertise and neuroanatomical knowledge of the researcher performing the tracing. In the current study, the researcher had ten years of specialized training in clinical neuroanatomy with specialization in neuroimaging. The experience of the researcher partially negates potential inaccuracies in the interpretation of imaging anatomy during the tracing, however this fact makes potential multicenter studies potentially difficult if different researchers are used to independently trace structures. Additionally, comparing manual and automated techniques for segmentation would have enriched the thesis and addressed, in part at least, the question regarding what the better methodological approach is towards quantifying cerebral volumes. This is however would require separate and extensive validation of the manual tracing protocol utilized in this study, which might not have fit into the scope of this thesis, however this is an important next step in future research.

c) Limitations in cortical thickness analysis:

The precision of the thickness measurements is constrained by the contrast-to-noise ratio and fidelity of the underlying MRI data. Although previous studies (Fischl et al., 2000) indicate that the methods are relatively insensitive to the specifics of the MRI protocol and scanner, it should be noted that gray/white matter contrast varies across the cortex. In particular, primary sensory areas tend to have a high degree of myelination, resulting in reduced contrast in these regions. To overcome this potential limitation, and to obtain accurate measurements throughout the cortex a unique T1WI sequence was developed by to maximize the spatial resolution and T1 contrast.

d) Limitations in white matter tractography:

Noise, patient movement, and distortion from imaging artifacts are almost unavoidable factors in imaging of individuals who are not completely immobilized or anaesthetized. These factors produce uncertainty in the orientation of the diffusion ellipsoid determining diffusion direction in DTI imaging, and are therefore detrimental to deterministic streamline fiber tracking. To overcome this potential limitation, probabilistic fiber tracking techniques were utilized in the current study, which incorporate the expected uncertainty into the tracking algorithm, which was then used to produce a connectivity metric for each voxel.

3) Relating current findings to previous research:

In the following section, I summarize the findings of previous structural studies utilizing manual tracing, cortical thickness and white matter tractography in SAD in order to draw comparisons with the findings presented in the current study. First (a) I summarize findings of previous manual tracing studies in SAD, (b) then go on to summarize the findings of previous cortical thickness studies and (c) white matter tractography studies in SAD.

a) Manual tracing in SAD:

One previous study sought to manually segment subcortical gray matter structures in SAD (Machado-de-Sousa et al., 2014). These authors utilized manual tracing to determine the volumes of the amygdala and hippocampus and found that the amygdala was significantly enlarged bilaterally, as well as the left hippocampus in individuals with SAD relative to controls. Potential limitations to this study include the manual segmentation protocol used by the authors (Schumman et al. 2004) is relatively out dated considering advances in the last 11 years in gradient and receiver coil technology and magnetic field strength, which has significantly increased imaging resolution and anatomical detail. A second limitation includes the relatively small sample size (n=12), which could potentially affect the sensitivity of the analyses.

b) Cortical thickness in SAD:

Three previous studies investigated cortical thickness in SAD. Syal et al. (2012) was the first to investigate cortical thickness in SAD and found bilateral thinning of the fusiform and the post central cortices as well as significant right hemisphere specific thinning in the right frontal pole, the right dorsolateral prefrontal cortex and right medial orbitofrontal cortex in subjects with SAD compared to HC's. Additional right hemisphere thinning was noted in the right precentral and paracentral regions; the adjacent right superior marginal gyrus within the inferior parietal lobule, the right temporal pole and right inferior temporal cortex within the temporal lobe, and the right insular cortex of patients.

In 2013, Frick et al. found significantly thicker left hemispheric lingual and fusiform gyri in patients with SAD. In the SAD group a negative association was found between social anxiety symptom severity and thickness of the right rostral anterior cingulate cortex.

Recently Brühl et al. (2014) conducted a large study with 46 patients with SAD and 46 healthy controls in which they found patients with SAD had significantly increased cortical thickness in the right temporal pole, anterior cingulate cortex and left anterior insula as well as in the right dorsolateral prefrontal cortex and the right superior parietal lobule and angular gyrus which extended in part into the right precuneus and inferior parietal lobule.

c) White matter tractography in SAD:

Several studies have investigated white matter alterations associated with social anxiety disorder. Overall, the global white matter volume was not significantly different between SAD and HC in four studies, one study reported reduced global white matter (Baur et al., 2013a) and one study reported globally reduced fractional anisotropy (FA), (Baur et al., 2013a). Significant FA changes were detected in the left uncinate fasciculus in SAD when compared to HC in three studies (Baur et al., 2013a, 2011; Qiu et al., 2014), with one study finding no difference in the left, but reduced FA in the right uncinate fasciculus in SAD compared to HC (Phan et al., 2009).

In the superior longitudinal fasciculus, apparent diffusion coefficient (ADC) was reduced bilaterally in one study, which also reported reduced FA on the left side (Qiu et al., 2014), which is paralleled by another study (Baur et al., 2011). However, two studies found no difference in at least one side of the superior longitudinal

fasciculus (Baur et al., 2011; Phan et al., 2009) No changes in FA were reported for the inferior fronto-occipital fasciculus in two studies (Baur et al., 2013a; Phan et al., 2009), while one study showed reduced ADC (Qiu et al., 2014). There is no evidence for increased FA in white matter in most of the existing studies (Phan et al., 2009; Baur et al., 2013a; Qiu et al., 2014) except for increased FA and fiber density in one study (Liao et al., 2011).

4) Interpretation of current findings:

In this section, (a) I present a synopsis of the findings provided by the various techniques used in the present study. This is done to provide a final summary of the data in the context of the findings described above, before presenting the (b) models of neural circuitry that may help to explain the neurobiological underpinnings of SAD.

a) Structural neuroimaging in SAD:

Utilizing manual tracing to segment and calculate the volumes of the macroscopically visible subcortical gray matter structures in SAD, I found that the right globus pallidus was significantly enlarged in individuals with SAD compared to healthy controls. In analyses of cortical thickness, we found significant thinning in the left isthmus of the cingulate gyrus, the left superior temporal gyrus and the left temporal pole. In DTI analyses, we found decreased FA in the genu of the corpus callosum, the splenium of the corpus callosum, the fornix, bilateral corticospinal tracts, the right superior aspect of the corona radiata, bilateral aspects of the sagittal striatum, the right cingulum and the tapetum bilaterally.

b) Neural circuitry:

In a recent activation likelihood estimate (ALE) meta-analysis in SAD (Hattingh et al., 2012), the right globus pallidus has been reported as hyperactive in response to emotion recognition. Individuals with SAD are constantly confronted with aversive stimuli as social situations are an integral part of being a functional human being. Hypervigilance to spot negative evaluation by others in a social situation is a known feature of SAD (American Psychiatric Association, 2013). Research on stress-induced brain plasticity has shown that chronic immobilization stress increases anxiety-like

behavior in rats and that this is accompanied by dendritic hypertrophy (Vyas et al., 2004). Considering previous evidence of right globus pallidus hyperactivity during emotion recognition, dendritic hypertrophy and consequent increase in the volume of the right globus pallidus found here may be a plausible explanation.

Hyperactivity of the cingulate gyrus in response to emotion recognition (Hattingh et al., 2012), the superior temporal gyrus in response to fearful faces (Blair et al., 2008b) and the temporal pole in response to speech anticipatory anxiety (Lorberbaum et al., 2004) have previously been reported in SAD. These findings suggest that the hypervigilance associated with SAD, is directed towards recognizing emotion in others, especially emotion that is negatively valenced such as fear, which then leads to a propagation of anticipatory anxiety. This circuit then completes as the anticipatory anxiety feeds into hypervigilance, priming the individual further for emotion recognition. The thinning of these regions in context of previously reported hyperactivity seem to suggest that in anxiety states, there is exposure to chronic stress which increases excitatory neurotransmission which may lead to consequent excitotoxic apoptosis and thinning in regions which are chronically hyperactive (Gorman et al. 2010).

The DTI analyses in the current study demonstrated decreased structural integrity in distinct elements of the circuit of Papez – the cingulum and fornix. The cingulum is the principle input pathway into the circuit and the fornix the principle output pathway. These findings are consistent with impaired emotional regulation in SAD (Sung et al., 2012). Hyperactivity of the cortical components to the circuit of Papez, the cingulate cortex, and the parahippocampal/entorhinal and hippocampal complex has previously been reported in SAD (Freitas-Ferrari et al., 2010). Hyperactivity, and consequent hyperstimulation of the cingulum and fornix could once again lead to excitotoxic damage to these fiber bundles, which might explain the reduced FA seen in SAD.

The exact underpinnings of the described changes can at present only be speculated about. Because the study was cross-sectional, it is difficult to know whether the detected reductions represent neurotoxic effects of anxiety, effects of other factors, such as nitric oxide, or a pre-existing condition that could have rendered the brain more vulnerable to the development of pathological anxiety responses. Owing to the strict selection criteria, it is, nevertheless, possible to exclude potential

confounding factors such as major life traumas, psychiatric premorbidity and comorbidity, chronic pain, and pharmacological treatment.

Speculatively, cortical hyperactivity in a wide array of brain areas has extensively been reported in SAD (Etkin et al., 2007; Freitas-Ferrari et al., 2010; Brühl et al., 2014). Hyperactive cortical regions project via the limbic loop of the basal ganglia through the globus pallidus. Because the globus pallidus is the primary output nucleus (Standring et al., 2008) of the basal ganglia circuitry, this increased work results in dendritic hypertrophy in the globus pallidi. The increased excitatory neurotransmission that follows from chronic cortical hyperactivity, over time leads to decreased cortical thickness via excitotoxic apoptosis. The limbic white matter circuits found to be affected here, also become altered by chronic excitatory neurotransmission, feeding to and from the cortex and subcortical structures, and eventually lose integrity, seen in the decreased FA, as a result of excitotoxic effects. This hypothesis suggests a synthesis between the current structural findings of this thesis, and some of the most prominent findings of the functional literature.

The study did not directly examine the cellular correlates of the neuroimaging differences identified. Cortical thickness reflects cell-packing density, cell size, the number of cortical neurons, and the dendritic length (Kruggel et al., 2003), factors, which also contribute to subcortical volumes. The molecular underpinnings of the observed morphological changes will primarily be discussed in relation to neuronal modulation by anxiety. Two mediators of this modulation, the glucocorticoids and glutamate as well as their effects have been studied in animal models in detail (Conrad 2008; Leuner and Shors 2012) and involve dendritic retraction, neurotoxicity, and, in some cases, apoptosis (Bremner et al. 2008). Both glutamate and glucocorticoids have neuronal influences on their own, but are also reported to interact (Magarinos and McEwen 1995; Brown et al. 2010).

5) Future directions:

In order to progress the findings presented here, and to test the hypotheses that have been proposed, future directions could include:

a) Repeating analyses used here in larger samples to maximize the statistical power. Using larger sample sizes will add considerable significance to the various observations.
b) Metabolic techniques such as magnetic resonance spectroscopy could provide additional information regarding chemical processes occurring in various structures implicated by current findings. This additional information will add to our current understanding of SAD neurobiology.
c) Longitudinal follow-up imaging will potentially provide insight as to how brain structure in SAD changes over time, which may lend further support to the excitotoxic hypothesis.
d) Multi-center studies could potentially add test-retest reliability to the tracing protocol and manual volumetry results presented here.
e) Repeat measures at higher field strength eg 7Tesla will theoretically increase spatial resolution, adding sensitivity to the various structural measures used in the current study.

6) Concluding remarks:

The current findings provide an integrated perspective of brain structure in SAD and allow these structural measures to be viewed in context of the larger functional literature in SAD. The current impression is that SAD involves various aspects of limbic circuitry with involvement of proximal basal ganglia structures and distal cortical projections. These structural findings and novel manual tracing protocol provide a basis for further investigations into the neurobiology of SAD. It is my hope that with this growing body of neuroimaging literature, that safer, more effective treatments may be developed for individuals suffering with SAD.

References:

1. American Psychiatric Association, 2013. Diagnostic and Statistical Manual of Mental Disorders, Fifth Edition (DSM-5). American Psychiatric Association, Washington, DC.
2. Baur, V., Brühl, A. B., Herwig, U., Eberle, T., Rufer, M., Delsignore, A., et al. (2013). Evidence of frontotemporal structural hypoconnectivity in social anxiety disorder: A quantitative fiber tractography study. *Human Brain Mapping*, *34*(2), 437–446. doi:10.1002/hbm.21447
3. Baur, V., Hänggi, J., Rufer, M., Delsignore, A., Jäncke, L., Herwig, U., & Brühl, A. B. (2011). White matter alterations in social anxiety disorder. *Journal of Psychiatric Research*, *45*(10), 1366–1372. doi:10.1016/j.jpsychires.2011.05.007
4. Blair, K., Geraci, M., Devido, J., McCaffrey, D., Chen, G., Vythilingam, M., et al. (2008). Neural response to self- and other referential praise and criticism in generalized social phobia. *Archives of General Psychiatry*, *65*(10), 1176–1184. doi:10.1001/archpsyc.65.10.1176
5. Bremner JD, Elzinga B, Schmahl C, Vermetten E. 2008. Structural and functional plasticity of the human brain in posttraumatic stress dis- order. Prog Brain Res. 167:171–186.
6. Brown ES, Zaidel L, Allen G, McColl R, Vazquez M, Ringe WK. 2010. Effects of lamotrigine on hippocampal activation in corticosteroid- treated patients. J Affect Disord. 126:415–419.
7. Brühl, A. B., Delsignore, A., Komossa, K., & Weidt, S. (2014). Neuroimaging in social anxiety disorder—A meta-analytic review resulting in a new neurofunctional model. Neuroscience & Biobehavioral Reviews, 1–21. doi:10.1016/j.neubiorev.2014.08.003
8. Conrad CD. 2008. Chronic stress-induced hippocampal vulnerability: the glucocorticoid vulnerability hypothesis. Rev Neurosci. 19:395–411.
9. Etkin, A., Wager, T.D., 2007. Functional neuroimaging of anxiety: a meta-analysis of 1105 emotional processing in PTSD, social anxiety disorder, and specific phobia. Am. 1106 J. Psychiatry 164, 1476–1488.

10. Fischl, B. (2004). Automatically Parcellating the Human Cerebral Cortex. *Cerebral Cortex*, *14*(1), 11–22. doi:10.1093/cercor/bhg087
11. Freitas-Ferrari, M. C., Hallak, J. E. C., Trzesniak, C., Filho, A. S., Machado-de-Sousa, J. P., Chagas, M. H. N., et al. (2010). Neuroimaging in social anxiety disorder: A systematic review of the literature. Progress in Neuropsychopharmacology & Biological Psychiatry, 1–16. doi:10.1016/j.pnpbp.2010.02.028
12. Frick, A., Howner, K., Fischer, H., Eskildsen, S. F., Kristiansson, M., & Furmark, T. (2013). Cortical thickness alterations in social anxiety disorder. *Neuroscience Letters*, *536*, 52–55. doi:10.1016/j.neulet.2012.12.060
13. Gorman, J. M., Docherty, J. P., (2010). A Hypothesized Role for Dendritic Remodeling in the Etiology of Mood and Anxiety Disorders, 1–9.
14. Hattingh, C.J., Ipser, J., Tromp, S., Syal, S., Lochner, C., Brooks, S.J., Stein, D.J., 2013. Functional magnetic resonance imaging during emotion recognition in social anxiety disorder: an activation likelihood meta-analysis. Front. Hum. Neurosci., 6.
15. Klumpp, H., Keutmann, M. K., Fitzgerald, D. A., Shankman, S. A., & Phan, K. L. (2014). Resting state amygdala-prefrontal connectivity predicts symptom change after cognitive behavioral therapy in generalized social anxiety disorder. *Biology of Mood & Anxiety Disorders*, *4*(1), 14. doi:10.1186/s13587-014-0014-5
16. Kruggel F, Bruckner MK, Arendt T, Wiggins CJ, von Cramon DY. 2003. Analyzing the neocortical fine-structure. Med Image Anal. 7:251–264.
17. Leuner B, Shors TJ. 2012. Stress, anxiety, and dendritic spines: what are the connections? Neuroscience. 251:108–119.
18. Liao, W., Xu, Q., Mantini, D., Ding, J., Machado-de-Sousa, J. P., Hallak, J. E. C., et al. (2011). Altered gray matter morphometry and resting-state functional and structural connectivity in social anxiety disorder. Brain Research, 1388(C), 167–177. doi:10.1016/j.brainres.2011.03.018
19. Lorberbaum, J. P., Kose, S., Johnson, M. R., Arana, G. W., Sullivan, L. K., Hamner, M. B., et al. (2004). Neural correlates of speech anticipatory anxiety in generalized social phobia. *NeuroReport*, *15*(18), 2701–2705.
20. Machado-de-Sousa, J. P., Osório, F. de L., Jackowski, A. P., Bressan, R. A., Chagas, M. H. N., Torro-Alves, N., et al. (2014). Increased Amygdalar and

Hippocampal Volumes in Young Adults with Social Anxiety. PLoS ONE, 9(2), e88523. doi:10.1371/journal.pone.0088523

21. Magarinos AM, McEwen BS. 1995. Stress-induced atrophy of apical dendrites of hippocampal CA3c neurons: involvement of glucocorticoid secretion and excitatory amino acid receptors. Neuroscience. 69:89–98.
22. Phan, K. L., Orlichenko, A., Boyd, E., Angstadt, M., Coccaro, E. F., Liberzon, I., & Arfanakis, K. (2009). Preliminary Evidence of White Matter Abnormality in the Uncinate Fasciculus in Generalized Social Anxiety Disorder. *Bps*, *66*(7), 691–694. doi:10.1016/j.biopsych.2009.02.028
23. Qiu, C., Zhu, C., Zhang, J., Nie, X., Feng, Y., Meng, Y., et al. (2014). Diffusion Tensor Imaging Studies on Chinese Patients with Social Anxiety Disorder. *BioMed Research International*, *2014*(3), 1–8. doi:10.1155/2014/860658
24. Savic, I. (2013). Structural Changes of the Brain in Relation to Occupational Stress. *Cerebral Cortex (New York, N.Y. 1991)*, bht348. doi:10.1093/cercor/bht348
25. Schumann CM, Hamstra J, Goodlin-Jones BL, Lotspeich LJ, Kwon H, et al. (2004) The amygdala is enlarged in children but not adolescents with autism; the hippocampus is enlarged at all ages. J Neurosci 24: 6392–6401.
26. Standring, S. (2008). Gray's Anatomy: The Anatomical Basis of Clinical Practice 40th ed. Churchill Livingstone
27. Sung, S. C., Porter, E., Robinaugh, D. J., Marks, E. H., Marques, L. M., Otto, M. W., et al. (2012). Mood regulation and quality of life in social anxiety disorder: An examination of generalized expectancies for negative mood regulation. *Journal of Anxiety Disorders*, *26*(3), 435–441. doi:10.1016/j.janxdis.2012.01.004
28. Syal, S., Hattingh, C. J., Fouché, J.-P., Spottiswoode, B., Carey, P. D., Lochner, C., & Stein, D. J. (2012). Grey matter abnormalities in social anxiety disorder: a pilot study. *Metabolic Brain Disease*, *27*(3), 299–309. doi:10.1007/s11011-012-9299-5
29. Talati, A., Pantazatos, S. P., Hirsch, J., & Schneier, F. (2015). A pilot study of gray matter volume changes associated with paroxetine treatment and response in social anxiety disorder. *Psychiatry Research: Neuroimaging*, 1–25. doi:10.1016/j.pscychresns.2015.01.008

30. Vyas A, Pillai AG, Chattarji S (2004) Recovery after chronic stress fails to reverseamygdaloid neuronal hypertrophy and enhanced anxiety-like behavior. Neurosci 128: 667–673.